Recontamination in food processing - quantitative modelling for risk assessment

Promotoren:

Prof. dr. M. van Schothorst

Voormalig hoogleraar van de European Chair in Food Safety Microbiology

Prof. dr. ir. R.M. Boom

Hoogleraar in de Levensmiddelenproceskunde

Copromotor:

Dr. ir. M.H. Zwietering

Voormalig universitair hoofddocent bij de sectie Levensmiddelenproceskunde, thans werkzaam bij Danone Vitapole, Palaiseau, Frankrijk

Promotiecommissie:

Prof. dr. ir. M.A.J.S. van Boekel (Wageningen Universiteit)

Prof. dr. L.G.M. Gorris (Wageningen Universiteit)

Prof. dr. ir. H.J. Busscher (Rijksuniversiteit Groningen)

Dr. ir. M.C. te Giffel (NIZO Food Research, Ede)

Esther den Aantrekker

Recontamination in food processing - quantitative modelling for risk assessment

Proefschrift

ter verkrijging van de graad van doctor
op gezag van de rector magnificus
van Wageningen Universiteit,
prof. dr. ir. L. Speelman,
in het openbaar te verdedigen
op woensdag 2 oktober 2002
des namiddags te vier uur in de Aula

ISBN 90-5808-695-X

The research described in this thesis was part of the research program of the Graduate School VLAG and was financially supported by Unilever Research & Development, the Netherlands

E.D. den Aantrekker- Recontamination in food processing - quantitative modelling for risk assessment-2002

Thesis Wageningen University, Wageningen, The Netherlands

Contents

Chapter 1	Introduction	7
Chapter 2	Quantifying recontamination through factory environments-a review	15
Chapter 3	A model for biofilm formation relevant to the food industry	35
Chapter 4	Estimating the probability of recontamination via the air using Monte Carlo simulations	51
Chapter 5	Modelling the effect of water recycling on the quality of potato products	73
Chapter 6	Discussion: application of recontamination models	87
	References	111
	Summary	121
	Samenvatting	123
	Dankwoord	125
	Curriculum Vitae	127

1

Introduction

1. Food safety

People have been preserving food for ages. In the early times, they will not have been aware of the mechanistic background of methods like fermenting food products. Such conservation techniques not only prolonged the shelf life of the foods but also prevented outgrowth of pathogenic bacteria and thus foodborne illnesses. The first reported case of food poisoning dates from the Middle Ages where 40.000 deaths occurred, probably due to ergot poisoning caused by *Claviceps purpurea*, a fungus that grows on rye and other grains. In 1820, the first bacterial food poisoning case was reported and was caused by the consumption of sausage, probably infected by *Clostridium botulinum* [62].

Since then food processing technologies and conservation methods have been improved tremendously due to increased knowledge of pathogens and processing methods. Nevertheless, outbreaks of foodborne illnesses still occur. Since there is an increased consumer preference for fresh, ready-to-eat products, there is a tendency to reduce the severity of conservation, which makes products microbiologically more vulnerable [46]. The minimum estimate of foodborne illnesses in the United States is 6 million cases per year on a population of 268 million people. Surveys in other countries suggest that up to 10% of the population may annually suffer from a foodborne disease [64]. In the Netherlands, the number of foodborne illnesses is estimated to be one quarter to one million cases annually on a total population of around 16 million [46]. Depending on the pathogenic bacteria involved, food poisoning can cause acute effects like vomiting or diarrhoea and can even lead to death. Chronic health problems can occur as well, such as cardiovascular disease or immune system disorders. Some foodborne diseases (like listeriosis) are particularly dangerous during pregnancy as they can be either fatal to the foetus or cause severe deformations [64]. Therefore, some population groups are more vulnerable to certain pathogens than others.

A survey amongst 605 consumers in the USA indicated that 69% were aware of the presence of pathogenic bacteria in poultry meat. However, 20% of the questioned people did not know how to reduce risks related to microbiological hazards [14].

In the food industry, the risks of potential foodborne illnesses are reduced by taking preventive measures. The production process of food products usually contains steps like pasteurisation or sterilisation to reduce the number of pathogens. Furthermore, the addition of ingredients like salts or acids, or storage at low temperatures can prevent the outgrowth of pathogens. Despite these preventive measures, food products can still occasionally be contaminated with pathogens. Therefore, in order to further control food safety, various tools have been developed. The most widely used system at this moment is Hazard Analysis Critical Control Points (HACCP). Using this system, the most important steps (Critical Control Points) in a food production process are identified that significantly influence food safety and measures are taken to control these steps. The effectiveness of these control measures is then monitored to determine whether the process parameters remain within predetermined limits designed to achieve food safety requirements [60].

Although HACCP can increase the safety of food products, the presence of pathogenic bacteria can never be completely excluded. Whether or not a product is safe enough for consumption has traditionally been evaluated in a subjective manner with respect to local manufacturing and consumption of foods. The increase in global trade urged the development of a more quantitative and structured system to estimate the risk of illness related to foodborne pathogens. This has resulted in the development of Microbiological Risk Assessment [70].

2. Microbiological Risk Assessment

Risk assessment procedures are already widely used in economic forecasting, toxicology and environmental sciences [139]. Recently, the same approach is applied to food microbiological issues resulting in Microbiological Risk Assessments (MRA). Based on the outcome of an MRA, the risk manager can decide whether the expected risk is acceptable and inform the consumer or to implement actions to reduce the risk to a tolerable level [109]. Due to the structured approach, various management options can be evaluated to assess the influence on the risk estimate.

MRA consists of four stages: (1) hazard identification, (2) hazard characterisation, (3) exposure assessment and (4) risk characterisation [70]. In the first step of MRA, the hazard identification, those biological hazards (usually pathogenic bacteria and their toxins) are identified that can cause foodborne illness after consumption of the product. For example, *Listeria monocytogenes* is identified as one of the hazards in soft cheese prepared from raw milk, which can cause listeriosis after consumption. In the second step, the hazard characterisation, the effect of the identified hazard is determined. This is done in so-called dose-response relationships in which the relation between concentration of the pathogen and probability of illness are established. For the soft cheese example, epidemiological and outbreak data [16] or animal experiments [97] can be used to establish such a dose-response relationship for *L. monocytogenes*. In the third stage of MRA, the exposure assessment, all factors affecting the presence and numbers of micro-organisms up to the point of consumption should be considered. This includes the source, frequency and level of contamination at any point of the food chain. In the example of soft cheese, the production process of soft cheese is evaluated to determine whether *L. monocytogenes* can grow or is inactivated in either of the production steps. By evaluating all production steps, the final concentration of *L. monocytogenes* in the soft cheese prior to consumption can be estimated. Finally, in the fourth step of MRA, the risk characterisation, the outcome of step 3 is coupled to that of step 2 to estimate the probability of becoming ill after consuming the food product. For the soft cheese example, the concentration of *L. monocytogenes* at the moment of consumption is then coupled to the predetermined dose-response relationship. This gives the probability of illness after eating soft cheese. When the number of products that is sold

annually is taken into account, the number of listeriosis cases caused by this product can be estimated. Bemrah et al. [11] performed an MRA on soft cheese and estimated between 3 to 25 listeriosis cases per year on a total of 10 million vulnerable people such as pregnant women.

In this thesis, the third step of an MRA, the exposure assessment, is further investigated as is explained in the next sections.

3. Exposure assessment

For the exposure assessment, a total farm-to-fork evaluation is often applied to incorporate all steps in the production chain that could influence the level of pathogenic bacteria [70]. Predictive modelling techniques can be combined with process engineering models to evaluate the effect of food processing steps on microbial survival and food safety, as was demonstrated by Zwietering and Hasting [148]. Each stage in the chain from raw materials until consumption was evaluated using balances:

Accumulation = in – out + production

The 'in' and 'out' term represent the transport of bacteria in the production steps due to product flow. The 'production' term can be either growth or inactivation in the production step. Various growth and inactivation models have been developed to describe the effect of temperature, *pH* and water activity on the survival of micro-organisms [131]. Such mathematical models can reduce the number of traditional challenge tests and are therefore less time consuming. These models will, however, never accurately describe reality but will rather give orders of magnitude values that can help to determine the most important steps in a food production process. Using these modelling techniques, several scenarios can be evaluated easily to assess the effect of changing process parameters on the level of pathogens in the product.

An example of a process evaluation is given in figure 1. It can be seen that by combining predictive microbiology and process modelling the most important process steps can be determined. The heating step is an important step causing a 2.5-log reduction. During storage a slight increase occurs in the product. This is therefore also an important step. In this case the level of bacteria at the moment of consumption is estimated as 1.5 log cfu g^{-1}.

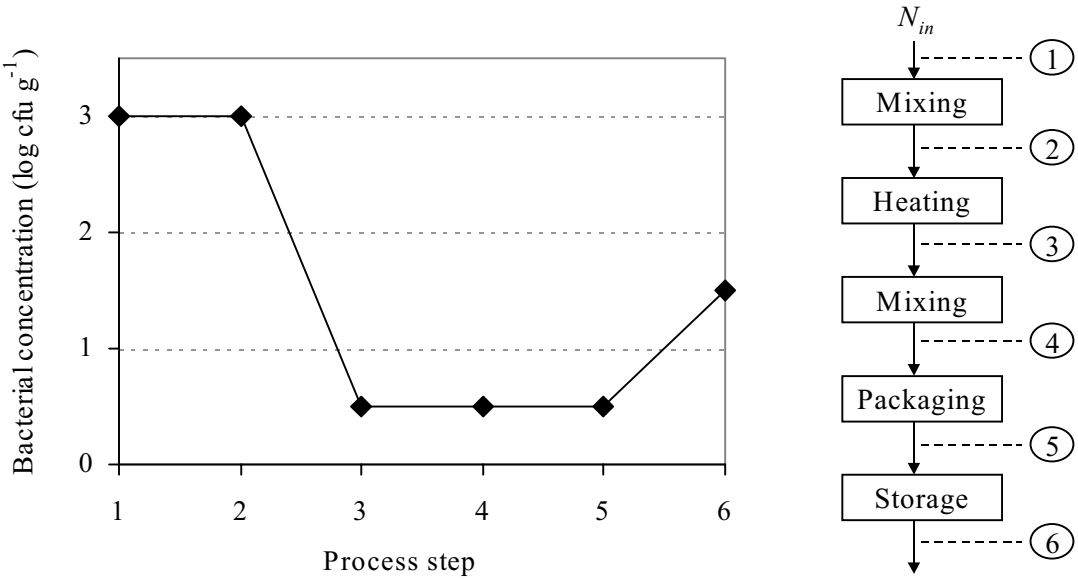

Figure 1. Process evaluation of an imaginary production process.

Most MRA studies indeed use a farm-to-fork approach taking into account all process steps from the ingredients to the final product [17, 139]. Usually, only growth or inactivation in the different process steps is considered and introduction of bacteria in the production process is not taken into account. However, when pathogens re-enter the product after an inactivation step, this can cause foodborne illness. Indeed, such recontamination has been reported as a source of food spoilage and food infections [37, 47, 55, 117]. A survey performed by WHO [140] revealed that 25% of the outbreaks in Europe were related to recontamination. It is therefore relevant to quantify recontamination so that it can be incorporated in MRA.

4. Recontamination

Recontamination can occur via the factory environment or by addition of contaminated ingredients after an inactivation step. The latter route can relatively easily be incorporated in a process evaluation. Therefore, in this thesis only recontamination via the factory environment is considered. There are several recontamination routes through which bacteria can re-enter the product. One of the routes is via aerial transfer. Bacteria can be present on floors or equipment or in drains in a factory environment. When the factory is cleaned with high-pressure hoses, aerosols are produced which consist of droplets of water vapour in the air. In this way bacteria can be transferred from the surface into the air. Due to sedimentation, the bacteria can be deposited on the products that are exposed to the factory air. A schematic picture of recontamination via aerosols is given in figure 2. Apart from aerosol formation, bacteria can be transferred through the air attached to dust or skin particles.

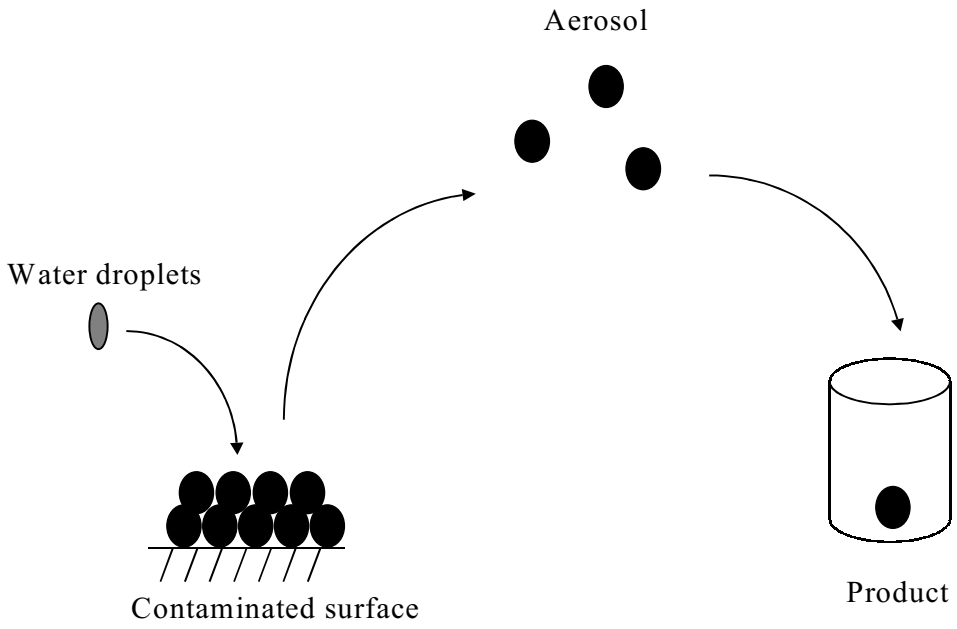

Figure 2. Recontamination via aerosols. A contaminated surface is sprayed with water causing aerosol formation in which pathogens can travel through the air. Due to sedimentation the bacteria can end up in the final product.

Given the labour-intensive production process, ready-to-eat meals are vulnerable for manual contact [47, 61], which is another source of recontamination. When contaminated hands contact the product, pathogens may be introduced into the product.
A product can also be contaminated due to contact with a contaminated surface. This is usually an important source of recontamination for poultry and dairy products [95, 117]. In the meat industry, products may come into contact with contaminated cutting boards, knifes, a slicing machine etc. In poultry processing, for example, bacteria adhere to defeathering and evisceration equipment and thus cause cross contamination on carcasses passing through the equipment [96].
In for example the dairy industry, product contamination can occur due to biofilm formation inside heat exchangers, tanks or on the wall of pipelines. A biofilm consists of layers of bacteria that have attached to the surface together with their extracellular products (see figure 3). Bacteria present in a product flow can attach to the wall due to for example van der Waals forces and electrostatic interactions. When they start producing extracellular products, usually polysaccharides, these act as anchors between the bacteria and the wall causing irreversible attachment to the wall. The formation of such biofilms protects the bacteria from hostile environments, and thus they are much more resistant against detergents and disinfectants. When bacteria are released from the surface, they can cause food spoilage or foodborne illnesses if pathogenic bacteria are present [68].

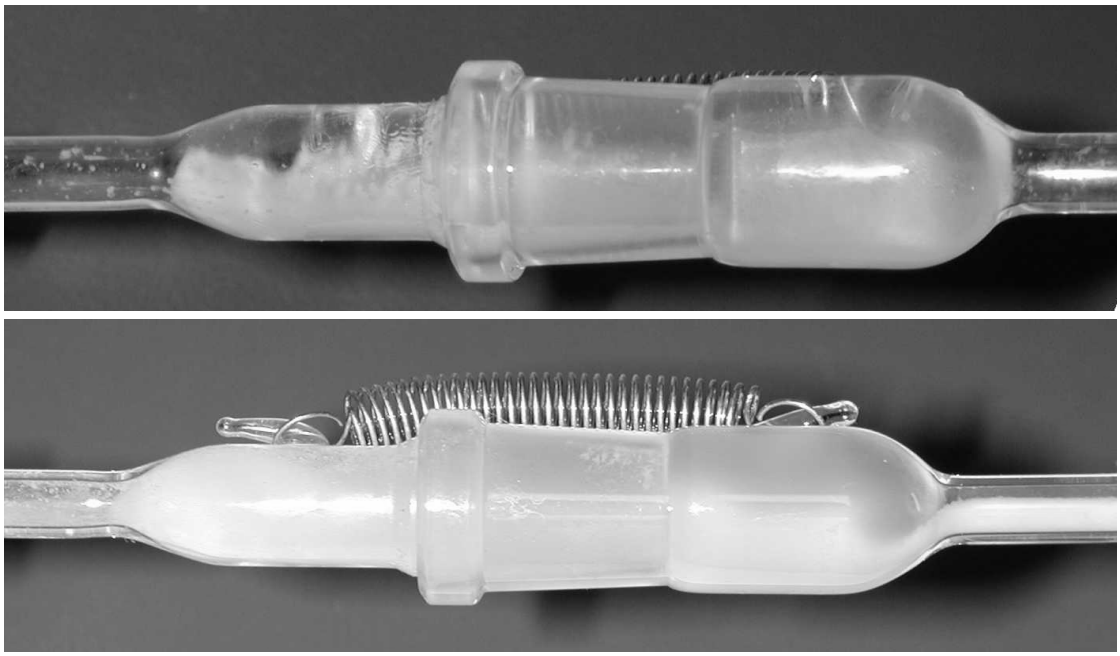

Figure 3. Biofilm formation in a glass connection after 48h and 216h.

5. Objective of this thesis

Although recontamination is an important source causing foodborne illness, it is usually not included in MRA at present due to the lack of quantitative insight. The objective of this thesis is therefore to quantify recontamination using predictive modelling techniques so that it can be used as an element in exposure assessment. The aim is to develop models that contain as few parameters as possible so that they can easily be applied in food process evaluations. For this purpose, two recontamination routes were further investigated: recontamination through biofilm formation and recontamination via aerial transfer.

Once recontamination is quantified, its importance can be determined in an overall risk assessment by comparing this recontamination factor to other contamination sources and possibilities for growth or inactivation in the production process. When all factors that can influence food safety are incorporated in an MRA, this will give a better estimate of the probability of becoming ill after consuming a food product.

6. Outline of this thesis

Several predictive models have been presented in literature that quantify one of the different recontamination routes. **Chapter 2** gives a review of available models that can be used to quantify recontamination. The applicability of the models for the food industry is discussed and a generic model framework is proposed that can be used to quantify recontamination. **Chapter 3** describes a route towards quantification of recontamination via biofilms. A model is developed that describes the biofilm formation process, based on mass balances. The

outcome of this model is a single value or a 'point estimate'. The parameters for the model are obtained in biofilm experiments with *Staphylococcus aureus* on silicon rubber tubing under several flow conditions. In **Chapter 4** another recontamination route is quantified: recontamination via the air. Data were gathered on the number of micro-organisms present in the air and the settling velocity of the micro-organisms. These were described using stochastic distributions and were used as input parameters in a model to assess the effect of airborne exposure for three example products.

As described previously, in the third step of MRA, the production process is evaluated to determine the effect of different process steps on the level of micro-organisms in the product. **Chapter 5** shows that the same approach can be applied for other parameters than for micro-organisms. The effect of process steps on the final quality of potato products was assessed with regard to salt concentration. This demonstrates that a chemical exposure assessment is analogous to a microbiological one in many aspects.

Chapter 6 describes a microbial risk assessment in relation to recontamination. The developed biofilm and aerial contamination model are applied in an example production process to demonstrate how the models can be incorporated in an MRA. For the airborne contamination model, the outcome of the exposure assessment is coupled to a dose-response relationship. This results in an estimate of the probability of becoming ill after eating a product that is contaminated via the air. Furthermore, possibilities for future research are discussed with regard to quantifying recontamination and improving food safety.

2

Quantifying recontamination through factory environments-a review

Esther D. den Aantrekker, Remko M. Boom, Marcel H. Zwietering, Mick van Schothorst

Abstract

Recontamination of food products can be the origin of foodborne illnesses and should therefore be included in quantitative microbial risk assessment studies. In order to do this, recontamination should be quantified using predictive models. This paper gives an overview of the relevant modelling approaches that are available in literature to quantify recontamination via factory environment. Different recontamination routes are described: recontamination via air, via processing equipment or via manual contact. Unfortunately, not many available models are directly applicable to the food industry; most models are developed for aquatic or environmental systems. Finally, a general systematic approach is proposed for modelling contamination from surfaces via air, hands or liquid into the product and ranges for the parameters are given.

Accepted in the International Journal of Food Microbiology

1. Introduction

Food has to meet high standards regarding food safety and food quality. GMP (Good Manufacturing Practices) and HACCP (Hazard Analysis Critical Control Points) systems are applied to improve the microbial quality of food. However, even with the best control measures in place, a food product may still pose a risk to the consumer. In order to quantify this risk, quantitative microbial risk assessment (MRA) can be implemented [98]. MRA consists of four stages: (1) hazard identification (the identification of biological agents that are capable of causing adverse health effects and that may be present in a particular food or group of foods), (2) hazard characterisation (the evaluation of the nature of the adverse effects associated with biological agents that may be present in food), (3) exposure assessment (the evaluation of the likely intake of the biological agent via food) and (4) risk characterisation (the estimation of the probability of occurrence and severity of known or potential adverse health effects in a given population based on the previously mentioned hazard identification, hazard characterisation and exposure assessment) [70].

In the third stage of MRA, the exposure assessment, all factors affecting the presence and numbers of micro-organisms up to the point of consumption should be considered. This includes the source, frequency and level of contamination at any point of the food chain [70]. Most MRA studies indeed use a farm-to-fork approach taking into account all process steps from the ingredients to the final product [17, 139]. However, recontamination of food products is often not considered. Since food poisoning outbreaks are often caused by recontamination [37, 47, 55, 117], this factor should not be ignored in an MRA study.

In this paper, recontamination is defined as the introduction of pathogens into the product after an inactivation step via the factory environment. Since only the factory environment is considered here, the addition of contaminated ingredients after an inactivation is not included. Recontamination of products occurs via direct or indirect contact of environmental vectors with the product. Direct contact occurs when the product comes into contact with surfaces or hands containing bacteria. Indirect contact can be caused for example by contamination via the air.

It depends on the type of product or process which recontamination route is the most important. Given the labour-intensive production process, ready-to-eat meals are more vulnerable for manual contact [47, 61] and surface contact [37, 95, 117]. Poultry and dairy products are found more vulnerable for surface contact [95, 117]. Air contamination is more important for products that are exposed to air or use air for food preparation like ice cream and instant powders [65]. These conclusions are mainly based on reported sources of foodborne illness and expert knowledge. When recontamination is incorporated in MRA, the importance of this factor can be assessed more quantitatively by performing a sensitivity analysis [150] or a rank correlation [18].

A limited number of studies did include recontamination in their risk assessment study. Jacobs et al. [61] did an MRA study only on recontamination. They investigated the risk of

foodborne infection due to handling of foods by food service workers. Mossel et al. [88] determined the probability of recontamination by multiplying the number of bacteria in the environment with a certain transfer factor describing the transfer velocity between environment and product stream. Van Gerwen et al. [130] included recontamination in their structured method for MRA. In their MRA study on cheese spread, recontamination was found to be an important factor affecting food safety of the product. McNab [85] also included recontamination in his framework of MRA. Van Gerwen [130] and McNab [85], however, did not mention the source of recontamination and only made an estimation of the probability of overall recontamination.

In order to use a more quantitative approach to describe recontamination, predictive modelling techniques can be used. Different types of models are available in predictive microbiology. Polynomial, empirical models are easy to use and no detailed knowledge of the process is needed. The disadvantage of this type of models is that they do not contribute to the knowledge of the underlying process and need many parameters to describe the data. Furthermore, an extensive and systematic data set is needed to obtain the right parameters for the model. Other empirical models often need less parameters, but (like the polynomial models) can only be used for the range of experimental conditions that are covered in the original data set. Mechanistic models are based on fundamental physical principles and therefore give more insight into the process. However, like the polynomial models, the mechanistic models often also contain many parameters and still can describe only a limited range of conditions [149].
As input parameters for the different models, one can use point estimates (like average or worst-case values) or probability distributions [126]. MRA studies often use Monte Carlo simulations based on probability density functions (PDFs) as input parameters. The advantage of the use of PDFs is that both variability (random effects of chance) and uncertainty (lack of precise knowledge) of the parameters can be taken into account [133]. Therefore, it gives a more realistic description of the actual situation.

This review gives a summary of predictive models that can be used to describe and quantify recontamination. The following sections describe the different recontamination routes and models separately. Finally, an attempt is made to incorporate the models in an overall approach that can be used as a general framework to quantitatively describe recontamination.

2. Recontamination through equipment

When bacteria attach to a surface they can form biofilms, which consist of bacteria and their extracellular products. Bacteria in such a biofilm are more resistant to cleaning and disinfection, which makes it more difficult to remove these attached bacteria from food

production systems than free living cells. Biofilms can then cause recontamination of products when bacteria detach from the biofilm and end up in the final product.
Biofilms are formed in several steps (figure 1). First, nutrients adhere to the contact surfaces, providing a conditioning of the surface. This conditioning film is, however, not always necessary for the second step of the process: adhesion of cells. The bacteria are first reversibly attached, meaning that there are weak interactions between the bacterial cell and the surface. The bacteria can still be removed easily from the surface by rinsing. However, after an induction period, the bacteria start to produce extracellular polymeric substances (EPS). These EPS allow bacteria to firmly attach to the surface causing an irreversible attachment. In this phase, much stronger forces are necessary to remove the biofilm (like scraping or scrubbing). During and after the attachment process, the bacteria start to multiply and the biofilm increases in thickness. As the biofilm ages, the attached cells can be detached individually or sloughed off in large clumps of cells by the product in contact with the surface and thus recontaminating the product [68].

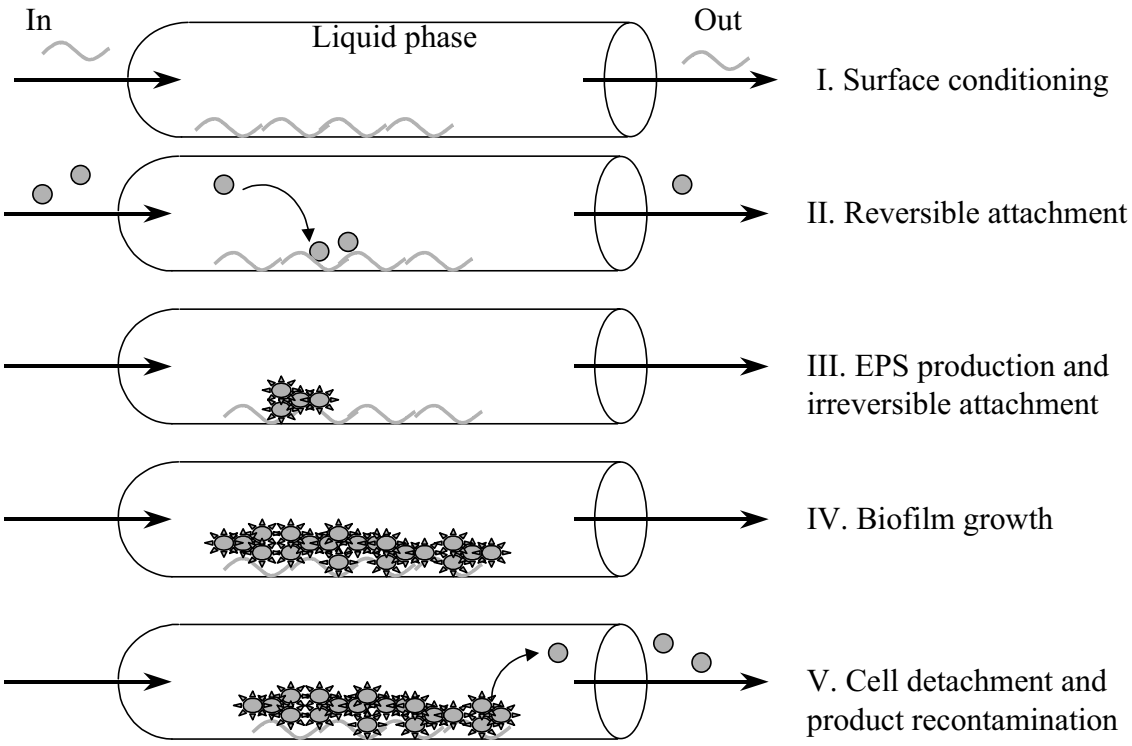

Figure 1. Biofilm process in a pipeline. First the surface is conditioned with nutrients flowing into the pipeline. Then bacteria attach to the conditioned surface and start to produce extracellular polysaccharides (EPS), which causes an irreversible attachment. The biofilm increases and cells detach again, causing recontamination.

Since biofilms can cause recontamination of food products leading to food spoilage or even foodborne illnesses, the formation of biofilms in food processing systems is not desired [68]. However, in aquatic systems biofilms are widely utilised in biofilm reactors, e.g. for the treatment of wastewater. Therefore, most models describing biofilm formation are developed for aquatic systems describing biofilm formation in reactors or pipelines. Because of their application in the wastewater treatment, these biofilms are much further developed than the ones found in the food industry.

Depending on the purpose of modelling biofilm formation, one dimensional, two or three dimensional models can be used [87]. Figure 2 depicts the spatial structure of the biofilm that is described in a 1D, 2D or 3D model.

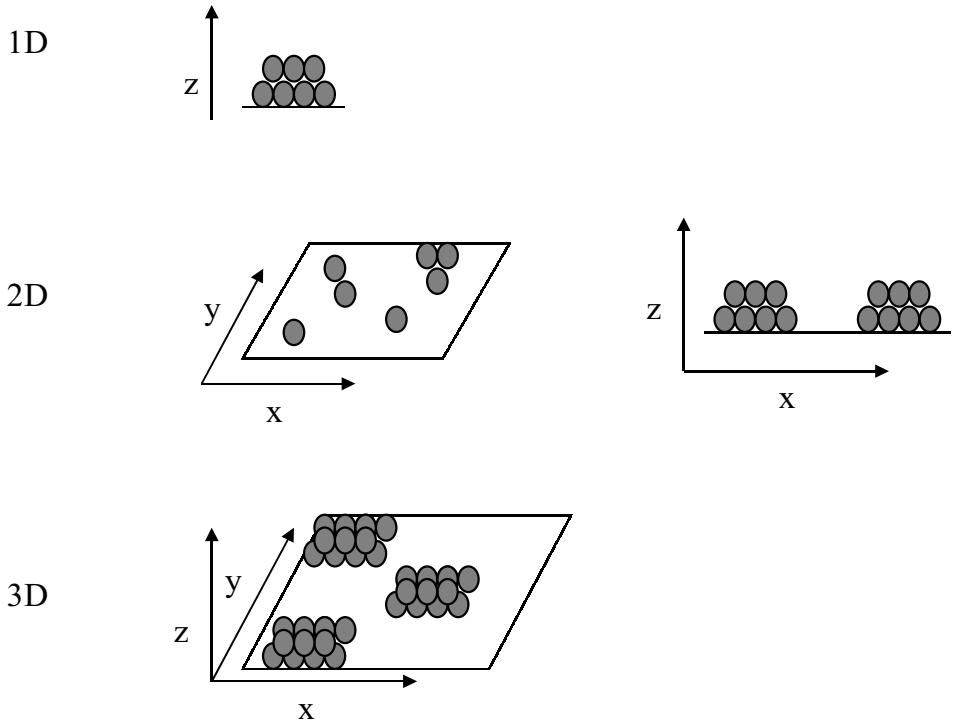

Figure 2. Spatial distribution of cells along a surface for 1D, 2D and 3D models.

Most biofilm models describe biofilms as uniform films containing a single type of organism, often only described in one spatial dimension. Those 1D models are usually a mixture of mechanistic and empirical models. They include a mechanistic basis, which basically consists of a set of differential equations describing attachment, growth and detachment of cells, but they may also include purely empirical expressions, for example to describe biofilm growth [136]. An example of a general 1D model based on substrate consumption is given by Characklis [20].

Substrate balance:

$$V\frac{\mathrm{d}S}{\mathrm{d}t} = \phi(S_0 - S) - r_S A - \frac{(\mu - m)XV}{Y_{XS}} \quad (1)$$

Liquid phase balance:

$$V\frac{\mathrm{d}X}{\mathrm{d}t} = \phi(X_o - X) + \mu VX - r_A A + r_D A \quad (2)$$

Biofilm balance:

$$\frac{\mathrm{d}B}{\mathrm{d}t} = r_S A Y_{BS} + r_A A - r_D A - r_E B \quad (3)$$

with A: wetted surface area (m^2)
B: biofilm mass (kg)
r_A: rate of suspended biomass attachment onto the biofilm (kg $m^{-2}h^{-1}$)
r_D: rate of biofilm detachment (kg $m^{-2}h^{-1}$)
r_E: rate of biofilm decay (e.g., lysis, endogenous respiration) (h^{-1})
r_S: substrate flux into the biofilm (kg $m^{-2}h^{-1}$)
m: maintenance coefficient (h^{-1})
S (S_0): (input) substrate concentration (kg m^{-3})
t: time (h)
V: volume (m^3)
X (X_0): (input) suspended biomass concentration (kg m^{-3})
Y_{BS}: yield coefficient for biofilm on substrate (kg biofilm/kg substrate)
Y_{XS}: yield coefficient for suspended biomass on substrate (kg biomass/kg substrate)
ϕ: flow rate ($m^3 h^{-1}$)
μ: specific growth rate of suspended biomass (h^{-1})

Such models can be expanded with the introduction of EPS production [5] or O_2 consumption and transport [91, 121].

In the model described above (equations 1 to 3), growth is described semi-empirically using Monod kinetics. There are several empirical relations to describe the detachment rate (r_D), incorporating different factors. Detachment was found to be dependent on the density and thickness of the biofilm with different power laws, describing the non-linear behaviour of detachment [123]:

$$r_D = k_D \rho L_B^n \quad (4)$$

with k_D: detachment rate coefficient ($m^{1-n} h^{-1}$)
ρ: biofilm density (kg biomass m^{-3})
L_B: biofilm thickness (m)
n: power (-)

The unity of the detachment rate coefficient (k_D) depends on the type of model used and on the power factors applied.
De Jong et al. [30] incorporated the growth rate in their detachment model. Another factor that can be incorporated in the detachment model is shear stress resulting in e.g.:

$$r_D = k_D \rho \tau^n \quad (5)$$

with τ is the fluid shear stress (N m^{-2})

Equation 4 and 5 can be applied with different power factors (n) with typical values between 0.5 and 2 [123].
Dickinson and Cooper [33] developed a model in which detachment obeys an Arrhenius relation in which the cells need to overcome a certain adhesion energy to detach. Variation in this adhesion energy results from probabilistic variations in the state of adhesion. Therefore, the input parameters of the model follow a probability distribution. Another stochastic model is presented by Stewart [123] assuming that every cell has a certain probability of detachment from the biofilm. This model is presented as:

$$r_D = F_D (L_B - z_D) A_p \rho \quad (6)$$

with F_D: overall frequency of detachment events per unit area (m^{-2}h^{-1})
z_D: biofilm thickness after detachment ((L_B-z_D) is size of detached particle) (m)
A_p: particle area (m^2)

This model is the basis for many empirical equations (like equations 4 and 5).
Since there are not many experimental detachment rate data to verify the different models, it is difficult to determine which model gives the best description of detachment [123].

Another biofilm model (different from equations 1 to 3) is described by Belkhadir et al. [8] and is based on the concept that a biofilm consists of an active and an inactive layer. This inactive layer is developed at the inner side of the biofilm due to substrate and O_2 supply limitations and accumulation of toxic compounds.
Some models are specifically developed to describe the operation of a specific reactor type. Bakke et al. [5] described a model to determine biofilm formation in an annular reactor.
Recontamination of drinking water was described by Dahi and Thøgerson [27], assuming that the biofilm and liquid phase are in steady state condition. The increase in biomass in the liquid phase due to growth and detachment of cells for a distance dl in a pipeline can be described by:

$$\frac{\mathrm{d}N}{\mathrm{d}l} = \frac{\mu}{v} N + \frac{2}{v R_p} k_D \quad (7)$$

with N: bacterial density in liquid phase (cfu m^{-3})
l: positional axial co-ordinate (m)
μ: specific growth rate (h^{-1})
v: flow velocity (m h^{-1})
R_p: radius of the pipe (m)
k_D: detachment rate coefficient (cfu $m^{-2}h^{-1}$)

The models mentioned above are mainly single species models. Wanner and Gujer [137] developed a mixed-culture multi-substrate biofilm model, which described the spatial distribution and development in time of particulate components such as microbial species, EPS etc. A computer model, AQUASIM, was developed to solve the differential equations [136]. The liquid phase was not included, it only considered the biofilm itself. Therefore, this model is less applicable to describe recontamination during food processing. Clement et al. [22] did include a description of the liquid phase. They developed a model to describe the change in biomass in both biofilm and liquid phase in time and in place. The model includes diffusion of substrates into the biofilm perpendicular to the surface, using Fick's second law of diffusion.

Although most biofilm models are based on the assumption that biofilms form a uniform layer on the surface, in reality this will not happen. Therefore, 2D and 3D models were developed describing biofilm formation not only perpendicular to the surface but also in other directions. Lu et al. [78] developed a biofilm model in 2 spatial dimensions in order to describe microbial behaviour in drinking water systems. They only described the change in biomass in the liquid phase, assuming that the biofilm was in steady state. Biomass concentration in the pipeline depended on the place in the pipeline but also on the detachment of cells from the biofilm, which was influenced by the radial distance of the cells. This model used 13 differential equations with 64 parameters to describe simultaneous transport of biomass, substrate, NH_4-N, NO_x-N, O_2, alkaline substances and Cl. Since this model assumed steady state conditions, the time factor was ignored, which makes this model less applicable for quantification of recontamination. Furthermore, this model is far too complicated and detailed to use for the evaluation of the risk of recontamination.
Richter et al. [111] used a different approach to describe biofilm formation in place. They used Monte Carlo simulations, based on the probability that a micro-organism will grow or move to a certain place. This model only focused on the spatial distribution of a biofilm and not on changes in the liquid phase.
Apart from 2D models, there are 3D models that describe biofilm formation in time and in three spatial dimensions. Picioreanu et al. [100] developed a model based on relations describing diffusion of substrate in the biofilm in x, y and z-direction. Growth in the biofilm was modelled using cellular automata with if/then statements. The liquid phase was not

included. The same approach was used by Noguera et al. [94], who also used grid cells to model growth. When the number of bacteria reach a certain value they are moved to neighbouring elements.
Such models can be used to better understand the mechanism of biofilm development and detachment. For example, it can be used to describe the effect of different Reynolds numbers on the shape of a biofilm [101] or to investigate which circumstances promote detachment (causing recontamination). This knowledge can be applied to prevent biofilm formation or detachment by cleaning more often or change flow velocities etc.

Although these 2D and 3D models give more morphological and geometrical details than 1D models and give more insight into the biofilm process, they are less suitable for practical applications. Biofilm models should only include those processes that are important for the purpose of the model with as little parameters as necessary [87]. For the food industry, the detachment rate is the most important factor for predicting the number of cells in the liquid. Since detachment is a result of the complete biofilm formation process, the attachment and growth factor should also be taken into account in a recontamination model. In order to estimate the probability of recontamination, these 3 factors (attachment, growth and detachment) should be averaged over a large contact area. Then, spatial details largely disappear in the overall numbers [136].
Since in the food industry, biofilm substrate and O_2 consumption rates are largely unknown, models based on this concept are less useful. Furthermore, since production lines are cleaned regularly, the time for biofilm formation may be limited. For the food industry, biofilms are therefore more associated with the attachment and growth of micro-organisms on surfaces rather than the development of thick biological films over time [53]. Oxygen and nutrient gradients are in this case less important than in wastewater treatment systems. However, the modelling approach used in aquatic systems, based on mass balances, could be applied to describe biofilm formation and detachment in food factories. De Jong et al. [30] developed such a model and implemented it in an expert system: NIZO-PCS. This computer program can simulate bacterial attachment, growth and detachment in dairy factories and mainly consists of 2 mass balances. The desorption factor is in this case dependent on the growth rate in the biofilm, meaning that cells are only released when the biofilm is growing.

Biofilm balance:

$$\frac{dC_B}{dt} = \mu C_B\left(1 - k_D\right) + k_A X \tag{8}$$

Liquid phase balance (for a tank reactor):

$$V\frac{dX}{dt} = \phi\left(X_0 - X\right) + \left(\mu - k_I\right)VX - k_A AX + k_D \mu A C_B \tag{9}$$

with A: surface area (m^2)
C_B: biofilm concentration (cfu m^{-2})
k_A: adsorption coefficient (m h^{-1})
k_D: fraction of cells detached from surface (-)
k_I: destruction constant (h^{-1})
$X(X_0)$: (input) biomass concentration (cfu m^{-3})
V: tank volume (m^3)
ϕ: flow rate (m^3 h^{-1})
μ: specific growth rate (h^{-1})

Since the model was developed to describe attachment in heat exchangers it contains a destruction constant (k_I) describing the inactivation of bacteria due to high temperatures.
Zwietering and Hasting [148] also used mass balances to describe growth and exchange between dead spaces and the bulk product flow. Although their system describes transfer in 2 liquid phases, instead of transfer between a solid and liquid phase, as described in equations 8 and 9, the approach is comparable.

3. Recontamination via the air

Contamination of products via air can occur through dust particles ('dry' air) or via aerosols. Aerosols are for instance formed when contaminated floors or drains are sprayed with high-pressure jets, resulting in the formation of droplets that can be suspended in the air.
There are only a few models that describe recontamination of food products via the air. Radmore et al. [106] found an empirical, quadratic relationship between the number of bacteria present in the air and the number of bacteria found in contaminated products. When the concentration in the air increases linearly, the concentration in the product increases quadratically. Contamination via the air can also be described using the settling velocity of particles. The level of recontamination is then given by [141]:

$$L_c = v_s C_{air} A t \qquad (10)$$

with A: exposed product area (m^2)
C_{air}: number of cells in the air (cfu m^{-3})
L_c: contamination level (cfu/product)
t: exposure time (h)
v_s: settling velocity (m h^{-1})

This contamination level (L_c) gives the number of bacteria that enter the product via the air. A L_c of 10^{-3} then means that one out of 10^3 products is contaminated with one cell. The settling velocity (v_s) can be calculated by dividing the rate of sedimentation (SR in cfu $m^{-2}h^{-1}$) by the number of cells in the air (C_{air} in cfu m^{-3}). The latter can be measured using air samplers and

the sedimentation rate can be measured by exposing petri dishes to the air for a certain period of time. Whyte [141] proved that gravitational forces were dominant under different air movement situations. Horizontal airflows can therefore be neglected. Vertical airflows were not considered in this study. However, it is unlikely that airflows are unidirectional, since flows are usually obstructed by machinery or people causing stagnant areas in which gravitation plays an important role again [141].
The model proposed by Whyte [141] assumes a linear relationship between the number of cells in the product and the concentration of bacteria in the air. This is therefore in contrast with the empirical, quadratic relationship found by Radmore et al. [106]. Whyte [141] validated his model by filling different sized bottles with sterile liquid. His model gave a good description of the actual contamination rate of the different bottles, suggesting that the assumption of a linear relationship is justified. The data Radmore et al. [106] used for their model have a large variation. Therefore, it is difficult to determine whether the relationship between the number of cells in the product and the concentration in the air is linear or quadratic.

A different approach to describe airborne contamination can be found in phytopathology. Pielaat and van den Bosch [104] studied the distribution of spores during a rain event. Spores of pathogens can be present on plant leafs. When it starts raining, a layer of water is formed on the leafs. A droplet can then result in splashing of the spores from the leafs to another location. This mechanism is basically the same as the contamination of food products via aerosols that are formed by spraying contaminated floors. A schematic picture is given in figure 3.

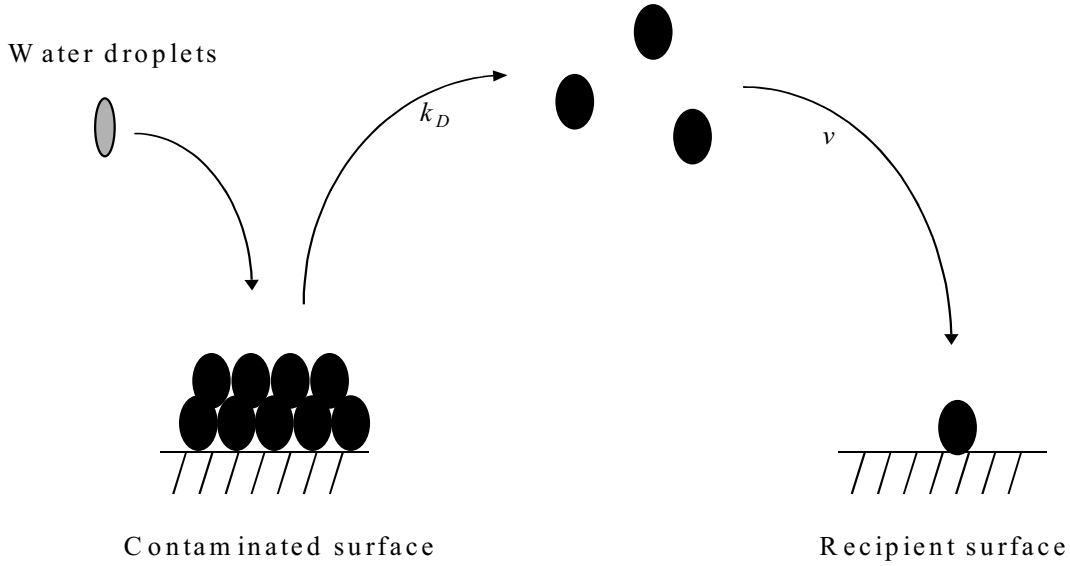

Figure 3. Removal of bacteria from a surface. When water hits a contaminated surface, bacteria will be removed to the air and will be deposited to another surface (in case of vegetation) or into a product (in food industry). k_D is the detachment rate and v is the sedimentation rate.

Pielaat and van den Bosch [104] used a stochastic model to describe the probability per unit length of finding a spore at position x at time t. This probability depends on the probability that a spore will be splashed ('desorbed') from a certain place and the probability that a spore will move from place q to place x. Therefore, the model not only depends on time but also on location:

$$\frac{\partial P(t,x)}{\partial t} = -k_D P(t,x) + \int_{-\infty}^{\infty} \varepsilon k_D P(t,q) v(x-q) dq \qquad (11)$$

desorption *displacement*

with k_D: probability per unit time of a spore being removed (h^{-1})
$P(t,x)$: probability per unit length of finding a spore at position x at time t (m^{-1})
$v(x-q)$:probability density function for a spore to move from position q to position x
ε: probability of a spore staying in the process ((1-ε) is a sort of 'loss factor')

During a rain event, spores can be removed from the system by washing off into the soil. Therefore, a factor ε was introduced into equation 11 to indicate that not all spores remain in the process.

Aerial transfer models are also found in environmental studies in which transfer of dioxin-like compounds from the air to vegetation was modelled [35, 45, 77].
The dioxin compounds can be deposited by dry air, wet air (rain) or via aerosols. The concentration of dioxin compounds on vegetation due to dry and wet deposition was described by Lorber et al. [77]:

$$C_{PPA} = \frac{v_D + r_w v_w}{k_w Y} \qquad (12)$$

with C_{PPA}: vegetative concentration due to settling of contaminated particulates onto plant matter (ng kg^{-1})
k_w: weathering dissipation constant ($year^{-1}$)
r_w: retention of wet deposition on plants (-)
v_D: dry deposition rate (ng $m^{-2}year^{-1}$)
v_w: wet deposition rate (ng $m^{-2}year^{-1}$)
Y: crop yield (kg m^{-2})

During rain, the concentration of dioxin compounds on vegetation depends on how well the plant will retain the compounds. Therefore, a retention factor (r_w) was included in the model. Furthermore, weathering processes like wind and rainfall can remove compounds that are deposited on the plant. Therefore, a weathering factor (k_w) was included as well [35].
The dry deposition rate v_D was described as [77]:

$$v_D = C_a v_s I \tag{13}$$

with C_a: concentration of compounds in the air (ng m^{-3})
I: fraction of compounds intercepted by the plant (-)
v_D: dry deposition rate (ng $m^{-2}year^{-1}$)
v_s: settling velocity (m $year^{-1}$)

The concentration of compounds on vegetation due to aerosols was described by [77]:

$$C_{VPA} = \frac{B_{VPA} C_{VA} f}{\rho} \tag{14}$$

with B_{VPA}: air-to-leaf biotransfer factor (-)
[(µg compound/kg plant)/(µg compound/kg air)]
C_{VA}: concentration of compounds in the aerosol (ng m^{-3})
$C_{VPA:}$ vegetative concentration due to settling of contaminated particulates via aerosols onto plant matter (ng kg^{-1})
f: empirical correction factor (-)
ρ: density of air (kg m^{-3})

The environmental model for wet and dry deposition (equation 12 to 14) resembles the food microbiological model (equation 10), since in both cases the concentration of particles in the product or on the vegetation depends on the settling velocity and the concentration of the particles in the air. In the environmental model, of course, weather conditions play an important role resulting in the introduction of additional parameters.

Quantitative risk assessment studies are also applied in environmental studies. Beer and Ricci [7] did a QRA study to estimate the risk of exposure to airborne components. In order to assess exposure, an area in Australia was divided in cells of 1x1 km. The average number of times the concentration of a compound exceeded a reference value was counted. Furthermore, the frequency of exceedances in time was determined. Using these data, an empirical model could be developed in order to predict the exposure of a compound exceeding a reference value.

This section summarised different approaches to model contamination via air. The environmental models deal with the probability of contamination of pollutants via the air, which causes 'infection' of vegetation. Although this is rather different from modelling bacterial contamination via air into food, the same approach might be applied in the food industry, due to the mechanistic analogy between the processes.

4. Recontamination via hands

There are not many models that quantitatively describe contamination of products via manual contact. According to Bloomfield and Scott [12] the risk of foodborne illness due to contact with hands or surfaces depends on the level of contamination and the probability of transfer. The latter was estimated to be 50% in an MRA study to estimate the risk of *Shigella* infection by handling infected laundry [40]. Bacterial transfer via hands was further quantified by Mackintosh and Hoffman [81] who performed experiments to determine transfer from infected cloth via hands to recipient cloth. However, they did not use the obtained transfer rates for incorporation in an MRA study. Chen et al. [21] determined the transfer of *Enterobacter aerogenes* from chicken via hands to lettuce. The experimentally obtained transfer rates were used to obtain frequency histograms. Those were then fitted with frequency distributions using BestFit (Palisade Corp., Newfield, NY). The transfer rates found were mainly lognormally distributed.

The same approach was used to determine the effect of wearing gloves during food preparation [86]. The data from Mackintosh and Hoffman [81] could be treated similarly to quantify hand contamination. The obtained probability density functions can then be used in Monte Carlo simulations to calculate the risk of foodborne illness due to food handling.

Therefore, more experimental data on hand transfer are necessary to reliably quantify the risk of recontamination via hand contact with different food products.

5. Conclusions

Since many foodborne illnesses are caused by recontamination, it is important to study this in more detail. In order to quantify recontamination via biofilms, the whole biofilm process should be considered, meaning that attachment, growth and detachment should be included. This approach was followed by De Jong et al. [30] who included their model in an expert system. The model was validated with data from a whey plant and gave a good correlation. The other biofilm models described in this chapter are based on substrate consumption, which is appropriate for wastewater treatment, but less relevant for the food industry.

There are various models available to quantify air contamination. Most models were developed for air contamination in the environment where weather influences are important [35, 45, 77, 104].

Whyte [141] developed an air contamination model (equation 10), describing transfer from the air to the product, which can be used in the food industry. This model can be combined with the model of Pielaat and van den Bosch [104] in order to describe the complete contamination process (from the floor to the product). Whether this model will then be able to estimate the risk of recontamination via air needs to be validated by comparison with experimental data from food factories. The number of bacteria on the floor and in the air needs to be measured as well as the contamination of the product.

For hand contamination there are not many models described. In this case, Whyte's model [141] for air contamination might be used to describe hand contamination. The number of bacteria on the hand is then multiplied with the transfer from the hand to the product and the time and area that the product is exposed to the hand. The probability density functions (PDFs) as determined by Chen et al. [21] and Montville et al. [86] could then be used as input parameters. The outcome will be a new PDF describing the risk of exposure by hands.

The different recontamination routes are described by different model types. Biofilm models are mainly described by a combination of mechanistic and empirical models. Air models are usually empirical models but in some cases stochastic models are used. For hand transfer only one model was described which was an empirical probabilistic model.
Since there is a large distribution in number of bacteria present on surfaces and also in the amount of transfer, it will be better to use PDFs as input parameters rather than point estimates in either mechanistic or empirical models [126].

The three different routes mentioned in this review can in fact be summarised by the same overall scheme. First, a source is contaminated with bacteria, then cells are released from this source and enter the intermediate phase after which the cells come into contact with the product. This is schematically depicted in figure 4.

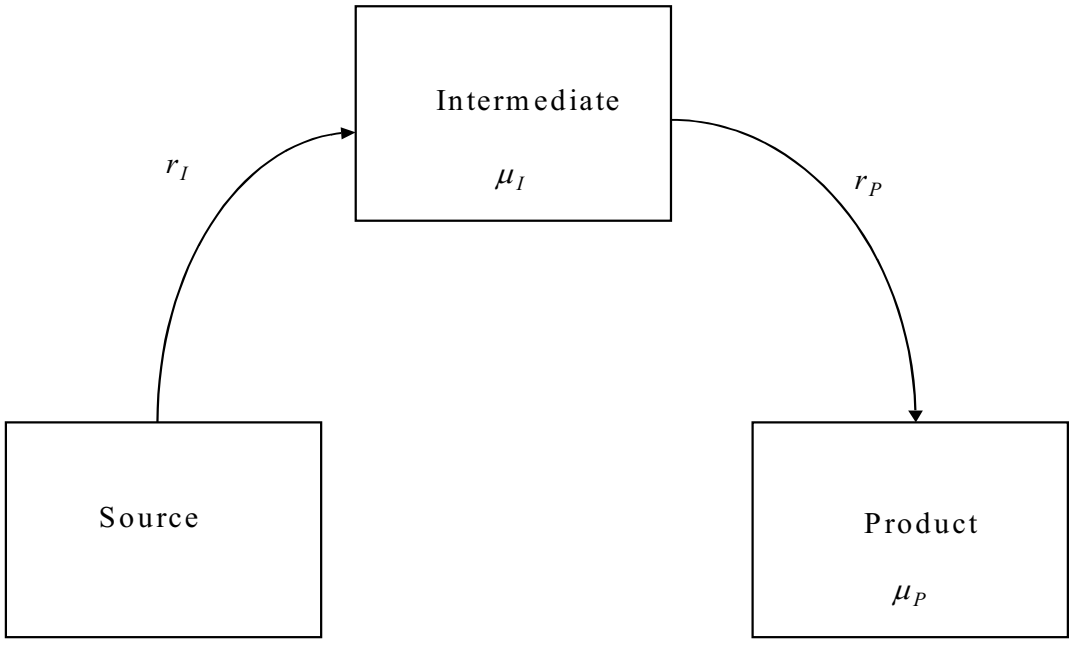

Figure 4. Schematic picture of a general recontamination model. A contaminated source (liquid, equipment or floor) releases cells to the intermediate phase (surface, hands or air). The cells can then be transferred to the product causing recontamination. r_I = transfer to intermediate phase (cfu $m^{-2}h^{-1}$ or cfu $m^{-3}h^{-1}$), r_P = transfer rate to product (cfu $m^{-3}h^{-1}$).

In case of biofilm formation, the source is contaminated liquid flowing into a pipeline. Cells from the liquid can attach to the surface (the intermediate phase) and can then be released to the product passing the contaminated surface.
In case of contamination via the air, the source can be the floor. Cells can be released from the floor e.g. by spraying causing aerosol formation (intermediate phase). The cells can then enter the product via sedimentation.
In case of manual transfer, the source can be contaminated equipment or material. When a person touches the equipment, the cells are transferred from the equipment to the hand (which is then the intermediate phase). By touching the product, the cells are transferred from the hands to the final product.
The general process as depicted in figure 4 can be modelled by describing the number of bacteria that are transferred from the source to the intermediate phase, the growth in the intermediate phase and the transfer from the intermediate phase to the product:

Intermediate phase (biofilm, air or hands):

$$\frac{dC_I}{dt} = r_I - r_P + \mu_I C_I \qquad (15)$$

Product:

$$\frac{dC_P}{dt} = r_P + \mu_p C_p \qquad (16)$$

with C_I: concentration of cells in the intermediate phase (cfu m^{-2} or cfu m^{-3})
C_P: concentration of cells in the product (cfu m^{-3})
r_I: transfer rate to the intermediate phase (cfu $m^{-2}h^{-1}$ or cfu $m^{-3}h^{-1}$)
r_P: transfer rate to the product (cfu $m^{-3}h^{-1}$)
μ_I: specific growth rate in the intermediate phase (h^{-1})
μ_P: specific growth rate in the product (h^{-1})

The transfer rates (r_I and r_P) and growth rates in equation 15 are further specified for the different recontamination routes in table 1. The terms in table 1 are only meant to guide the reader. In order to become practically applicable, they will probably have to be expanded with additional parameters specific for each situation.

Table 1. Description of transfer and growth rates for the intermediate phase (equation 15) for the different recontamination routes[1].

	r_I	r_P	*growth*
Biofilm	$k_I C_L$	$k_P C_S$	$\mu_S C_S$
Air	$\frac{A_S}{V_{air}} k_I C_S$	$\frac{A_P}{V_{air}} k_P C_{air}$	$\mu_{air} C_{air}$
Hands	$\frac{A_S}{A_H} k_I C_S$	$\frac{A_P}{A_H} k_P C_H$	$\mu_H C_H$

r_I = rate of transfer to the intermediate phase (cfu $m^{-2}h^{-1}$ or cfu $m^{-3}h^{-1}$); r_P = rate of transfer to the product (cfu $m^{-3}h^{-1}$); k_I = transfer rate coefficient from source to intermediate (m h^{-1} or h^{-1}); k_P = transfer rate coefficient from intermediate to product (m h^{-1} or h^{-1}); μ = specific growth rate (h^{-1}); A = area (m^2); V = volume (m^3); C = concentration (cfu m^{-2} or cfu m^{-3}). The indices L, S and H stand for liquid, surface and hand respectively.

[1]: Please note that this table only gives an example of transfer rates for a simple recontamination model. Actual use of the model may necessitate the inclusion of additional factors (e.g. shear rate in r_P) or powers (e.g. $k_P C_S^n$ for r_P).

Since different articles use different models to describe transfer via biofilms, air or liquid, it is difficult to quantify the transfer rate coefficients (k_I and k_P) and growth rates. Those articles that used the same unity in the transfer rates as in table 1 were used to obtain orders of magnitude for the transfer rates of the different recontamination routes. The different transfer and growth rates are given in table 2. Table 3 then gives a summarised range of values for all the transfer and growth rates found.

Table 2. Reported values of the transfer and growth rates for the different recontamination routes.

	k_I	k_P	μ_I	References
Biofilm	(m h^{-1})	(h^{-1})	(h^{-1})	
	4.7E-4-2.2E-3	0-0.32	0-0.51	[90]
	9.0E-5-1.8E-3	0.09	0.2-0.33	[89]
	4.8E-6-3.0E-4	1E-3-1E2		[33]
	2.3E-4			[30]
		0.119-0.198	0.119-0.198	[5]
		0.001-0.1	0.01-0.2	[101]
		4.32-27.7	0.7-0.96	[105]
		0.013-0.3		[22]
		0.067-0.31		[19]
			2.5	[27]
			0.024-0.054	[82]
Air	(h^{-1})	(m h^{-1})	(h^{-1})	
		17.5-175		[71]
		10.8		[26]
Hands	(h^{-1})	(h^{-1})	(h^{-1})	
	0.025-6	40.8-206.4		[81]
		0.0018-60		[21]

k_I is transfer rate coefficient from source to intermediate (m h^{-1} or h^{-1}); k_P is transfer rate coefficient from intermediate to product (m h^{-1} or h^{-1}); μ_I is specific growth rate in the intermediate phase(h^{-1})

Table 3. Summarised range of transfer and growth rates for the different recontamination routes based on the values in table 2.

	k_I	k_P	μ_I
Biofilm	0.00001–0.001 m h^{-1}	0.001–100 h^{-1}	0.01-2.5 h^{-1}
Air	-	10-200 m h^{-1}	-
Hands	0.01–10 h^{-1}	0.001–200 h^{-1}	-

k_I is transfer rate coefficient from source to intermediate (m h^{-1} or h^{-1}); k_P is transfer rate coefficient from intermediate to product (m h^{-1} or h^{-1}); μ_I is specific growth rate in the intermediate phase (h^{-1}); - no data available

For biofilms it can be seen that the growth rate and desorption rate vary around the same values. In case of recontamination via air, the transfer rate from the surface to the air (k_I) is usually not mentioned. The transfer rate from the air to the product (k_P) was calculated by dividing the sedimentation rate (cfu $m^{-2}h^{-1}$) by the concentration of bacteria in the air (cfu m^{-3}) for data from Langeveld et al. [71].
For hands, the transfer rates k_I and k_P are usually given in percentages per contact event. k_I is then between 0.007 and 100% and the transfer from hands to the product (k_P) is between 0.001 and 86% [21, 40, 81, 86]. Some of these articles [21, 81] did mention the time period for transfer, which can then be used to calculate the transfer rates in h^{-1}. When the percentages are compared, k_I and k_P are in the same order of magnitude. When the time factor is included, it seems that the transfer from hands to the product (k_P) is faster than from surfaces to hands (k_I).
Both for hand and for air transfer no values for growth rates are given. However, since the circumstances for growth are not favourable in the air, it can be assumed that growth in the air is negligible. Mackintosh and Hoffman [81] investigated the survival of different microbial strains on hands and found a survival rate between 0.59 and 62%, 5 minutes after contamination. Furthermore, hands are washed frequently causing a 2.5 to 4.5 log reduction of cells [81]. This suggests that growth on hands can also be neglected. However, more research is needed to confirm this hypothesis.

It is necessary to obtain more data on the transfer rates of the different recontamination routes in order to compare the different processes better. Those values can then be used in the general model as described in equations 15 and 16 and table 1. This general model could be used in MRA studies to estimate the recontamination frequency and assess the relative importance of the various phenomena. Including recontamination in MRA studies can indicate which routes (via air, biofilms or liquid) are the most important for a certain production process and should therefore be controlled to maintain product quality and safety.

3

A model for biofilm formation relevant to the food industry

Esther D. den Aantrekker, Wouter W. Vernooij, Martine W. Reij, Marcel H. Zwietering, Rijkelt R. Beumer, Mick van Schothorst, Remko M. Boom

Abstract

Bacteria that attach to the inner walls of process equipment can cause recontamination of food products. In order to quantify this recontamination, a one-dimensional biofilm model was developed based on mass balances. The parameters of the model were obtained in biofilm experiments in which both biofilm formation and the release of cells into the flowing liquid were measured in time for up to nine days. Staphylococcus aureus *was chosen as a model pathogen and silicon tubing was used as testing material. The experiments were performed in duplicate for different flow conditions (Reynolds = 3.2, 32 and 170). It was found that at higher Reynolds (Re) number, the biofilm developed faster, probably due to an increase in transfer of nutrients to the surface. The number of detached cells into the liquid increased accordingly. At the highest Re number, the growth rate in the biofilm approximated the growth rate of free living cells.*

Using the specific growth rate in the biofilm and the desorption coefficient as fit parameters, the proposed biofilm model was capable of describing the obtained data for the three different flow conditions.

Submitted for publication

1. Introduction

Bacteria can adsorb reversibly to surfaces as a result of (amongst others) van der Waals forces and electrostatic interactions. When adsorbed, the cells are still readily removed by mild rinsing. Bacteria can also adsorb irreversibly by producing extracellular products, usually polysaccharides that act as anchors between the bacteria and the surface. Such layers of bacteria and their extracellular products are called biofilms [56]. Biofilms can be found in all sorts of environments: bridges, rocks, teeth, ship hulls, kitchen sinks etc. [95]. They may have a positive or a negative effect on the environment. An example of a positive effect can be found in wastewater treatment, where biofilms are used to remove organic and inorganic compounds from wastewater. Another example is the production of vinegar. Here, biofilms are grown on wood chips, which is an efficient way to produce vinegar [56].

However, the formation of biofilms can also cause problems. In the food industry, biofilms may be formed in pipelines and cause corrosion. Furthermore, the formation of biofilms protects the bacteria from hostile conditions, and thus they are much more resistant against detergents and disinfectants [95]. This can cause premature spoilage of products or even health risks when food spoilage or pathogenic micro-organisms attach to a food contact surface and (re)contaminate the product [56].

In order to quantify this recontamination, the biofilm process can be described using mathematical models. Such biofilm models have been presented before [20], but these are mainly designed for aquatic systems for which the focus is on substrate and/or oxygen consumption and where the biofilm is well developed and mature. In the food processing industry, however, biofilms will be much thinner due to regular cleaning of the equipment. Further, the substrate consumption is usually unknown and much smaller. Therefore, models based on this concept are less useful for the food industry.

The aim of this paper is thus to develop a simple biofilm model with as few parameters as possible, that can be used to quantify recontamination in the food industry. The values of the model parameters are obtained in biofilm experiments following both biofilm and liquid counts for several days. Experiments are performed under different flow conditions using *Staphylococcus aureus* as model pathogen, capable of biofilm formation [39, 74, 96]. Silicon rubber is used as a test surface both for practical reasons and for its high adsorption properties, since *S. aureus* usually attaches better to hydrophobic than to hydrophilic surfaces [10, 25, 34].

2. Theory

It was assumed that biofilm formation depends on only two phases: a liquid bulk phase and a biofilm phase. Another assumption is that the biofilm is homogeneous with a constant density during time and can therefore be described by a one-dimensional model.

The number of cells in the biofilm phase depends on the number of cells adhering to the wall, the growth of adsorbed cells and the number of cells detaching from the wall. Effects of the wall surface (like specific interactions or roughness of the surface) are not investigated. The number of cells in the bulk liquid depends on the number of cells flowing into the system, the number of cells released from the wall, growth in the bulk liquid, adsorption of cells to the wall and the number of cells flowing out of the system. The biofilm formation process for both the biofilm and liquid phase is given in figure 1.

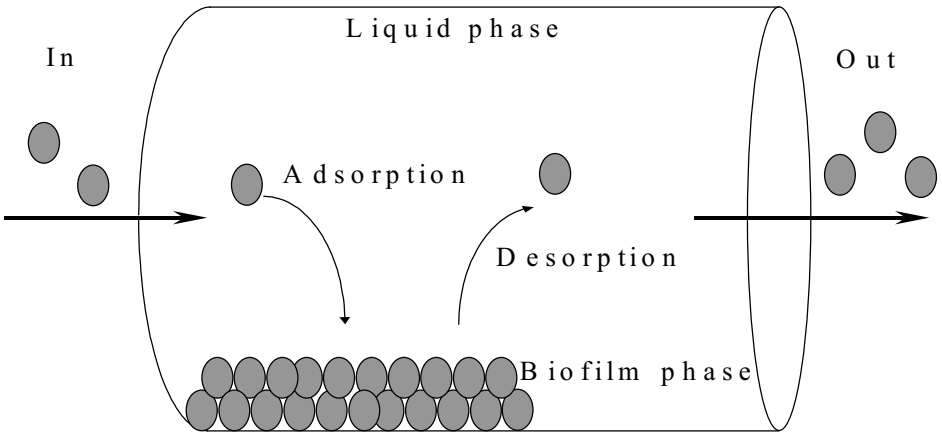

Figure 1. Biofilm formation in a pipeline. Cells enter the pipeline and adsorb to the wall where they can grow and form a biofilm. Cells can then be desorbed again from the biofilm and end up in the liquid phase after which they flow out of the system.

The accumulation of cells in the biofilm phase is described by:

$$A_B \frac{dN_B}{dt} = k_A A_L X_L - k_D A_B N_B^n + \mu_B A_B N_B \qquad (1)$$

accumulation adsorption desorption growth

with A_B: biofilm area (m^2)
N_B: number of adsorbed cells (cfu m^{-2})
k_A: adsorption coefficient (m h^{-1})
A_L: surface area (m^2)
X_L: concentration of cells in the liquid (cfu m^{-3})
k_D: desorption coefficient ($m^{2n-2}cfu^{1-n}h^{-1}$)
n: power factor describing non-linearity for desorption
μ_B: growth rate in the biofilm (h^{-1})

Adsorption is assumed to be a first order process, while desorption is assumed to be a higher order process. The rate of desorption in a developing biofilm must be less than the growth rate when the biofilm is thinner than steady state thickness and must equal the growth rate for biofilms that reach steady state thickness. This requires a higher order

dependence on the number of adsorbed cells (N_B) for the desorption rate than for the growth rate [123]. This was achieved by introducing the power factor n in the desorption process. Physically this means that when the layer becomes thicker, cells are more susceptible to be removed from the biofilm by shear forces, probably in clumps of cells.

Assuming that the biofilm spreads evenly along the surface area of the system ($A_B = A_L$), equation 1 can be rewritten as:

$$\frac{dN_B}{dt} = k_A X_L - k_D N_B^n + \mu_B N_B \tag{2}$$

For the bulk liquid phase the mass balance is (assuming that the volume of the system is constant):

$$V_L \frac{dX_L}{dt} = \phi_L X_0 + k_D A_B N_B^n - \phi_L X_L - k_A A_L X_L + \mu_L V_L X_L \tag{3}$$

accumulation in desorption out adsorption growth

with V_L: liquid volume of the system (m^3)
ϕ_L: liquid flow ($m^3\ h^{-1}$)
X_0: concentration of cells entering the system (cfu m^{-3})
μ_L: growth rate in the liquid (h^{-1})

Since it is assumed that $A_B = A_L$ and $\phi_L/V_L = D_L$ (dilution rate) equation 3 can be rewritten as:

$$\frac{dX_L}{dt} = D_L X_0 + a_L k_D N_B^n + (\mu_L - a_L k_A - D_L) X_L \tag{4}$$

with a_L is the specific surface ($a_L = A_L/V_L$) in m^{-1}.

Equations 2 and 4 are used to describe biofilm formation.

3. Materials and methods

3.1 Test organism

The test organism was *Staphylococcus aureus* ATCC 6538. The strain was stored at -80 °C in cryo vials containing 0.2 ml glycerol, 0.5 ml of the bacterial culture and 6 glass beads. *S. aureus* was pre-cultured by adding one glass bead to 10 ml of Tryptone Soy Broth (TSB, Oxoid) and incubating for 24 h at 37 °C to obtain approximately 10^9 cfu ml^{-1}.

3.2 Experimental set-up

Biofilms were developed on silicon rubber surfaces in the following experimental set-up. Prior to inoculation, the experimental system was sterilised for one hour at 121°C.

One Erlenmeyer beaker containing around 750 ml diluted TSB (1:10) was inoculated with pre-cultured *S. aureus* to a final concentration of around 10^6 cfu ml^{-1}. This was pumped with a peristaltic pump (Watson Marlow 205 U) through 8 parallel silicon rubber tubes. After 2 hours, the inoculation suspension was changed for sterile medium by replacing the Erlenmeyer beaker with sterile diluted TSB (1:10), which was pumped via a dropper through the tubes during 216 hours (see figure 2). The length of the sampling tubes was 20 cm with an internal diameter of 5 mm. The experiments were performed at 23 °C.

Three different flow rates were tested in separate experiments: 45 ml h^{-1}, 450 ml h^{-1} and 2400 ml h^{-1} inside each sampling tubes. For each flow rate the experiment was performed twice. For the experiments at 450 ml h^{-1} and 2400 ml h^{-1} a loop was inserted in the existing experimental set-up to increase the flow rate in the sampling tubes. The flow rate in the loop was respectively around 7 times and 37 times the flow rate in the main stream. The dilution rate of the total system was at least 10 times the planktonic growth rate of *S. aureus* to prevent planktonic growth.

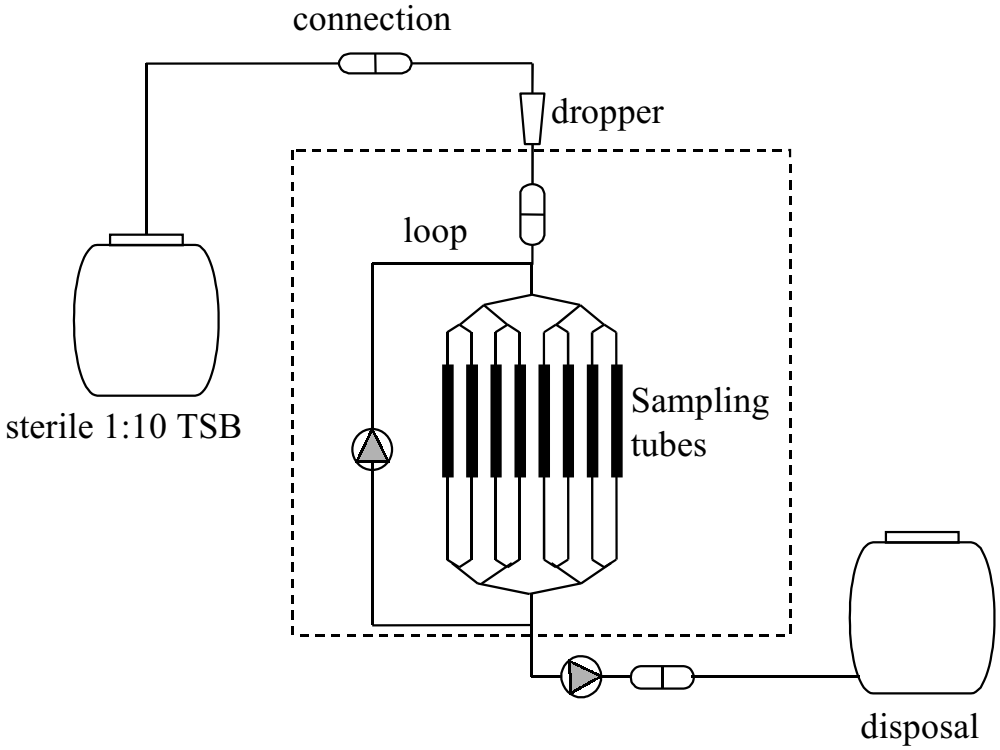

Figure 2. Experimental set-up for biofilm formation in a continuous system with silicon rubber tubes. After 2 hours of inoculation with *Staphylococcus aureus* (10^6 cfu ml^{-1}), this set-up is used to monitor biofilm formation for 216 hours. The loop was inserted to obtain flow rates of 450 ml h^{-1} and 2400 ml h^{-1} in the sampling tubes. Each day, one of the sampling tubes was removed for sampling. The system boundary for the model calculations is given with the dotted line.

3.3 Sampling

After 2 hours and once each following day, the bulk liquid was sampled by inserting a syringe into one of the sampling tubes. The syringe, inevitably, went through the developed biofilm on the inner-side of the sampling tube to reach the liquid phase. In order to reduce an interference between biofilm and liquid cells, the syringe was left in the tube for some moments so that biofilm cells on the tip of the needle would be washed out by passing liquid. Then a liquid sample of around 3 ml was withdrawn from the sampling tube. This sample was diluted and plated on Tryptone Soy Agar (TSA, Oxoid). The number of liquid cells on the plates was counted after incubation at 37 °C for 24 hours and represented the biomass concentration in the liquid phase (X_L).

After the liquid sample was taken from one of the sampling tubes, this tube was removed to determine the number of adsorbed cells. First, the liquid in the tube was collected by emptying the tube in a sterile bottle and plating this on TSA. This liquid contained both loosely attached cells and bulk liquid cells. The number of loosely attached cells was determined by subtracting the counts of the outflowing liquid from the bulk liquid counts obtained with the syringe method. Three pieces of 1 cm each were cut from the upper, centre and lower part of the silicon rubber tube. The sampling pieces were chosen outside the region of liquid sampling. The cylindrical samples were cut into 4 pieces resulting in 12 silicon rubber surfaces. These were first rinsed in 0.067 M phosphate buffer pH 7. The rinsing liquid was plated on TSA to determine the number of reversibly attached cells. After rinsing, the surfaces were transferred into an Erlenmeyer beaker containing 20 ml PSS (peptone saline solution) and 20 g glass beads (diameter is 3 mm). This was put in a shaker at 160 rpm for 30 minutes at room temperature to determine the number of irreversibly attached cells [75]. The samples were counted by plating on TSA and incubating them at 37 °C for 24 hours. The number of loosely, reversibly and irreversibly attached cells were added and represented the total number of adsorbed cells on the surface (N_B).

Each time when a sampling tube was removed, the total flow rate in the system was adjusted in such a way that the flow rate in the sampling tubes remained constant during the whole biofilm experiment. By removing a sampling tube the specific surface and the dilution rate of the system changed slightly. However, this effect was negligible for the total system.

3.4 Model fitting

The biofilm model as described in equations 2 and 4 contains three unknown parameters: μ_B, k_D and n. These were obtained by fitting equations 2 and 4 simultaneously through the data points of the liquid and biofilm phase for each of the 3 different flow rates. It was assumed that biofilms could be formed from the dropper to the sampling point. The system boundaries are given in figure 2. The software environment Matlab (The MathWorks Inc.,

Natick, USA) was used to solve the differential equations. All other parameters (A_L, V_L, D_L, X_0, μ_L and k_A) were known or could be easily determined independently.

4. Results

Biofilm experiments were performed at 45 ml h^{-1}, 450 ml h^{-1} and 2400 ml h^{-1}, corresponding to Reynolds (*Re*) numbers of 3.2, 32 and 170 respectively. Table 1 contains the parameters of the biofilm experiments at the 3 different Reynolds numbers. Average values of two experiments were used for each *Re* number. It is assumed that the total number of adsorbed cells (N_B) is zero at t = 0h. After t = 2h, the ingoing concentration of cells (X_0) is assumed to be zero.

The growth rate of planktonic cells (μ_L) was determined in a separate growth experiment to be 0.6 h^{-1} for growth in diluted 1: 10 TSB at T = 23 °C with a lag phase of 5.5h (results not shown). The adsorption coefficient (k_A) was determined experimentally during the 2 hours of inoculation. It is assumed that in the first 2 hours no desorption takes place and growth in the biofilm was negligible. Solving differential equation 2 then gives the adsorption coefficient, via $k_A = \frac{N_B}{X_L t}$, in which t = 2h and N_B and X_L are the total number of adsorbed cells and liquid cells after 2 hours (X_L was constant in time).

Table 1. Parameters of the biofilm model for three different flow conditions

Parameter	*Re* = 3.2	*Re* = 32	*Re* = 170
X_0^*	1.14E12 cfu m^{-3}	2.12E12 cfu m^{-3}	1.88E12 cfu m^{-3}
A_L^{**}	2.61E-2 m^2	5.14E-2 m^2	5.14E-2 m^2
V_L^{**}	4.00E-5 m^3	7.12E-5 m^3	7.12E-5 m^3
D_L^{**}	4.09 h^{-1}	10.52 h^{-1}	13.82 h^{-1}
μ_L	0.60 h^{-1}	0.60 h^{-1}	0.60 h^{-1}
k_A	7.41E-5 m h^{-1}	2.17E-5 m h^{-1}	2.94E-5 m h^{-1}

*: X_0 was set to zero after 2 hours, when inoculation was stopped.

**: Values are average values for the duration of the biofilm experiments

Fitting the experimental results of the different flow conditions with the biofilm model using the fit parameters n, μ_B and k_D, showed that n was always around 1.15 (range between 1.14 and 1.16). Therefore, it was decided to set this power factor to 1.15 and to fit the data points with μ_B and k_D. Figure 3 shows the obtained fit parameters for the different flow conditions. The growth rates in the biofilm were between 0.16 h^{-1} and 0.49 h^{-1} and the desorption coefficient varied from 0.0014 to 0.0049 $m^{0.3}cfu^{-0.15}h^{-1}$.

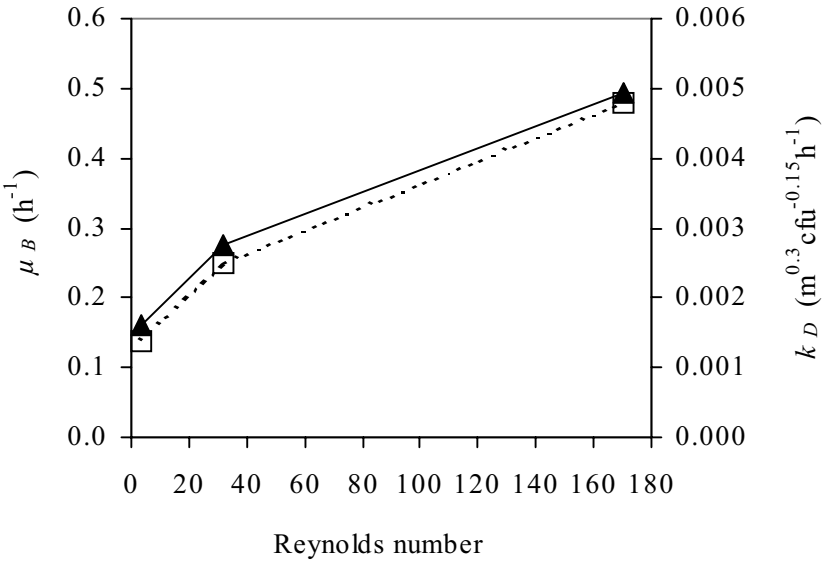

Figure 3. Values for the fit parameters at different Reynolds numbers. Closed triangles connected with a solid line represent the specific growth rate in the biofilm (μ_B). Open squares connected with a dotted line represent the desorption coefficient (k_D).

Figures 4 to 6 show the results of the model description of the data points in the biofilm phase and bulk liquid. The cell concentration in the bulk liquid decreased sharply after 2 hours, due to the change from inoculation suspension to sterile medium. Since the dilution rate (D_L) is larger than the specific growth rate in the liquid (μ_L), the inoculated cells will be washed out of the system. After this change, the concentrations in both the biofilm and bulk liquid increased rapidly to a maximum concentration of cells released into the liquid of around 10^9 cfu ml^{-1}. The maximum concentration of total adsorbed cells was around 3 10^9 cfu cm^{-2}. This includes the number of loosely, reversibly and irreversibly attached cells, which were at equal levels throughout the biofilm experiments (results not shown). When the total number of absorbed cells is 1.5 10^8 cfu cm^{-2}, a 100% surface coverage is reached (calculated with an average cell diameter of 0.93 μm [79]. Therefore, when the maximum concentration of attached cells is reached, on average 20 layers of cells are formed.

In view of the variance between duplicate experiments, the biofilm model describes the data satisfactorily except for the liquid concentration at t = 24h. This data point is systematically higher than the model describes. In the model calculations, the experimental set-up is approximated as an ideally stirred tank reactor, assuming that after 2 hours, X_0 is zero and liquid cells are washed out rapidly due to the high dilution rate in the system. However, since the flow in the system is laminar (*Re* is maximum 170), there may be a residence time distribution. It may therefore be possible that the medium near the wall is refreshed more slowly than in the centre of the tube causing a deviation between the model descriptions and experimental values. This hypothesis was tested by assuming X_0 remained at the inoculation level after the switch to sterile medium, which is the

opposite situation compared to $X_0 = 0$. Indeed, a better agreement with the data points at t = 24h was obtained, as can be seen in figures 4 to 6 represented by a dotted line. The values of the parameters μ_B and k_D remained the same. Therefore, although the model assuming the experimental system to be a perfect stirrer can not describe the data points satisfactorily at t = 24h, the obtained parameters are not influenced by this. However, some effect of fluid retention is observed, having a significant influence in the first moments of biofilm formation. Therefore, in reality, X_0 is somewhere between the two extreme situations tested here, in which X_0 was either zero or at the initial concentration after the switch to sterile medium.

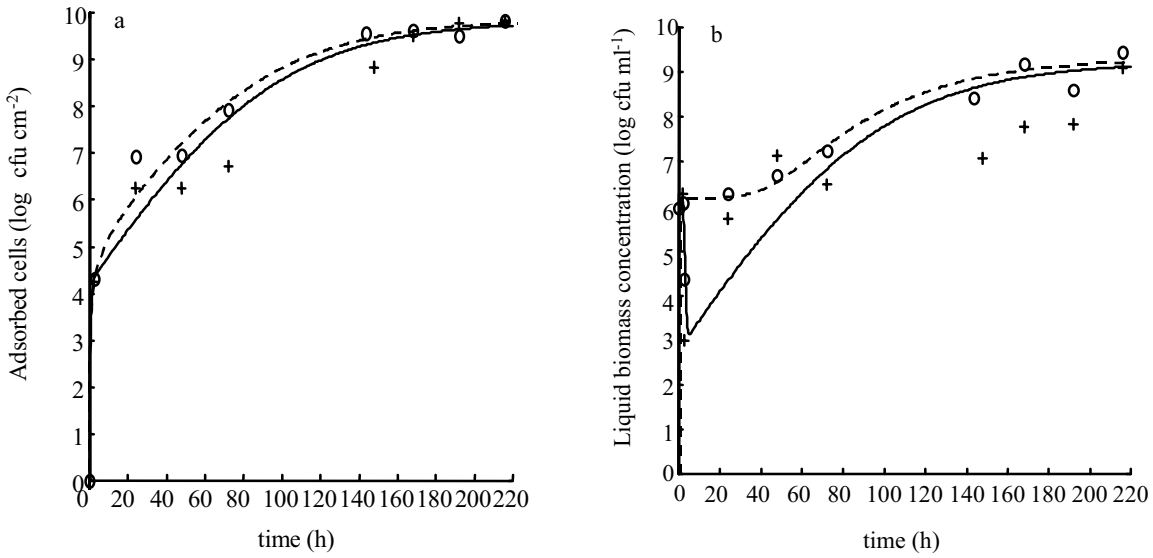

Figure 4. Biofilm formation at *Re* = 3.2 for both the number of adsorbed cells (**a**) and the number of released cells from the biofilm (**b**). The + and o signs depict data points of two separate biofilm experiments and the solid line is the description of the model for $\mu_B = 0.16$ h^{-1} and $k_D = 0.0014$ $m^{0.3}cfu^{-0.15}h^{-1}$. The dotted line gives the model description assuming there is no switch to sterile medium after 2 hours.

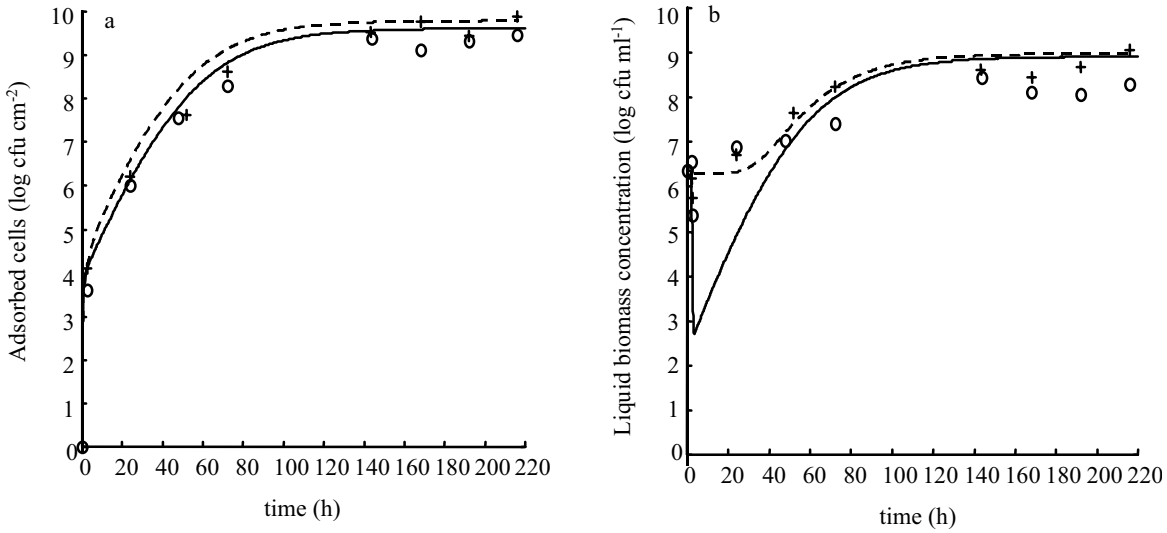

Figure 5. Biofilm formation at *Re* = 32 for both the number of adsorbed cells (**a**) and the number of released cells from the biofilm (**b**). The + and o signs depict data points of two separate biofilm experiments and the solid line is the description of the model for μ_B = 0.27 h^{-1} and k_D = 0.0027 $m^{0.3}cfu^{-0.15}h^{-1}$. The dotted line gives the model description assuming there is no switch to sterile medium after 2 hours.

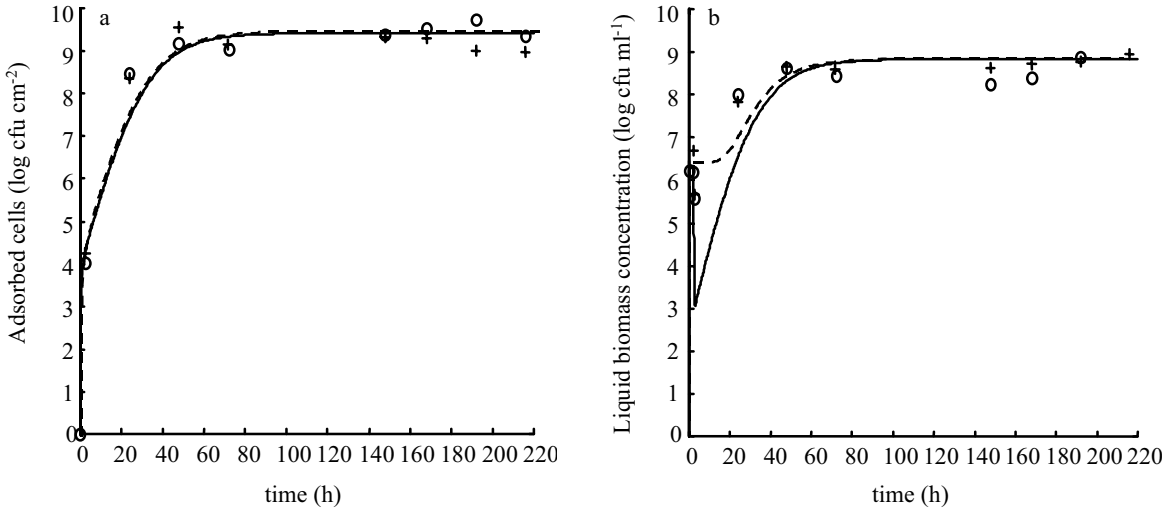

Figure 6. Biofilm formation at *Re* = 170 for both the number of adsorbed cells (**a**) and the number of released cells from the biofilm (**b**). The + and o signs depict data points of two separate biofilm experiments and the solid line is the description of the model for μ_B = 0.49 h^{-1} and k_D = 0.0048 $m^{0.3}cfu^{-0.15}h^{-1}$. The dotted line gives the model description assuming there is no switch to sterile medium after 2 hours.

The performance of the model is further analysed by comparing the model descriptions with the experimental values, using the mean square error (*MSE*, the residual sum of squares divided by the degrees of freedom), the correlation coefficient (*r*, the covariance of *x* and *y* divided by the product of the standard deviations of *x* and *y*) and the bias and accuracy factors (as described by Ross [114]). The lower the *MSE*, the better is the performance of the model. The correlation factor *r* and the bias and accuracy factor should approximate 1 to give a good description of the data.
Table 2 gives the quantitative comparison between the model description and the data points for the 3 different flow conditions calculated for log values. The *MSE* values were either calculated by comparing the data with the model descriptions (MSE_{model}) or by comparing the data with the average values of the duplicate measurements ($MSE_{duplicate}$).

Table 2. Quantitative comparison between model descriptions and observed data from biofilm experiments at different flow conditions. $MSE_{duplicate}$ is the comparison between the data with the average values of the duplicate measurements.

	Re = 3.2		*Re* = 32		*Re* = 170	
	Biofilm	Liquid	Biofilm	Liquid	Biofilm	Liquid
$MSE_{duplicate}$	0.18	0.38	0.06	0.12	0.06	0.15
MSE_{model}	0.48	1.22	0.08	0.73	0.22	0.86
r	0.94	0.80	0.99	0.90	0.97	0.88
Bias	1.20	1.23	0.95	0.43	0.86	0.38
Accuracy	3.13	7.44	1.73	4.03	2.04	4.41

When MSE_{model} is compared to $MSE_{duplicate}$ (which is a measure for the measurement error of the duplicate experiments), it can be seen that there is only a small difference for the biofilm data with a larger deviation for the liquid data. Furthermore, for the biofilm data, both the *r* and bias factor are around 1. For the liquid phase there is a larger deviation from 1 and also the accuracy factor is larger than for the biofilm data. The model therefore gives a better description of the biofilm than of the liquid phase.

5. Discussion

5.1 Model parameters and performance of the model

The adsorption coefficient (k_A) was determined experimentally as described before and was found to be in the range of 2E-5 to 7.5E-5 m h^{-1}. Benito et al. [10] found a slightly faster attachment of *S. aureus* to meat surfaces. In their batch system, the adsorption coefficient could be calculated to be 9.7E-5 m h^{-1}, which is still in the same order of magnitude as the values found in this study. It seems that, in the flow regime tested in this study, the adsorption coefficient was independent of *Re*. De Jong [31] also found that the

adsorption coefficient is constant in the laminar flow regime. Their adsorption coefficients for *Streptococcus thermophilus* coincide well (range between 8E-6 and 2E-4 m h^{-1}) with the values found in this study.
The obtained specific growth rate in the biofilm (μ_B) ranged from 0.16 h^{-1} to 0.49 h^{-1} depending on the *Re* number. Hodgson et al. [51] found a lower growth rate in the biofilm of 0.06 h^{-1} for *S. aureus*. The fastest increase in cell counts took place in the first 24h of their experiment. For this time period, the growth rate was calculated to be 0.17 h^{-1} for flow rates of 27 ml h^{-1} and 60 ml h^{-1}, which are comparable to the lowest flow rate tested in this study.
When the different factors, namely adsorption, desorption and growth are compared for *Re* 170 (figure 7), it can be seen that adsorption is only important at the initial stage of biofilm formation. After this initial stage, adsorption is negligible and desorption and growth increase simultaneously to reach a steady state biofilm thickness. This can only be described when the power factor *n* is larger than 1 (as is explained in the theory section). In this study, a power factor of 1.15 was found. The reason for this specific value is unclear. It may be that it is a characteristic of the structure of the biofilms formed by *S. aureus*.

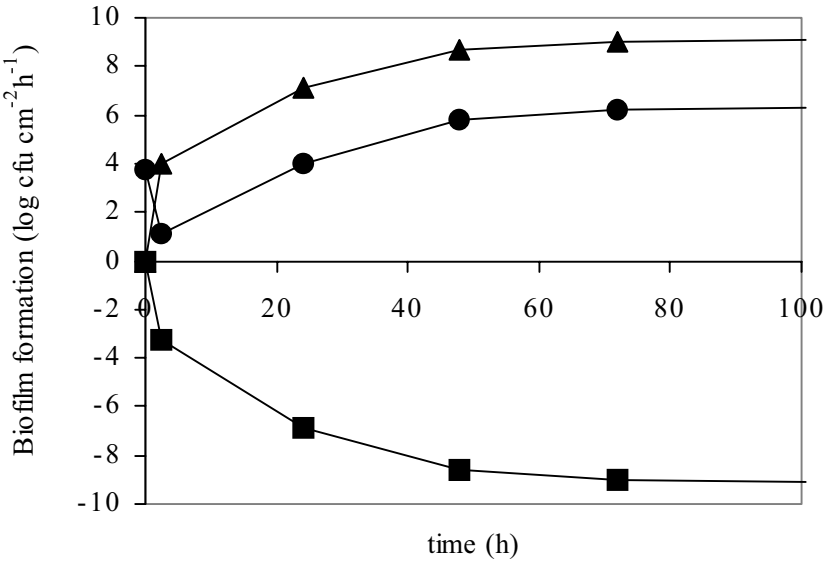

Figure 7. Influence of different factors on biofilm formation (equation 2) for *Re* = 170. Triangles give the growth factor ($\mu_B N_B$), the circles represent the adsorption factor ($k_A X_L$) and the squares the desorption factor ($k_D N_B^n$).

As can be seen in figure 3, the value of the desorption factor (k_D) is around 1% of the specific growth rate in the biofilm (μ_B) for each of the *Re* numbers. The parameters, therefore, seem to be correlated. This correlation strongly depends on the power factor (*n*), as follows from equation 2. At steady state conditions and assuming adsorption is negligible, equation 2 can be solved as: $k_D = \mu_B N_B^{1-n}$. The relation between k_D and μ_B can be calculated using the maximum concentration of cells on the wall (N_B = 3 10^9 cfu cm^{-2})

and the power factor found. The fact that detachment is growth-related is described earlier [69, 99, 103]. Apparently, dividing cells continuously release part of their daughter cells to the liquid phase. The relationship between the desorption factor (k_D) and the growth rate (μ_B) might be different at higher *Re* numbers where shear forces become more important causing higher desorption rates.
De Jong [31] developed a biofilm model where indeed it was assumed that part of the dividing cells are released to the liquid. When the biofilm thickness increases this part becomes larger until finally all dividing cells are released to the liquid. The effect of different flow rates on either growth or desorption was not investigated. Using their desorption parameter values and the specific growth rate of *S. aureus* yields a desorption rate that coincides very well with the rate found in this study (< 5% difference). This is remarkable since their parameter values were obtained for a different micro-organism (*Streptococcus thermophilus*) and a different surface material (stainless steel).

The outcome of the model calculations was compared quantitatively with the experimental data in table 2. Such quantitative comparisons are usually applied to validate a model with newly observed data. In this case, the experimental data were used to obtain parameters of the biofilm model and are therefore related to the model descriptions. Nevertheless, this table can be used to evaluate the performance of the biofilm model for the obtained data sets. It can be seen that the model describes the biofilm data well, but there is a larger deviation for the liquid data.
The accuracy of the model may increase by elaborating the model. However, since the aim was to develop a simple model that can be applied in the food industry, the model should contain as little parameters as possible while still giving a proper fit to the data. Therefore, in our opinion this model has the desired balance between simplicity and performance.

5.2 The effect of increasing flow rates on biofilm formation

Figures 4 to 6 show that at higher flow velocities or *Re* numbers the cell concentration increases more rapidly. At *Re* = 3.2 the maximum concentration is reached after 140h, whereas at *Re* = 170 the maximum concentration is already reached after 80h. The same trend can be seen for the fit parameters (figure 3). At higher *Re* numbers, the growth rate in the biofilm increases and approaches the growth rates of planktonic cells (μ_L = 0.6 h^{-1}). The desorption coefficient increases as well, which explains that even though the cells in the biofilm grow faster at higher *Re*, the maximum cell concentration (i.e. steady state biofilm thickness) remains the same.
When the flow rate increases, two mechanisms play a role: on the one hand, mass transfer to the surface increases causing higher growth due to the higher availability of nutrients and removal of metabolic products from the surface. On the other hand higher flow velocities cause higher shear stress resulting in a higher cell desorption rate [20, 73]. Which of these mechanisms dominates the biofilm process depends on the region of the

flow velocities. According to Trulear and Characklis [127] and Stoodley et al. [124] there is a plateau value of biofilm production at increasing flow velocities. Below this plateau value, biofilm growth is mass transfer limited and above this value shear forces reduce the biofilm thickness.
Several authors find a decreasing biofilm production at increasing flow velocities [15, 36, 73]. These effects were measured at Reynolds numbers above 7000 or with shear stress above 2 N m^{-2}. In this study, *Re* was maximum 170 and the corresponding shear stress was 0.05 N m^{-2}. At these low flow velocities, shear stress apparently does not yet influence biofilm thickness, since in this study an increase in biofilm production is observed at higher *Re* numbers rather than a decrease. It can therefore be assumed that at the low *Re* numbers used in this study, mass transfer is the limiting factor determining the biofilm process. Benefield et al. [9], Characklis [20] and Piciorenau et al. [102] also described a faster growth in the biofilm at increasing fluid velocities due to a decrease in mass transfer boundary layer resulting in a higher effective substrate concentration at the biofilm-fluid interface.

In this study, laminar flow was used in the biofilm experiments (largest *Re* was 170), whereas in large-scale equipment turbulent flow is encountered more often. However, on specific locations in the process, the flow is often laminar, particularly in cracks, crevices and dead ends. Furthermore, for viscous products the flow is often laminar as well. Therefore, the experiments in this study can give relevant information regarding biofilm formation, but extension to higher *Re* is desirable. It would be useful to further validate the proposed biofilm model using other surfaces and other micro-organisms. The obtained growth rates and desorption factors may be different from the ones obtained for biofilm formation of *S. aureus* on silicon rubber surfaces. Both the number of adsorbed cells and the number of released cells into the liquid should be measured in order to obtain useful information regarding the desorption of cells. Usually only the number of adsorbed cells is followed in biofilm experiments and not the number of desorbed cells. However, especially for the food industry, the number of desorbed cells is very important, since it determines the rate of recontamination from a biofilm to the product.

6. Conclusions

The experimental set-up used in this study proved to be useful for the generation of data for the biofilm model. Since both the adsorbed cells and desorbed cells in the liquid were measured, all parameters for the biofilm model could be obtained.
In the range of flow rates tested, the biofilm developed faster at higher flow rates probably due to an increase in mass transfer to and from the surface. The specific growth rate in the biofilm approximated the planktonic growth rate at the largest *Re* number.

The biofilm data were described adequately with the proposed biofilm model (equation 2 and 4) for each of the 3 different flow conditions. The description of the liquid data, however, gave a larger deviation. Especially the data points at t = 24h were underestimated. An adaptation of the model, however, gave a much better description of this time region.

The biofilm model has only 2 parameters that should be determined for a micro-organism, i.e. the specific growth rate in the biofilm (μ_B) and the desorption coefficient (k_D). In the flow regime tested in this study, the power factor n was 1.15, which gave a linear relationship between μ_B and k_D. This means that once μ_B is established, k_D can also be determined with N_B under steady state conditions. Whether this relationship is also valid for higher flow rates needs to be established.

Because of its simplicity, the model may be applied for the prediction of recontamination in food processing lines without necessitating much experimental data for the model parameters.

Acknowledgements

We thank Evelyn Serrarens for her work in the initial phase of this study. We are also grateful to Frans Rombouts (Wageningen University), Meike te Giffel (NIZO Food Research), Huub Lelieveld (Unilever Research & Development) and Taco Wijtzes (Wijtzes Food Consultancy) for valuable discussions and comments.

4

Estimating the probability of recontamination via the air using Monte Carlo simulations

Esther D. den Aantrekker, Rijkelt R. Beumer, Suzanne J.C. van Gerwen, Marcel H. Zwietering, Mick van Schothorst, Remko M. Boom

Abstract

Recontamination of food products can cause foodborne illnesses or spoilage of foods. It is therefore useful to quantify this recontamination so that it can be incorporated in microbial risk assessments (MRA). This article describes a first attempt to quantify one of the recontamination routes: via the air. Data on the number of airborne micro-organisms were collected from literature and industries. The settling velocities of different micro-organisms were calculated for different products by combining the data on aerial concentrations with sedimentation counts. Statistical analyses were performed to clarify the effect of different products and seasons on the number of airborne micro-organisms and the settling velocity. For both bacteria and moulds 3 significantly different product categories with regard to the level of airborne organisms were identified. The statistical distribution in these categories was described by a lognormal distribution. The settling velocity did not depend on the product, the season of sampling, or the type of micro-organism and had a geometrical mean value of 2.7 mm s^{-1}. The statistical distribution of the settling velocity was described by a lognormal distribution as well. The probability of recontamination via the air was estimated with the product of the number of bacteria in the air, the settling velocity, and the exposed area and time of the product. For three example products the contamination level as a result of airborne recontamination was estimated using Monte Carlo simulations. What-if scenarios were used to determine design criteria to control a specified contamination level.

Submitted for publication

1. Introduction

Microbiological risk assessment (MRA) has been developed as a science based tool used by governments or governmental bodies to facilitate the international trade in safe food. MRA is a procedure aimed at quantifying risks related to the consumption of a specific food product by a well-defined population. There are four steps in an MRA: hazard identification, hazard characterisation, exposure assessment and risk characterisation [70]. For the third step of MRA, the exposure assessment, it is advisable to apply a farm-to-fork approach meaning that all the steps in a food supply chain are quantified in order to estimate the probability of obtaining contaminated food and the level of contamination. Such farm-to-fork approaches are indeed applied for instance by Whiting and Buchanan [139] and Cassin et al. [17]. However, recontamination of products after an inactivation step has generally not been included in exposure assessment studies. Nevertheless, such recontamination has been reported as a source of food spoilage and food infections [37, 47, 55, 117]. It is therefore relevant to quantify recontamination so that it can be incorporated in MRA studies.

There are several routes of recontamination such as via surface contact, via personnel or via the air. This paper focuses on recontamination via the air. When the contribution of air contamination can be quantified, its importance can be determined in an overall risk assessment by comparing air contamination to other sources (initial contamination and other recontamination routes).

When micro-organisms are present on the factory floor, they can be transferred to the air by for instance spraying during cleaning, which causes aerosol formation (droplets of vapour in the air). Micro-organisms are not only present on floors, but also on other surfaces such as cable trays, pipes, light fittings and human skin. These micro-organisms can travel through the air while adhering to dust or skin particles. When products are exposed to the air of the product line environment, for example during product assembly or at the filling step, micro-organisms can end up in the product via several routes. Gravitational settling is the most important mechanism determining the deposition of particles in the air, compared to Brownian diffusion, inertial impaction, direct interception (by for example van der Waal's forces) and electrostatic attraction [141]. When there is no airflow, it can be understood that gravitation is the most important force working on particles in the air. When the air is fully turbulent, the air will be moving randomly in a room and gravitation will still be the most dominant force. In a unidirectional flow, the micro-organisms in the air will be influenced by the air flow. However, even in such situations, there are usually obstructions like machinery or operators working in the room, causing stagnant areas in which the bacteria will deposit by gravity [141].

In this study, it is therefore assumed that the main force determining deposition of micro-organisms is gravitation. The number of micro-organisms that enters the product via the air thus depends on the settling velocity of the micro-organisms, but also on the

concentration of micro-organisms in the air, and the exposed time and area of the product [141].

The aim of this paper is to apply this knowledge to estimate the contamination level of food products due to exposure to air. Therefore, data were collected of airborne concentrations and settling velocities for different food products. Statistical analyses were performed to determine whether there are significant differences between different food products and different seasons.

Assuming that airborne concentrations and settling velocities do not have a single, constant value, they were described by probability density functions (PDFs). Using these PDFs, both variability and uncertainty of the variables can be incorporated, which gives a more realistic estimation of the contamination level than by using point estimates [70]. The level of product contamination resulting from airborne contamination was estimated using Monte Carlo simulations. The result is a new PDF describing the contamination level of the product. On the basis of this procedure, some tentative applications to minimise the contamination level are given in the form of what-if scenario evaluations.

2. Materials and methods

2.1 Airborne recontamination model

Whyte [141] assumed a multiplicative relationship between concentration of airborne micro-organisms, settling velocity, and exposed area and time of the product:

$$L_c = C_{air} v_s A t \quad (1)$$

with L_c: contamination level (cfu/product)
C_{air}: concentration of micro-organisms in the air (cfu m^{-3})
v_s: settling velocity (m s^{-1})
A: exposed product area projected on a horizontal plane (m^2)
t: exposed time (s)

A contamination level of 10^3 cfu means that on average every product is contaminated with 10^3 cfu. A contamination level of 10^{-3} cfu means that one out of every 1000 products is contaminated with 1 cfu.

The settling velocity (v_s) can be calculated by dividing settle plate counts (cfu $m^{-2}s^{-1}$) by the airborne concentration (cfu m^{-3}). Equation 1 can then be rewritten in:

$$L_c = S_R A t \quad (2)$$

with S_R the sedimentation flux (cfu $m^{-2}s^{-1}$) = $C_{air} v_s$

2.2 Data collection

Data on airborne concentrations (C_{air}) and sedimentation fluxes (S_R) for bacteria, yeasts and moulds were collected from literature and from food manufacturers. Counts of less

than 5 cfu/plate were not included in this study due to the uncertainty in the colony counts. The data were classified into 6 different product groups reflecting different processing conditions: a dairy group containing solid products, a dairy group containing liquid products, a dry products group, a meat products group, a vegetable products group and a liquid products group. Relevant details were also recorded, for instance the location where the samples were taken, the season of sampling and the number of samples taken. When both C_{air} and S_R were known, the settling velocity (v_s) was calculated as described above.

2.3 Statistical analysis

Both the airborne counts (C_{air}) and the settling velocities (v_s) were log transformed in order to obtain normally distributed variables. The collected data originated from different sources and different measuring methods (culture media and equipment) and were based on different numbers of samples. Sometimes only the mean values were given together with the number of samples taken and in other cases all the measured microbial counts were reported. Therefore, in order to compare the different data, it was decided to weigh the data with the square root of the number of samples taken. The difference between product groups, products and seasons was then investigated using univariate analysis of variance. A significance level of 5% was used. The statistical analyses were performed in SPSS (SPSS Inc., Chicago, USA).

2.4 Probability density functions (PDFs) and Monte Carlo simulation

The log transformed data of C_{air} and v_s were fitted with cumulative theoretical frequency distributions using Excel spreadsheets (Microsoft Corporation, USA) and Bestfit (Palisade Corporation, Newfield, USA). The criterion for best fit was the root mean squared error (rms error). The obtained PDFs were used as input parameters to estimate the contamination level (L_c) using Latin Hypercube sampling (10.000 iterations) in @Risk software (Palisade Corporation, Newfield, USA).

3. Results and discussion

For an MRA study, only pathogenic bacteria are of interest, since these can cause an adverse health effect on the consumer [70]. Therefore, the number of airborne pathogens should be known in order to incorporate the airborne contamination model in an MRA study. However, since these data were not available in sufficient amounts, it was decided to collect data of total viable counts. Presumably, only a small part of the total viable count is pathogenic and therefore the result should be interpreted as a worst-case estimate. The estimate should, however, give a good description for spoilage causing bacteria.

Furthermore, data were collected of yeast and mould counts, since recontamination via the air can, apart from foodborne illness, also cause spoilage of food products, which reduces the shelf life of the products.

Statistical analyses showed that there were significant differences between concentrations of airborne bacteria, yeasts and moulds. The average log counts for the different micro-organisms for all available data are given in table 1.

Table 1. Average log counts for bacteria, yeasts and moulds for all product data.

Strain	*mu*	σ	*N*
Bacteria	3.07	0.96	829
Yeasts	1.29	0.89	216
Moulds	2.64	0.59	298
Yeasts/Moulds*	2.83	0.54	579

mu: average concentration in the air of the log transformed data (log cfu m^{-3})

σ: standard deviation of the log transformed data (log cfu m^{-3})

N: number of samples

*: the data did not distinguish between yeast and mould counts

It can be seen that the number of bacteria in the air is on average larger than the number of moulds and the number of yeasts in the air is the lowest. For a poultry-slaughtering factory, Lutgring et al. [80] indeed found that the number of airborne bacteria was higher than the number of yeasts and moulds. They suggest that the bacteria originated from the animals entering the factory and the primary source of yeast and moulds is the outside air. The different types of micro-organisms are treated separately in the next paragraphs.

3.1 Airborne concentrations for bacteria

Data on the airborne concentrations were classified in 6 product groups containing a total of 21 product types. For the meat data, the picking and hanging locations in poultry slaughtering houses were removed, because these locations are separated from cutting and packaging areas and are thus not relevant to estimate recontamination of the products. Table 2 contains the average bacterial concentrations and standard deviations for the different products in each product group. Statistical analyses were performed to determine whether all collected airborne counts could be combined into one PDF describing C_{air} for all products or that each product should be described with a different PDF. It was found that there were significant differences between the average concentrations of the different product groups and between the products within each product group. This is logical since the concentrations depend heavily on the specific process conditions.

The 21 different products can, therefore, not all be described by the same PDF. It was thus decided to seperate outlying products in order to reduce the number of PDFs and keep the analysis practical.

Table 2. Average bacterial concentration in the air and standard deviation (log cfu m^{-3}) for each product within the different product groups.

Product group	Product	*mu*	σ [a]	N_f	N_s	$\Sigma\sqrt{N}$ [b]	References
Vegetables	Vegetables[d]	2.99	1.27[c]	18	329	18	[52]
	Potato	2.43	1.33	6	226	158	[13, 54, 145]
	Sugar beet	4.68	0.34	1	24	16	[38]
Dry products	Dry products[d]	2.19	1.27[c]	21	241	16	[52]
	Milk powder	2.58	0.61	>9	126	44	[49, 66, 107]; Milk powder factory, 1999[e]
	Chocolate	2.02	0.32	1	9	9	Chocolate factory, 1999[e]
Liquid	Drinks[d]	2.51	1.32[c]	2	67	8	[52]
	Sauce	2.63	0.38	2	56	56	Sauce factory, 2001[e]
	Beer	3.67	0.07	10	302	46	[50]
	Soft drink	3.57	0.03	1	80	13	[50]
Dairy liquid	Dairy[d]	2.28	1.27[c]	14	342	18	[52]
	Milk	2.39	0.47	>1	26	16	[49]; Milk factory, 1999[e]
	UHT milk	2.24	1.38	8	47	8	[107]
	Condensed milk	2.11	0.91	2	14	7	[107]
Dairy solid	Butter	3.39	0.33	>2	8	3	[49, 107]
	Cheese	3.07	0.51	>12	107	22	[49, 107]
	Ice cream	3.18	0.19	>4	197	32	[49, 110]
Meat	Duck	3.79	0.38	2	800	160	[80]
	Turkey	3.58	0.85	2	780	156	[80]
	Pork	3.27	0.49	1	192	96	[67]
	Fish	3.06	1.63[c]	1	4	2	[52]

mu: average bacterial concentration in the air of the log transformed data (log cfu m^{-3})

σ: standard deviation of the log transformed data (log cfu m^{-3})

N_f: number of factories sampled

N_s: total number of samples taken

$\Sigma\sqrt{N}$: sum of square root number of samples

[a]: calculated from the available data unless mentioned otherwise

[b]: the data were weighed with the square root of the number of samples (as described in materials and methods; statistical analysis section)

[c]: standard deviation as was mentioned by Holah et al. [52]

[d]: the exact product is unknown

[e]: data obtained directly from industrial factories instead of literature references

The sugar beet data were removed from the vegetables group and the beer and soft drink data were removed from the liquid group since these values were significantly higher than the other data. Therefore, for the estimation of the contamination level in a beer or soft drink factory, specific beer or soft drink data need to be used (table 2) rather than the combined data in the liquid group. The same accounts for the sugar beet data. The high airborne counts in the beer and soft drink factories might have been caused by return bottles that are washed in the same hall as the filling machine. Due to the high ambient relative humidity of the air and the constant aerosol formation at the filling machine many micro-organisms are able to survive in the air [132].
After these modifications, statistical analyses of the different product groups showed that the vegetables group, dry products group, liquid group and dairy liquid group were not significantly different ($p > 0.05$) and also the products within these product groups were not significantly different from each other. It was decided to combine these data into one category: the low counts group. The other product groups, dairy solid and meat, were significantly different from each other and from the low counts category and were classified as the medium counts and high counts category respectively. Further statistical analyses of the different products within either the medium counts or high counts category showed that the products in the medium counts category (dairy solid group) were not significantly different from each other. The bacterial concentrations of the meat products in the high counts category, however, were significantly different. This means that according to statistical analysis, each product in the high counts category should be described by a different PDF. However, although the bacterial concentrations of the meat products were tested as significantly different, these differences can be considered as microbiologically not relevant. According to ISO standards, a 0.45 log difference between two independent test results tested by different people using the same sampling method on identical test material is still acceptable [3]. In this case, the samples originated from very different sources and are sampled with different sampling methods. The difference between the pork and duck products was only 0.5 log cfu m^{-3}, which can therefore be considered acceptable. The fish products were somewhat lower. However, the variability in the data set is quite large. Furthermore, the number of samples for fish ($N = 4$) is much smaller than for the other meat products and therefore does not play an important role in the overall meat data. Therefore, it was decided to combine the airborne concentrations in the high counts category into one PDF. If necessary specific data from table 2 can be used.

The low counts in the vegetables group can be explained by the fact that most samples were taken in the cutting and packaging areas, which are likely to have lower counts than at the entrance of the raw products. In dry environments, multiplication of bacteria is restricted, which might explain the lower counts in the dry products group compared to ‘wet’ factories like the dairy solid group. The liquid and dairy liquid group mainly contain

products that are produced in a closed system, which explains the relatively low counts in these groups.
The counts in the dairy solid group were about one log higher than in the dairy liquid group. The dairy solid group contains the products cheese, butter and ice cream. These products are produced in 'wet' factories that are cleaned regularly and for which it is more difficult to prevent aerosol formation.
It is not surprising that meat factories have higher airborne counts than other products. The source of the airborne concentrations found is usually the feathers of the birds [1, 80] or the hide of the animals [108]. High counts are also found in the faeces of the animals (10^{10}-10^{11} cfu g^{-1}) which partly become airborne in the hanging and picking area [1, 80]. Although these hanging and picking locations are separated from the other areas, they can still influence the bacterial air concentrations in the processing locations.
According to Kotula and Emswiler-Rose [67] the airborne counts in a meat factory can be ten times higher than in a dairy factory. This is in agreement with the results in this study: the average airborne counts in the meat group was 3.58 log cfu m^{-3} which is about 1 log higher than in the dairy liquid group (μ = 2.28 log cfu m^{-3}).
In general, the airborne counts strongly depend on the factory design, cleaning procedures and human activity [1, 48, 110].

Apart from the product groups, the effect of different seasons on airborne counts was investigated using statistical analysis for each of the three categories (low, medium and high counts). In this way the product type does not interfere with the effect of the season. However, there were no seasonal details available for the medium counts group. The seasonal counts for the low and high counts category are given in figure 1.

It can be seen that for both categories, the airborne counts in the summer were higher than in the other seasons. In the summer, temperatures are higher and micro-organisms are multiplying in all kinds of wet environmental niches. Subsequent drying and dust formation then causes release of high microbial numbers in the air due to the wind.
Moreover, because of harvesting in the summer, more particles are in the outside air, which might be another factor explaining the higher counts found in this season.
Although the average counts in the high counts group are quite similar (figure 1), statistical analysis showed that the different seasons were significantly different, both for the low and high counts category.

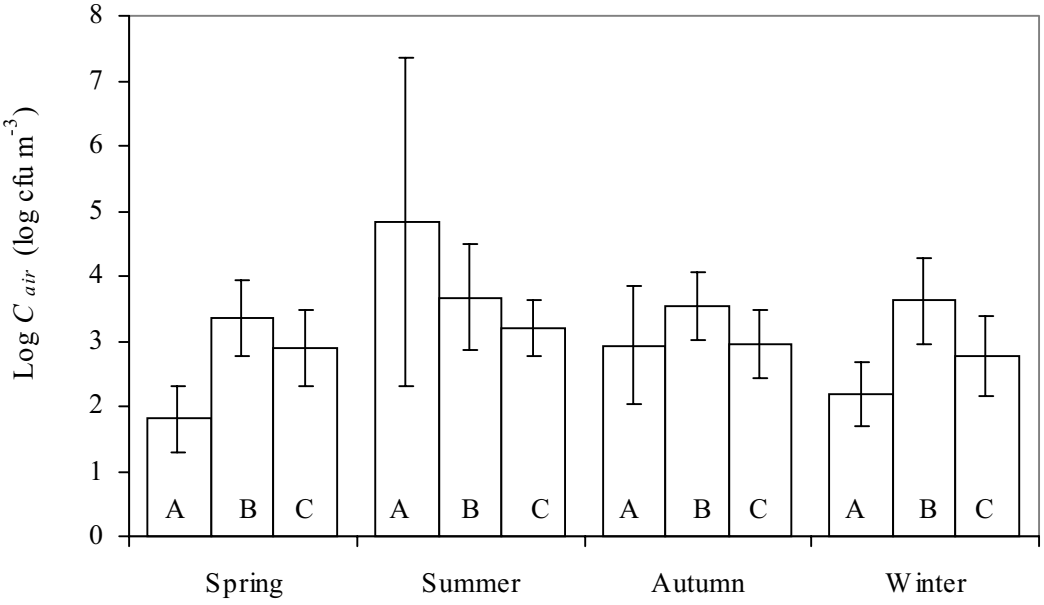

Figure 1. Concentrations (log cfu m^{-3}) of airborne bacteria (A, B) and moulds (C) in different seasons for the low counts (A) and high counts category (B, C). The error bars represent the standard deviation of the data set and not the uncertainty in the estimated mean value. The average summer count in the low counts group was based on only 5 samples, whereas the other seasons contained > 80 samples. The high count data (B, C) were based on ca. 100 samples in each season.

In the low counts group there were more than 80 samples in the seasons, except for the summer season for which only 5 samples were taken with a considerable standard deviation in the data. Therefore, more data are necessary to draw a reliable conclusion regarding the low counts group. In the high counts group the samples were more evenly distributed over the seasons (approximately 100 samples in each season). However, these data were only based on two references [67, 80], which makes it difficult to draw a reliable conclusion on the seasonal effect.

Most data on airborne counts did not mention the season of sampling. It is assumed that overall in all seasons samples were taken, so that the seasonal effect is already incorporated in the variability of the samples. Furthermore, the differences between the seasons in the high counts group were less than 0.45 log cfu m^{-3} (the maximum difference was 0.32 log cfu m^{-3}). It was therefore decided not to incorporate the season effect in the estimation of contamination levels.

3.2 Airborne concentrations of the spoilage micro-organisms yeasts and moulds

Data were available of yeast counts, mould counts and combined yeast and mould counts. Statistical analysis showed that the yeast counts were significantly different from the mould counts or combined yeast and mould counts. Since the yeast counts were much lower than the mould counts (table 1), it can be assumed that the combined yeast/mould

counts mainly consisted of moulds. The reason that the yeast counts are this low might be that moulds can better survive in the air due to their spore formation ability [1].
Comparison between the mould counts and combined yeast and mould counts showed that these groups were not significantly different from each other. Given the diversity of products, the available number of samples for the separate yeast counts was too small to draw conclusions regarding product groups or products. This paragraph therefore only focuses on mould counts (including the combined yeast/mould counts).
The average log counts and standard deviations are given in table 3. The same product groups were used for the statistical analysis as in the previous paragraph. The sugar beet data were removed again from the vegetables group for the same reasons as mentioned before.
Statistical analysis showed that for moulds the vegetables group was significantly different from all the other product groups and was characterised as the low counts category. The products within the low counts group were not significantly different from each other. The product groups: dairy solid and dairy liquid were not significantly different from each other and were combined in one category: the medium counts group. The products within this medium counts category were, however, significantly different from each other. The differences between the different products were regarded as microbiologically not relevant since the difference between the lowest concentration for butter and the highest concentration for cheese was only 0.4 log cfu m^{-3}. This is still acceptable according to ISO standards [3].
The remaining product groups: the dry products group, liquid group and meat group and the products within these groups were not significantly different from each other and these were combined in the high counts category.
The three different airborne categories (low, medium and high counts) therefore contain different products than for bacteria. For bacteria the low counts group consisted of not only vegetables but also dairy liquid, liquid and dry products. This is caused by the fact that the type of micro-organism found in the air is strongly related to the product produced. For example moulds survive better in dry environments than bacteria [132]. Therefore, the dry product group belongs to the high counts category for moulds and to the low counts category for bacteria. As mentioned before, the high bacterial counts in meat factories originate from the products entering the factory, whereas the mould counts originate from the outside air, which explains the higher bacterial counts in meat factories compared to mould counts [80]. Overall, the type and concentration of micro-organisms in the air depends on the processing conditions and factory design [1].

Table 3. Average mould concentrations[a] in the air and standard deviation (log cfu m^{-3}) for each product within the different product groups.

Product group	Product	*mu*	σ[b]	N_f	N_s	$\Sigma\sqrt{N}$[c]	References
Vegetables	Vegetables[e]	2.60	1.27[d]	18	268	16	[52]
	Potato	2.32	0.78	6	140	73	[13, 54, 145]
	Sugar beet	2.94	0.30	1	24	16	[38]
Dry products	Milk powder	2.94	0.20	>7	115	22	[49, 107]
Liquid	Beer	2.70	0.45	10	302	85	[50]
	Soft drink	2.77	0.46	1	83	13	[50]
Dairy liquid	Milk	2.55	0.32	>4	110	36	[49, 110]
	UHT milk	2.41	1.12	8	41	6	[107]
	Condensed milk	2.55	0.53	2	22	7	[107]
Dairy solid	Butter	2.38	0.30	>3	12	7	[49, 107], Butter factory, 1996 and 2001[f]
	Cheese	2.78	0.45	>14	314	152	[49, 107], Cheese factory, 1996-2001[f]
	Ice cream	2.30	0.17	>2	101	34	[49, 110]
Meat	Duck	3.15	0.53	2	800	160	[80]
	Turkey	2.98	0.58	2	780	156	[80]
	Pork	2.55	0.34	1	180	93	[67]
	Fish	2.57	1.71[d]	1	3	2	[52]

mu: average mould concentration in the air of the log transformed data (log cfu m^{-3})

σ: standard deviation of the log transformed data (log cfu m^{-3})

N_f: number of factories sampled

N_s: total number of samples

$\Sigma\sqrt{N}$: Sum of square root number of samples

[a]: the average concentrations in this table contain both mould and combined yeast and mould counts

[b]: calculated from the available data unless mentioned otherwise

[c]: the data were weighed with the square root of the number of samples (as described in materials and methods; statistical analysis section)

[d]: standard deviation as was mentioned by Holah et al. [52]

[e]: the exact product is unknown

[f]: data obtained directly from industrial factories instead of literature references

The same seasonal trend was found as for the bacteria: the summer counts were higher than in the other seasons (figure 1). There were only data available for meat products in the high counts category [67, 80]. For the same reasons as for the bacteria, the seasonal effect was not incorporated in the estimation of the contamination level (the deviation between the seasons was maximal 0.43 log cfu m^{-3}).

3.3 Settling velocity

The settling velocity was calculated for those cases that included data on both C_{air} and S_R. A total of 144 samples of different products and different micro-organisms was used to calculate the settling velocity. Since gravitational settling is the most important mechanism determining the deposition of micro-organisms [141], it was expected that the settling velocity would only be dependent on the size of the micro-organisms. Statistical analysis of the log settling velocities indeed showed that there were no significant differences between the different product groups and seasons ($p > 0.05$). However, the different micro-organisms (bacteria, yeasts and moulds) were not significantly different as well ($p > 0.05$).

If there are no predominant flow conditions, the settling velocity is the result of at least 3 forces that exert on a falling particle: the gravitational force, the drag force (described by Stokes law) and the buoyancy force (described by Archimedes' law). Combining those forces, the hydraulic diameter of a falling particle can be calculated when the settling velocity is known:

$$d_p = \sqrt{\frac{18 v_s \eta_{air}}{(\rho_p - \rho_{air}) g}} \qquad (3)$$

with d_p: diameter of the falling particle (m)
v_s: settling velocity (calculated by S_R/C_{air}) in m s^{-1}
η_{air}: viscosity of the air (17.1E-6 Pa s)
ρ_p: density of the particle (estimated at 10^3 kg m^{-3})
ρ_{air}: density of the air (1.29 kg m^{-3})
g: gravitational acceleration (9.81 m s^{-2})

For bacteria, yeasts and moulds the average log settling velocity was calculated. These values were transformed back to the original settling velocities to obtain the geometrical mean settling velocities, which are given in table 4, together with the calculated diameters of the particles.

Table 4. Geometric mean settling velocities and calculated settling particle diameters for different micro-organisms.

Micro-organism	v_s (m s^{-1})	Diameter (µm)	*N*
Bacteria	2.70E-3	9.21	110
Yeasts	2.85E-3	9.46	15
Moulds	2.55E-3	8.95	19
All strains[a]	2.70E-3	9.21	144

v_s: settling velocity (m s^{-1})

N: number of samples

[a]: data for bacteria, yeasts and moulds were combined

As can be seen in this table, the calculated diameter of the falling particles is between 9 and 10 µm. Most airborne micro-organisms will consist of bacterial or fungal spores, since spores survive better in the air than vegetative cells [1, 132]. The diameter of bacterial spores is between <1 and 2 µm, which is much smaller than the calculated diameter of the falling particles. The implied particle volume of the falling particles is 100-1000 times larger than for single spores. Mould spores are larger than bacterial spores and have a diameter between 2 and 5 µm [120], which again is smaller than the calculated diameter of 9 µm. This suggests that the yeasts, moulds and bacteria are either attached to each other or to dust particles or water droplets in aerosols. This hypothesis is further confirmed by the fact that the airborne concentration increases when cleaning or human activities increase [48, 119], suggesting that micro-organisms are indeed attached to either water droplets, dust or skin particles and are not present as single organisms in the air. When bacteria, yeasts and moulds are attached to these larger dust, skin or water particles, there will be no differences in settling velocities between the different types of micro-organisms.

The median bacteria-carrying particle diameters found in the pharmaceutical industry are between 7 and 17 µm depending on the clothes worn by the employees. The permeability of the fabrics as well as the pumping action of the clothing during motion play a role in the release of bacteria-carrying particles. This suggests that skin and dust particles do play an important role in the displacement of bacteria. For normal clothes, a median diameter of 12 µm was found [141]. This is somewhat larger than the calculated diameter of 9 µm in this study. It might be that the bacteria-carrying particles in the food industry are more dependent on aerosol formation, whereas in the pharmaceutical industry the type of clothing is the predominant factor influencing particle sizes. Furthermore, in equation 3, the particles are assumed to be spherical and dense. When the bacterial spores are attached to dust or skin particles, the particles will have another dimensional shape, which might be another factor explaining the higher measured diameter than the hydraulic diameter that was calculated in this study.

3.4 Probability density functions

The obtained log data on airborne counts of bacteria and moulds and the different settling velocities were fitted with cumulative theoretical distributions using Bestfit. For bacteria the low, medium and high counts group were fitted separately since they were significantly different. The best fits for these groups were respectively a loglogistic, beta general and a Weibull distribution. It would be more appropriate to use the same theoretical distribution for the different categories with different parameters for each category, considering that the underlying physical phenomena are the same. It was therefore decided to fit the log data with a normal distribution, since the number of bacteria in the air is a biological parameter for which it can be assumed that they follow a lognormal distribution. A lognormal distribution is used more often to describe bacterial concentrations [32, 83] and is the same as a normal distribution of the log counts [133]. The root mean squared (rms) error for the normal distributions was usually only 2 times higher than for the best fit. For example, the rms error for the loglogistic distribution of the low counts category was 6.4E-4 whereas the rms error for the normal distribution was 11E-4. When the different distributions are compared graphically, the best fit and normal distributions are very similar. An example is given in figure 2 for the low counts category.

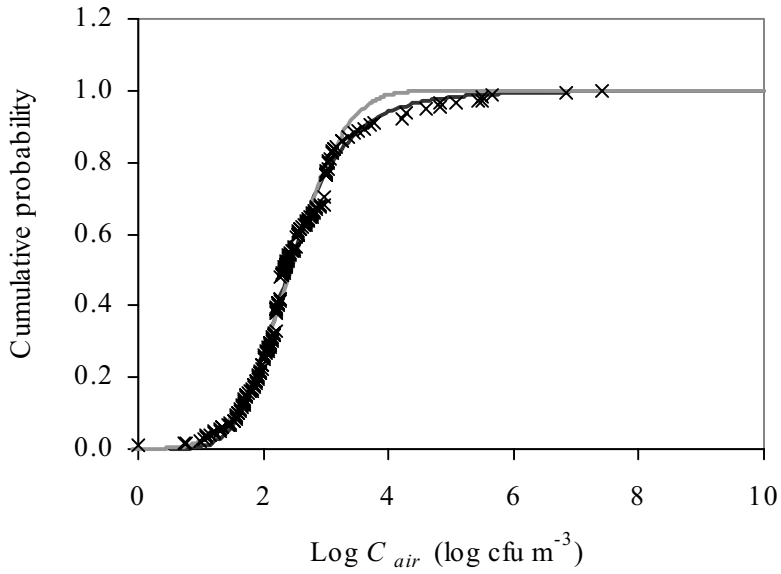

Figure 2. Cumulative probability density distributions of the measured log airborne concentrations (x) and the fitted theoretical distributions (lines) for the low counts group. The dark line represents the best fit (a loglogistic distribution) and the grey line is the normal distribution of the log data.

When the rms values of the different categories (low, medium and high counts) were added for each type of distribution (normal, loglogistic, beta general and Weibull distribution), the normal distribution gave overall the lowest value. Therefore, when the same type of theoretical distribution is to be used to describe all three categories, the normal distribution will give the best description of the log data.

The airborne mould counts were also fitted for the 3 different categories low, medium and high counts. As for the bacteria, it was decided to describe the log data in the different categories with a normal distribution. The parameters for the normal distributions for both bacteria and moulds are given in table 5.

Table 5. Parameters for the normal distribution of the bacteria and moulds concentrations in the air (log cfu m^{-3}) in different categories.

Micro-organism	Category	Product group	*mu*	σ
Bacteria	Low counts	Vegetables	2.44	0.71
		Dry products		
		Liquid products		
		Dairy liquid		
	Medium counts	Dairy solid	3.19	0.25
	High counts	Meat	3.39	0.73
Moulds	Low counts	Vegetables	2.38	0.82
	Medium counts	Dairy liquid	2.63	0.43
		Dairy solid		
	High counts	Dry products	2.88	0.53
		Liquid products		
		Meat		

mu: average mould concentration in the air of the log transformed data (log cfu m^{-3})

σ: standard deviation of the log transformed data (log cfu m^{-3})

The log values of the settling velocities for all available data (including different product groups and micro-organisms) were fitted together since they were not significantly different. This resulted in a logistic distribution. However, a lognormal distribution has been used before to describe particle size distribution of airborne particles [23, 93, 141]. In this case a normal distribution was fitted on the log transformed settling velocities. The obtained rms value was only 1.5 times larger than the best fit. The obtained average v_s was –2.59 log m s^{-1} and the standard deviation was 0.45 log m s^{-1}.

3.5 Monte Carlo simulations

Since both the airborne counts and the settling velocities were log transformed, the contamination level was also calculated in log numbers, resulting in:

$$\text{Log } L_c = \log C_{air} + \log v_s + \log (A*t) \quad (4)$$

Now that the different parameters are known for the lognormal distributions describing C_{air} and v_s, the contamination levels for different products can be calculated using the data from table 5 and the exposure time and area of the specific product.

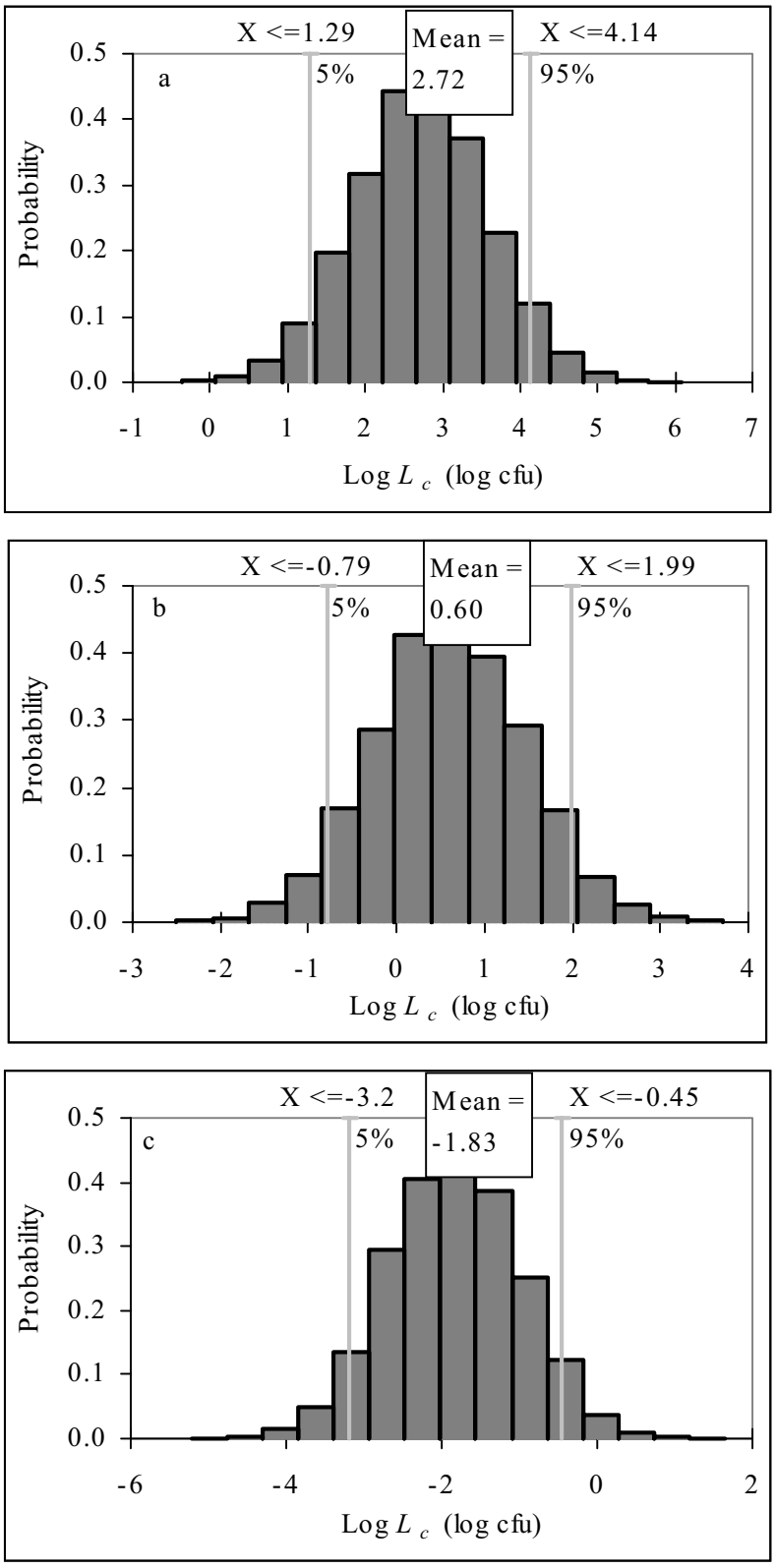

Figure 3. Probability density functions of the estimated bacterial contamination levels (log cfu/product) of (a) a pizza product, (b) a sliced meat product and (c) a sauce product including the 90% confidence interval.

In this paragraph three examples are calculated for airborne bacterial counts: one example for a pizza factory (figure 3a), one for a sliced meat factory (figure 3b) and one for a sauce factory (figure 3c).

A pizza usually contains several ingredients, like dough, tomato sauce, cheese, vegetables and meat and is usually assembled in an open space. According to the ingredients, a pizza could be classified in each of the 3 different categories: low counts category containing vegetables products, medium counts category containing cheese products and high counts category containing meat products. Using a worst-case approach, the pizza is classified in the high counts category. The area of a pizza is 380 cm^2 (diameter is 22 cm). The exposure time is 37 min (parameters obtained from a representative pizza factory). This gives an average log L_c per pizza of 2.72 log cfu. The median contamination level is thus 525 cfu/product. Using an average weight of a pizza of 300 g, the average contamination due to airborne exposure is 2 cfu g^{-1}. The probability density function of the L_c is given in figure 3a. It can be seen that the 90% confidence interval is between 1.29 log cfu/product and 4.14 log cfu/product. This means that 5% of the pizza's may have a contamination level of 19 cfu/product (0.06 cfu g^{-1}) or less, but also 5% of the pizza's may be contaminated with 1.4E4 cfu/product (47 cfu g^{-1}) or more assuming worst-case air contamination. It depends on other factors (like concentration of micro-organisms in the ingredients, the effect of heating prior to consumption and the type of contaminants) whether or not this L_c is acceptable.

Another example that belongs to the high counts category is sliced meat, for which an exposure area of 140 cm^2 and an exposure time of 45 s is assumed (parameters obtained from a representative meat factory). This results in an average log L_c of 0.6 log cfu/product (see also figure 3b). The median L_c is then 4 cfu per product or 0.2 cfu g^{-1} (assuming an average weight of 17 g per slice of meat). Five percent of the sliced meat products can be contaminated with more than 100 cfu/product (6 cfu g^{-1}) and 1% with more than 700 cfu/product (41 cfu g^{-1}). These values are lower than for the pizza product and are caused by the smaller exposed area and shorter exposure time. However, since the sliced meat products are not heated again prior to consumption and may allow growth of the organisms, this lower L_c might have a larger impact on food safety than the higher values for the pizza example. The contribution of air contamination to the final concentration of bacteria in the product should, however, be compared to the initial concentration of bacteria on the slices and to other recontamination sources (contact surfaces or personnel) to determine the importance of recontamination via the air for this product.

Another example is a sauce product, which belongs to the low counts category and has an exposure area of 28 cm^2 and an exposure time of 7.5 s (parameters obtained from a sauce factory). The average log L_c is then –1.83 log cfu/product. The median contamination level is 0.015 cfu/product, which means that one out of every 70 products is contaminated with 1 cfu. Figure 3c gives the average log L_c and its interval. In this case 5% of the sauce

products still only contain 0.35 cfu/product, which means that one out of 3 products is contaminated with 1 cfu. The contamination level of the sauce products can be as low as 6.4E-4 cfu/product. One out of every 1600 products is contaminated with 1 cfu.
When the three products are compared, it can be seen that the type of product and manufacturing conditions strongly influence the contamination level. There are differences between the different product groups but also the exposed area and time influence the probability of contamination via the air. This shows the utility of this type of quantification and data analysis.
Since the PDFs are log-symmetrical, the contamination level can also be calculated analytically using equation 4, by adding the different average log values and their standard deviations. For the sliced meat example, the average log contamination level is then: 3.39 (log C_{air}) -2.59 (log v_s) + log (1.4E-2*45) (area*time) = 0.60 log cfu/product. The standard deviation of log L_c can be calculated by the square root of the added quadratic standard deviations of C_{air} and v_s (assuming that the exposed area and time are exactly known): $\sqrt{0.73^2 + 0.45^2}$ =0.86. The confidence interval of the estimated log L_c is then calculated as:

$$\log L_c \pm t_{df,1-0.5\alpha} \sqrt{\left(1+\frac{1}{n}\right)\sigma^2} \qquad (5)$$

with $t_{df,1-0.5\alpha}$: Student's t value with df degrees of freedom and confidence level α
n: number of samples
σ: standard deviation of contamination level

The total number of samples in the meat group was 414. Using a 90% confidence interval, the Student's t-value is 1.645 resulting in a range of estimated log L_c between –0.82 and 2.01 log cfu/product. As can be seen in figure 3b the range calculated with Monte Carlo simulations is between –0.79 and 1.99 log cfu/product for the 90% confidence interval. This is therefore approximately equal to the analytical solution. The same can be done for the other products (pizza and sauce), for which the results again are very close to the Monte Carlo simulations. When the PDFs are not normally distributed, the analytical solution can not be used. Therefore, Monte Carlo simulations have a broader application and can be used more generally than analytical solutions. In this case, using normal distributions makes the calculations much easier, which is another reason for selecting normal distributions if the data justify this.
The applied air contamination model (equation 4) can be used in a total exposure assessment determining the concentration of pathogens in a product at the moment of consumption based on all aspects of the production process. In order to determine the risk of illness due to consumption of the product, the outcome of the exposure assessment should be coupled to a dose-response model. These models are usually based on actual

bacterial concentrations instead of log concentrations as determined in this study. Then the normal distribution of the log concentrations should be transformed to a lognormal distribution of the actual concentrations: log L_c = normal (mu,σ), thus L_c = lognormal(mu_l,σ_l). The mean and standard deviation of the lognormal distribution can be obtained from the mean and standard deviation of the normal distribution (using the natural logarithm instead of log values) as follows:

$$mu_l = \exp\left(mu_n + \frac{1}{2}\sigma_n^2 \right) \quad (6)$$

$$\sigma_l^2 = mu_l^2 \left(\exp\left(\sigma_n^2\right) - 1\right) \quad (7)$$

with mu_n = mu*ln(10) and σ_n = σ*ln(10). mu and σ are the average and standard deviations of the log values.

For the meat example the contamination level is described as: log L_c = normal(0.60, 0.86 log cfu/product), therefore L_c = lognormal(28, 199 cfu/product). Due to the lognormal distribution of the data the expected mean value is larger than the median value of 4 cfu/product calculated earlier.
The obtained lognormal distribution of the actual airborne concentrations can be used to evaluate the probability of becoming ill after consumption of sliced meat that is exposed to the air. This probability can for example be calculated with the exponential dose-response model:

$$P_{\text{inf}} = 1 - \exp\left(-rL_c\right) \quad (8)$$

with r the probability of causing an infection to the consumer [133]. Assuming r is 1E-10 and using L_c = lognormal(28, 199), the average probability of illness (P_{inf}) is 2.73E-9 with a 90% confidence interval between 1.49E-11 and 1.02E-8 per consumed slice of meat (obtained with Monte Carlo simulations). This is just an example of how the airborne model can be applied in risk assessments.

Since the practical contamination levels are not known, it is not possible to directly verify the results of the model calculations. However, for an open air system, the results seem to give the right order of magnitude. For an aseptic process, L_c is reported to be around 10^{-3} [143]. Whyte [141] determined the actual contamination level for the pharmaceutical industry by filling 9000 bottles with an area of 0.4 cm^2 and an exposure time of 20 min with a sterile medium. After incubation, the number of contaminated bottles was counted. This measured contamination level coincided well with their estimated contamination level. The obtained contamination levels were much lower (between 4.3E-4 and 1.12E-2 cfu) than the ones estimated in the food examples of the current study, since the exposure areas of the bottles used in the pharmaceutical experiment were much smaller (largest area was 4 cm^2) than the exposure areas of the food products. It would therefore be useful to

obtain more data on measured contamination levels for different food products in order to validate the estimated contamination levels in this study.

3.6 What-if scenario's

When a certain L_c should not be exceeded in a factory, the different parameters in equation 4 can be investigated to see which parameter is the most critical in controlling or decreasing the L_c. Although in specific cases, for example in forced flow conditions or air currents due to temperature differences, the settling velocity will vary, in this study, the settling velocity is assumed to be a constant parameter. The exposure area can vary in the order of magnitude from 1E-4 m^2 for a small bottle to 0.1 m^2 for a large cheese (or various m^2 for open tanks in a factory). This results in average bacterial L_c between 6.3E-4 cfu to 6.3E-1 cfu for different sized products (assuming an exposure time of 1 s and calculated for the high counts category) due to the linear relationship between the exposed area and L_c. Exposure times can vary between 1 s for UHT milk to 37 minutes for pizza's resulting in average L_c for the high counts category of 6.3E-4 to 0.37 cfu (assuming an area of 1E-4 m^2). The different combinations of areas and times are given in figure 4.

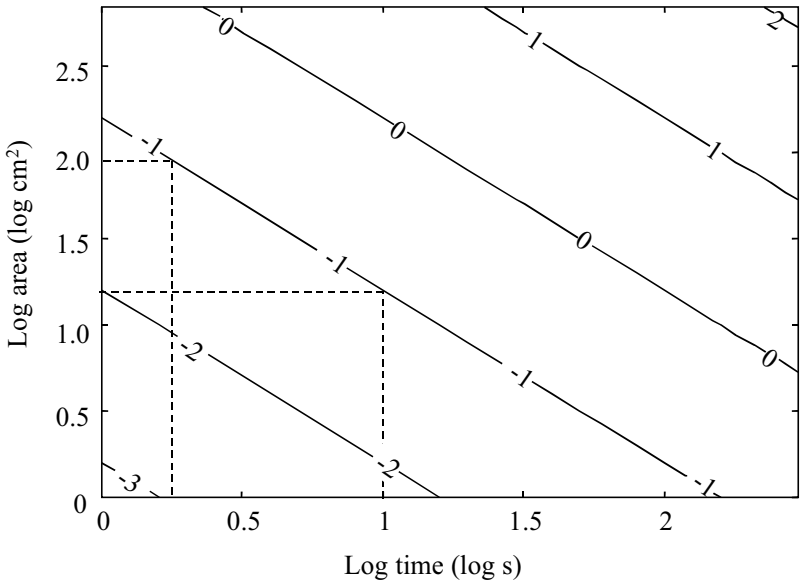

Figure 4. Estimated average bacterial contamination levels (log cfu/product) of meat products in the high counts category for different exposed areas and times. Dashed lines represent an example where the contamination level should not exceed –1 log cfu. The exposure time is either 0.2 log s (1.6 s) or 1 log s (10 s) corresponding to an exposure area of respectively 2 log cm^2 (100 cm^2) or 1.2 log cm^2 (16 cm^2).

This figure can be used to supply design criteria to control a certain average L_c value for meat products in the high counts category. Given a certain number of bacteria in the air, the L_c can be reduced by either changing the exposed area of the product or reducing the exposure time. The order of magnitude necessary for either of the parameters can be found

in figure 4. For example, in order to obtain an average log L_c of –1 (L_c = 0.1 cfu) using a product with an area of 100 cm^2 (log A = 2 cm^2), the exposure time should not exceed 1.6 s (log t = 0.2 s). The same contamination level can be achieved at an exposure time of 10s (log t = 1 s) and an exposed area of 16 cm^2 (log A = 1.2 cm^2).

The contamination level is also influenced by the airborne concentrations. C_{air} for bacteria can vary between 1.2 log cfu m^{-3} (lowest count in the low counts category) and 4.43 log cfu m^{-3} (highest count in high counts category). The average contamination level per m^2 per second is then between 4.04E-2 and 69 cfu $m^{-2}s^{-1}$.

When L_c in comparison to other sources is relevant, this factor has to be limited by adjusting C_{air}, t or A according to practical possibilities. In existing production facilities, the exposed area and probably also the exposure time are a fact. Then the most important factor determining L_c is C_{air}, which can be reduced by applying GMP procedures. This can be done by appropriate cleaning procedures, using filters, controlling or elimination of floor drains, using airflows that flow from clean areas to dirty areas and other GMP procedures [1, 48, 80].

For newly developed products or processes, apart from the airborne concentrations, the exposed area and time of the product can also be influenced to reduce the contamination level (as given in figure 4).

Further research may relate the air circulation and conditioning characteristics to local concentrations. This may lead to a further quantification of recontamination via the air.

4. Conclusions

This paper tentatively describes the quantitative estimation of the probability of recontamination via the air. Statistical analysis showed that the season of sampling influenced the level of airborne micro-organisms. It was, however, assumed that this effect is already incorporated in the variability of the samples and it was therefore not included in further calculations.

Both for bacteria and moulds, the airborne concentrations of different product groups could be classified in low, medium and high counts and could be described with a lognormal distribution with different *mu* and σ for each of the 3 categories.

In contrast to the level of airborne micro-organisms, there were no significant differences between different products, seasons or type of micro-organisms for the settling velocity. This settling velocity was also described with a lognormal distribution.

The level of contamination via the air was estimated for 3 example products, using Monte Carlo simulations with the obtained lognormal distributions for airborne concentrations and settling velocity as input parameters. This showed that the type of product and processing conditions strongly influences the contamination level.

What-if scenarios were performed to determine which parameter is best adjusted to minimise the contamination level due to airborne exposure. In existing production

facilities, GMP procedures can be applied to minimise concentrations of airborne micro-organisms.
The proposed quantification based on the airborne contamination model of Whyte [141] proved to be useful to obtain clues for intervention in reducing airborne contamination. Furthermore, it can be incorporated in a total farm-to-fork MRA, so that different contamination sources can be compared and the risk of consuming contaminated food due to airborne exposure can be estimated.

Acknowledgements
We are grateful to Gerrit Gort (Wageningen University) and Jan Hoekstra (Friesland Coberco Dairy Foods) for their contributions to this work.

Nomenclature

A: exposed product area projected on a horizontal plane (m^2)
C_{air}: concentration of micro-organisms in the air (cfu m^{-3})
d_p: diameter of the falling particle (m)
g: gravitational acceleration (m s^{-2})
L_c: contamination level (cfu/product)
mu: average airborne concentration of the log transformed data (log cfu m^{-3})
mu_l: average airborne concentration of the non-transformed data (cfu m^{-3})
N_f: number of factories sampled (-)
N_s: total number of samples taken (-)
P_{inf}: probability of illness (-)
r: probability of causing an infection (-)
S_R: sedimentation flux (cfu $m^{-2}h^{-1}$)
t: exposed time (s)
$t_{df,1-0.5\alpha}$:Student's t value with df degrees of freedom and confidence level α
v_s: settling velocity (m s^{-1})
η_{air}: viscosity of the air (Pa s)
ρ_{air}: density of the air (kg m^{-3})
ρ_p: density of the particle (kg m^{-3})
σ: standard deviation of the log transformed data (log cfu m^{-3})
σ_l: standard deviation of the non-transformed data (cfu m^{-3})

5

Modelling the effect of water recycling on the quality of potato products

Esther D. den Aantrekker, Albert van der Padt, Remko M. Boom

Abstract

Purifying and recycling process water is a way to minimise the use of potable water and the production of wastewater in the food industry. Water recycling should however never affect the quality of the final products. Therefore, a model is developed to investigate the possibilities of water recycling in a potato factory. One problem that could arise in a water recycling system is the accumulation of dissolved components, such as salts, in the process water loop, which would affect the product quality. Therefore, the quality of the potato products is associated with the amount of chloride ions present in the final product.

The model described in this article is based on mass balances; instationary diffusion is used to calculate the amount of chloride ions present in the process water and in the final product. The calculations show that chloride ions do accumulate in the water and in the potatoes during recycling, due to the addition of salts to the system. The approach used in this article proved to be a useful tool to obtain quantitative information of the process and find critical points in the system.

Accepted in the International Journal of Food Science & Technology

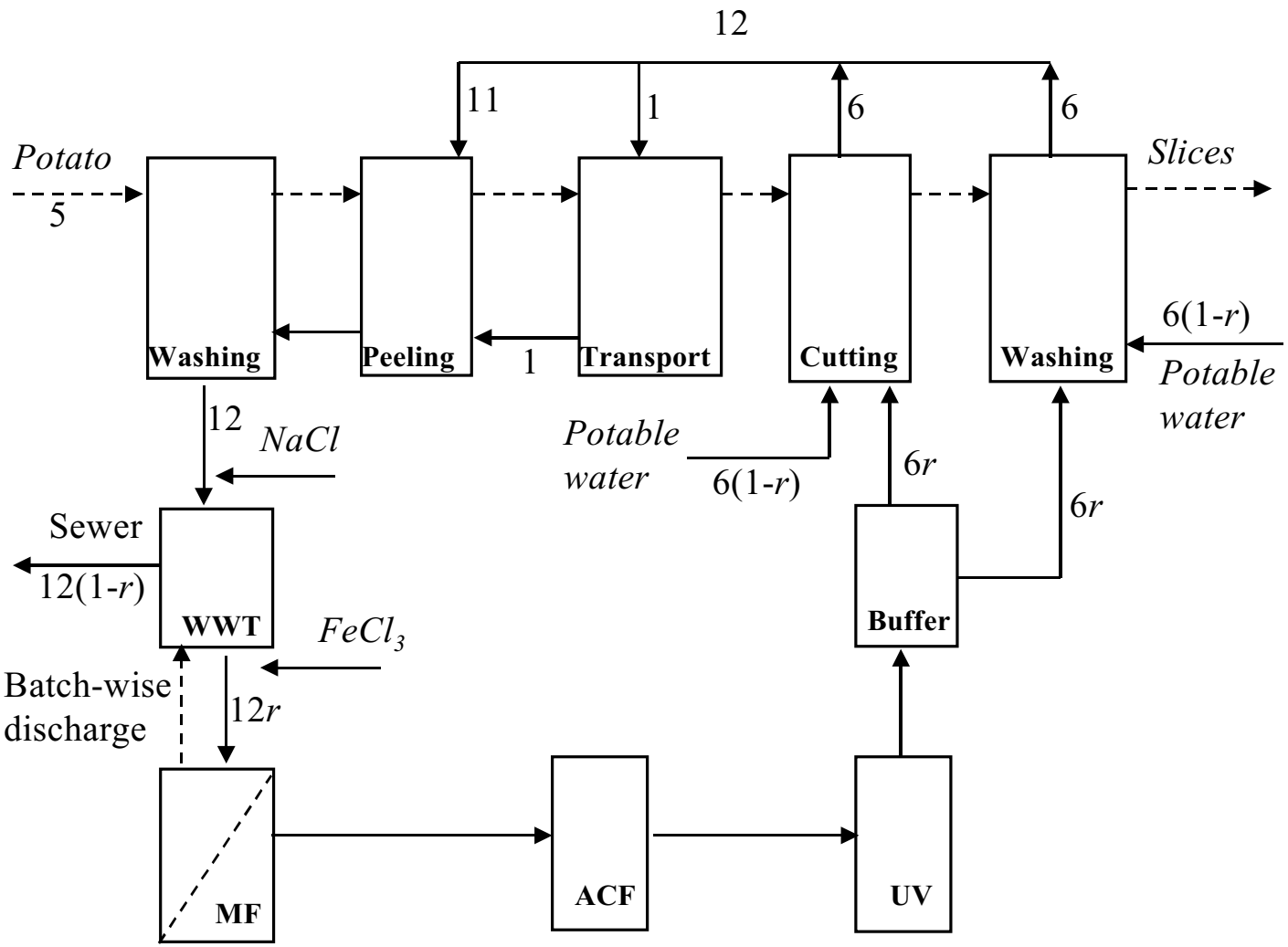

Figure 1. Production process of a potato factory together with the recycling system of the water. The flows ($m^3\ h^{-1}$) are given for each stream; r is the fraction of recycled water. WWT = wastewater treatment, MF = membrane filter, ACF = active carbon filter, UV = ultraviolet disinfection. The potatoes flow from left to right (dashed line) and the water in the opposite direction (solid line).

1. Introduction

Since environmental regulations are getting stricter, routes should be found to minimise the emission of wastewater in the food industry. This can be done either by reusing the water within the production process for example by using counter current systems within a production process or by recycling the water. Water recycling can be achieved by purifying the factory effluent to potable water quality and reusing this water in the production area so that the water system is closed. Water recycling systems are already widely used and investigated in the paper industry [2, 6] and the textile industry [118]. In the food industry, however, water systems are not closed yet and only water reuse within the production process is applied. Examples can be found in the blanching process of vegetables [125], in the production of a high dietary powder [72] and in the processing of shrimps [92].

Water system closure can only be applied if it does not affect the quality of the final products. In order to investigate the possibilities of system closure in food factories, it is important to obtain quantitative insight into these recycling processes and to determine the critical steps in the system. Maté and Singh [84] simulated a water recycling system with mathematical models in order to determine the effect of water recycling on the quality of the washing water in a peach canning plant. However, not only the water quality itself is important, but also the interaction of the water with the product. Therefore, the effect of water recycling should be examined for both water and product quality. Such information can be obtained by conducting an overall process evaluation. This approach has already been successfully applied to evaluate the microbiological safety of food processing steps [148]. In the present paper, the same approach is used to determine the effect of recycling water on the quality of food products. For this purpose, the potato industry is chosen as a case study. Chloride ions are chosen as a model compound related to the quality of the potato products, since salts are known to affect the texture of fruits and vegetables [128].

The potato factory studied currently uses a combination of counter current and cross flow within the production process and drains 100% of the process water to the sewer. A simplified flow chart of the potato and water flows in the factory is given in Figure 1. It should be noted that each process step is a co-current operation, since water is used to transport the potato slices. Potatoes enter the system on the left side where they are washed, peeled, sliced and washed again. Water enters on the right-hand side. A counter current process already ensures a minimal water use within the production process. An almost complete elimination of water use and drainage can be obtained by purifying the process water after the wastewater treatment step (WWT) and reusing this water in the production process. Triqua BV (Wageningen, the Netherlands) developed a purification system using a membrane filtration system (MF) with a pore diameter of 0.01 μm to remove suspended particles, active carbon filters (ACF) to remove dissolved chromophores and a UV-disinfection step (UV) to inactivate bacteria. In this recycling system, chloride ions are

introduced before the WWT and prior to the MF where ferric chloride is added to flocculate the suspended material (see Figure 1). This process guarantees both an effective removal of COD and a very good reduction of micro-organisms.

The different process steps in the potato handling and the recycling system have to be modelled to obtain an overall process evaluation of the implementation of this recycling system. Therefore, the aim of this work is the development of a simple model that can predict the accumulation of chloride ions during the recycling of process water in a potato factory. This model can then be used to obtain quantitative insight into the recycling process and to determine the critical steps in the process.

2. Theory

The potato factory consists of a water stream and a potato stream, which are contacted in a counter current fashion. In order to model the effect of water recycling on the product quality, both streams have to be taken into account.

Several assumptions are made in order to model the whole recycling process. The calculated chloride concentrations will therefore be an estimate of the real chloride concentrations. However, estimations can often help to determine critical steps in the process.

Since the aim of the work was to develop a simple model for the estimation of the chloride concentration, the wastewater treatment itself is assumed to have no effect on the chloride concentration. This is a ‘worst-case’ approach.

Another assumption is that the chloride ions are capable of passing the membrane filter, active carbon filters and the UV-disinfection step. These assumptions were confirmed by chloride measurements in an end-of-pipe set-up, which showed that the chloride concentration did not change during these purification steps (data not shown). This implies that only the residence time distribution of the recycling system has to be taken into account. Therefore, for the development of the model only the process steps in the potato factory are used.

At each process step, plug flow is assumed for both the potatoes and the water. This plug flow was approached by 5 ideally stirred tank reactors. Since the aim was to develop a simple model predicting the accumulation of chloride ions, it was assumed that the geometry of the potatoes does not change during the process. Therefore, the potatoes are assumed to be slices from the first production step (where the potatoes are washed) to the last step (where the slices are washed) and these slices are regarded as infinite slabs. This is justified by the fact that after the typical residence time, the chloride ions have not yet reached the centre of the potato slices. These simplifying assumptions again represent a ‘worst-case’ approach.

The quality of the water influences the product quality by exchange of compounds between the water and the potatoes due to diffusion. By calculating the Biot number for mass transfer (*Bi* = 24; calculations not shown) the main resistance of transfer of the chloride diffusion was found to be inside the potato itself and not in the film layer of water surrounding the potato. The diffusion process within the potatoes can be calculated with transient diffusion, which gives the change in chloride concentration in time and in place:

$$\frac{\partial C_p}{\partial t} = D\frac{\partial^2 C_p}{\partial x^2} \tag{1}$$

with C_p the chloride concentration in the potatoes (kg m^{-3}), x the depth in the slice (m), t is the time (s) and D the diffusion coefficient for salt in potatoes (m^2 s^{-1}).

Equation 1 is solved numerically with Euler centred spatially estimates [24]:

$$D\frac{\partial^2 C_p}{\partial x^2} \approx D\frac{C_p(x+\Delta x)-C_p(x)}{(\Delta x)^2} + D\frac{C_P(x-\Delta x)-C_P(x)}{(\Delta x)^2} \tag{2}$$

The error associated with the numerical estimation was less than 10% compared to the analytical solution, which is sufficient for our purposes.

Diffusion into the potatoes is calculated by dividing the potato slices in two halves (plane symmetry) and each half in five equidistant layers of thickness (Δx). Each potato layer is denoted as i and flows from left to right from one vessel to the next, within each process step. The different vessels are denoted as j. Diffusion within the potato slices only takes places in the x-direction (from the bottom to the top). Water from the next process step enters on the left side and exchanges chloride ions with the first layer of potatoes in each vessel. This approach is applied for each individual process step and is visualised in Figure 2.

Combining plug flow and diffusion, the chloride concentration in the potatoes can be calculated with:

$$V_{pl}\frac{\mathrm{d}C_p(i,j)}{\mathrm{d}t} = \phi_{pl}\left(C_p(i,j-1)-C_p(i,j)\right) + V_{pl}D\frac{C_p(i+1,j)-C_p(i,j)}{(\Delta x)^2} + V_{pl}D\frac{C_p(i-1,j)-C_p(i,j)}{(\Delta x)^2} \tag{3}$$

accumulation in out diffusion

with ϕ_{pl} the flow rate of a potato layer (m^3 s^{-1}), V_{pl} the volume of a potato layer (m^3), Δx layer thickness (m) and $C_p(i,j)$ the concentration of chloride in the potatoes in layer i (i = 1 to 5) and vessel j (j = 1 to 5) in kg m^{-3}. At i = 1, $C_p(i-1,j)$ is equal to the chloride concentration in the water ($C_w(j)$) and at i = 5 (centre slice), $C_p(i+1,j)$ is assumed to be $C_p(i,j)$ indicating symmetry between two potato halves. When j = 1, $C_p(i, j-1)$ is the concentration in the potato slice leaving the previous process step.

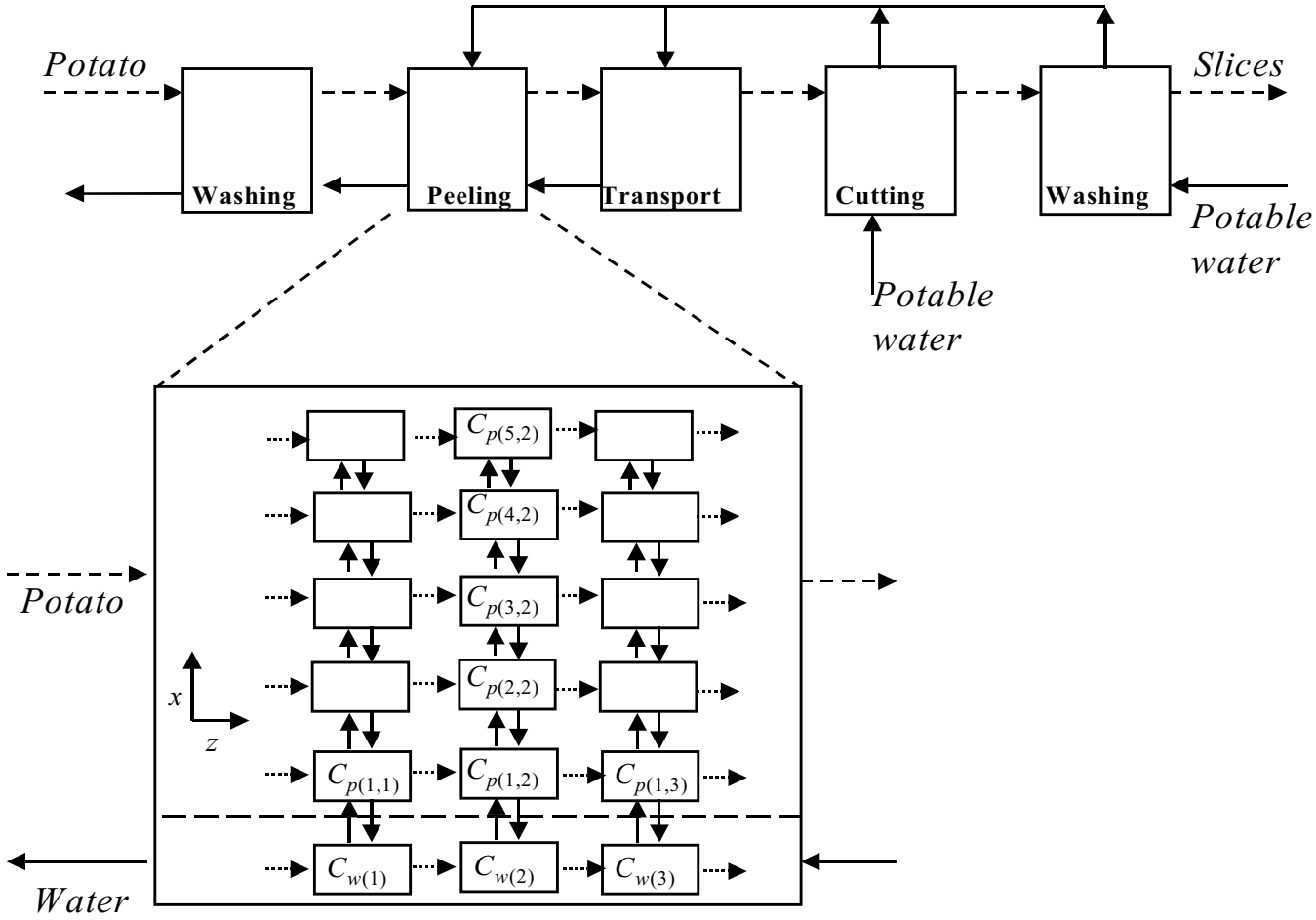

Figure 2. Modelling approach for the production process. The potatoes are divided in 5 layers (i = 1 to 5) and also in 5 vessels (j = 1 to 5), which gives a matrix of 5x5 for each process step. Each layer of potatoes flows from left to right (z-direction) and diffusion takes place from below to above (x-direction). The water is divided in 5 vessels (j =1 to 5) and flows from left to right within a process stage. In this figure the flow is given for j = 1 to 3 and diffusion is given for the second vessel (j= 2 and i = 1 to 5).

The concentration of chloride in the water can be calculated by using the general balance: accumulation = in – out + transfer. Transfer only takes place in the first layer of potatoes. Therefore: $J = -D\frac{\partial C_p}{\partial x}$. The chloride concentration in the water can then be calculated with:

$$V_w \frac{\mathrm{d}C_w(j)}{\mathrm{d}t} = \phi_w \left(C_w(j-1) - C_w(j)\right) - A_p D \frac{\partial C_p}{\partial x} \qquad (4)$$

accumulation in out exchange with potatoes

with V_w the water volume (m^3), $C_w(j)$ the chloride concentration in the water in vessel j (j = 1 to 5) in (kg m^{-3}), ϕ_w the water flow rate(m^3 s^{-1}) and A_p the exchange area of the potatoes (m^2).

This equation can be rewritten (using $\tau = V/\phi$ and $A_p = V_p/d_p$) as:

$$\frac{\mathrm{d}C_w(j)}{\mathrm{d}t} = \frac{C_w(j-1) - C_w(j)}{\tau_w} - \frac{\tau_p \phi_p}{\tau_w \phi_w} \frac{D}{d_p} \frac{C_w(j) - C_p(1,j)}{\Delta x} \qquad (5)$$

with V the volume of water or potato slices (m^3), ϕ the water or potato flow rate (m^3 s^{-1}), τ_w the residence time for water (s), τ_p the residence time for potatoes (s) and d_p the thickness of the potato slices (m).

The chloride concentrations in the different production steps are calculated with equation 3 (for the potatoes) and 5 (for the process water). These equations are solved numerically by using the *ode15s* solver in Matlab/Simulink software (The MathWorks Inc., Natick, USA).

Parameter values

The water flow rate (ϕ_w) and residence times of the potatoes (τ_p) and the water (τ_w) were measured at each process step (Table 1). The residence time of the potato layers (τ_{pl} for equation 3) is equal to the residence time of the whole potato slices (τ_p). The potato flow rate (ϕ_p) was constant during the production process at a level of 5 m^3 h^{-1}. The diffusion coefficient was assumed to be 4.2 10^{-10} m^2 s^{-1} [135]. The initial chloride concentration in the potatoes entering the factory ($C_p(0)$) was measured to be 0.035 kg m^{-3}. The initial chloride concentration in the water ($C_w(0)$) was measured to be 0.117 kg m^{-3}. The thickness (d_p) of the potato slices was estimated to be 1.5 mm.

Table 1. Process step depending parameters for the chloride model (measurements potato factory).

Parameter	Washing potatoes	Peeling	Transport	Cutting	Washing slices
τ_p (s)	270	40	5	10	15
τ_w (s)	1800	40	1200	360	750
ϕ_w ($m^3\ s^{-1}$)	3.33E-3	3.33E-3	2.78E-4	1.67E-3	1.67E-3

After the production process the water goes to the WWT where chloride is added at 9 g m^{-3}. Before the MF stage, 16 g of chloride is added to 1 m^3 of the water flow to achieve flocculation. The addition of these salts is incorporated in the model.

3. Results and discussion

In order to compare the effect of recycling to the current process without recycling, the chloride concentrations were first calculated for the case where there is no recycling. Subsequently, the effect of 67% and 100% recycling was calculated and compared with the current situation.

No recycling

Since potable water contains more chloride (0.117 kg m^{-3}) than the potatoes initially do (0.035 kg m^{-3}), the potatoes take up chloride from the water. Therefore, it was expected that the chloride concentration in the potatoes would increase during the contact time between potato and water and the concentration in the water would decrease during the contact time.

Indeed, for the current process, the model predictions show that during production, the average chloride concentration in the potatoes increased from 0.035 kg m^{-3} to 0.070 kg m^{-3} and the average chloride concentration in the water dropped to 0.116 kg m^{-3} at the last process step. Figure 3 gives the change in chloride concentration during the start-up of the process, calculated at the end of the production line (where the potato slices are washed). It is assumed that at the start of the production process, the factory is filled with ‘native’ potatoes (with a chloride concentration of 0.035 kg m^{-3}).

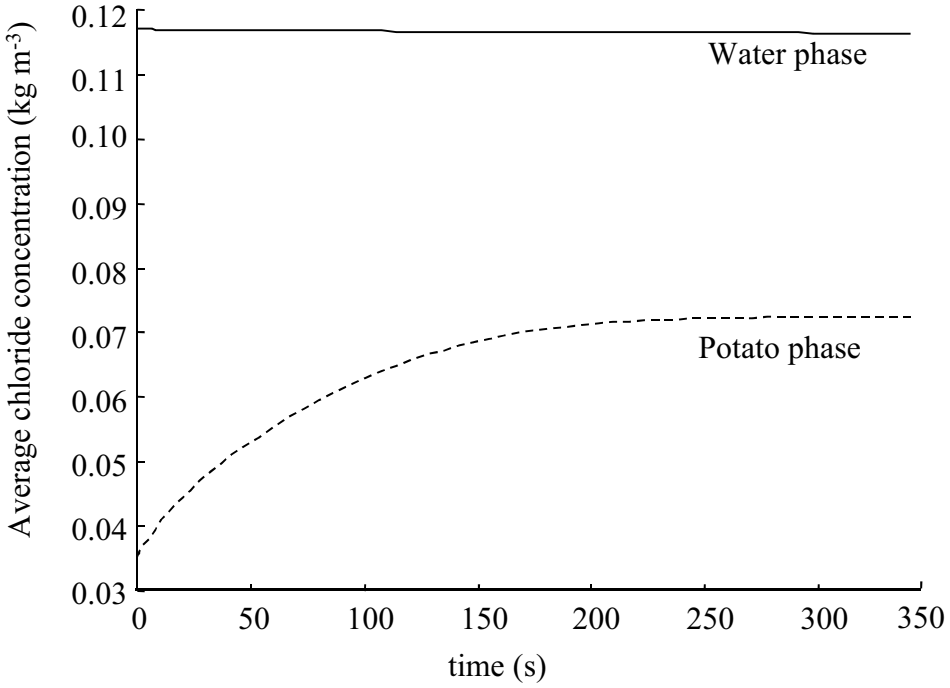

Figure 3. Change in chloride concentration at the last process step (washing slices) for 0% recycling; calculations were made for the time the potatoes are in the production process, which is 340 s. The solid line gives the chloride concentration in the water and the dashed line for the potatoes. Initial condition: all potatoes have a concentration of $C_p(i,j)|_{ini} = C_p(0)$ and $C_w(i)|_{ini} = C_w(0)$ at all process steps.

In order to find where the increase of chlorides took place in the potatoes, the chloride concentration was plotted versus the potato slice layer (i = 1 to 5) for each process step. Since diffusion is two-sided the chloride profile in the potatoes is the same in each potato half. Figure 4 shows that the most critical step is the first step (where the potatoes are washed). Here, the potatoes contact the water for the first time. Because of the large concentration difference between the water (C_w = 0.116 kg m^{-3}) and the potatoes (C_p = 0.035 kg m^{-3}), there is a large driving force for the exchange of chlorides. The residence time is also quite large in this step compared to the other steps. Therefore, most chlorides are exchanged in this first step. This explains why the chloride concentration in the potatoes reaches a steady state condition as could be seen in figure 3.

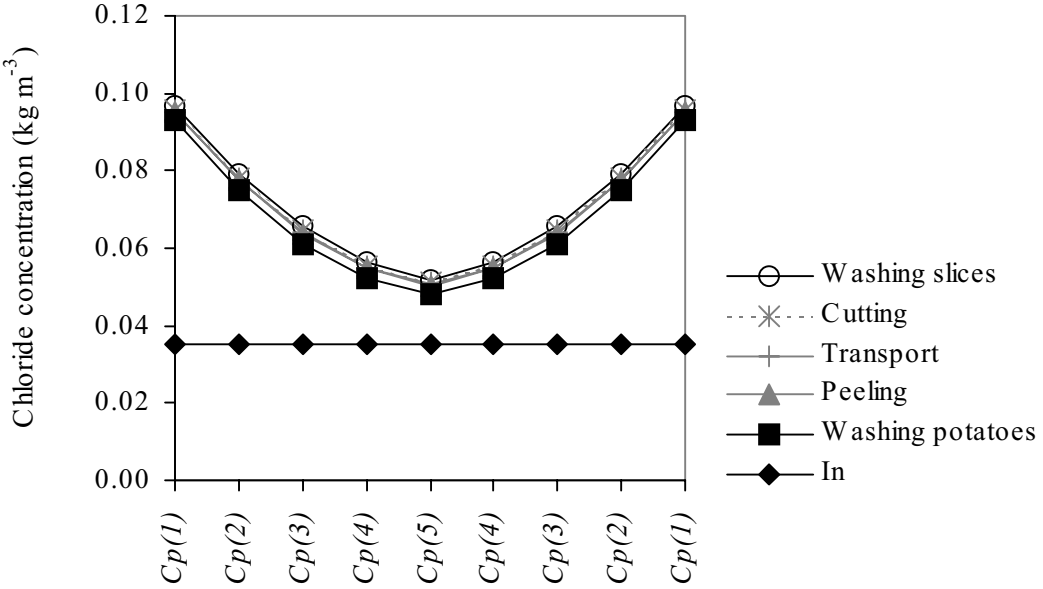

Figure 4. Chloride concentration profiles for every potato slice layer ($C_p(1)$ to $C_p(5)$), per process step in the no-recycle case. 'In' indicates the initial chloride concentration in the potato slice layers.

Recycling

The recycling processes were calculated for a time period necessary to reach a steady state condition (the condition in which the concentrations in the water and in the potatoes did not change anymore).

When 67% recycled water was used in the production process, the chloride concentration in the potatoes and in the water increased to C_p = 0.075 kg m^{-3} and C_w = 0.129 kg m^{-3}, respectively. This represents an increase in chloride concentration of 7% for the potatoes compared to the previous case. Steady state was reached after 7 recycling loops.

A recycling percentage of 100% gave a further increase in the chloride concentration to 0.091 kg m^{-3} in the potatoes and 0.167 kg m^{-3} in the water, corresponding to an increase of 30%. This increase in the recycling system could have been caused by the addition of chloride in the system. When water is recycled, these chlorides will accumulate in the water and will also cause an increase in chlorides in the potatoes due to diffusion. Finally, the chlorides will leave the system in the potato slices.

In order to test this hypothesis, the chloride concentration was calculated in case of 100% recycling without added salts. Table 2 shows that in this case all the chlorides are washed out by the potatoes and finally the water reached the same chloride concentration as the potatoes. This steady state condition was reached when the water was recycled 24 times.

Table 2. Predicted chloride concentrations for different percentages of recycled water at the last process step.

% recycled water	% potable water	C_p (kg m^{-3})	C_w (kg m^{-3})	% Increase[a]
initial concentration		0.035	0.117	
0	100	0.070	0.116	
67	33	0.075	0.129	+7%
100	0	0.091	0.167	+30%
100[b]	0	0.035	0.035	-50%

[a] : percentage increase compared to the current system for the chloride concentration in the potatoes

[b] : no salts added

C_p : average chloride concentration in the potato slices

C_w : average chloride concentration in the water

The fact that accumulation of chloride ions in the recycling system is caused by the addition of salts is further confirmed by plotting the chloride concentration versus the process stage in order to find where the increase takes place in the system. Figure 5 shows that the WWT and MF are the critical steps where chlorides are added to the process.

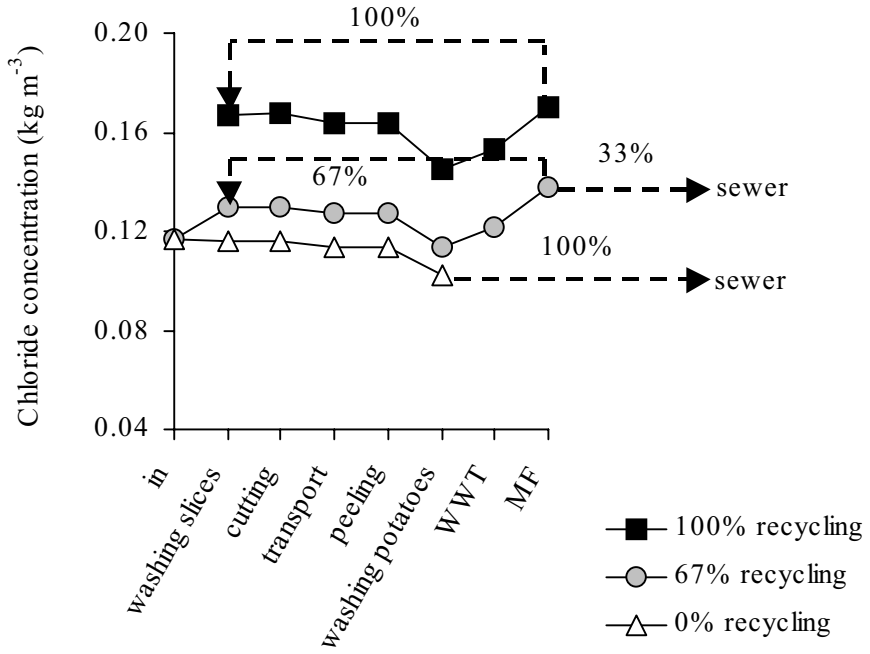

Figure 5. Chloride concentration in water per process step for different percentages of recycling, in case a steady state situation is reached. The arrows indicate the direction of the recycling process and 'in' indicates the potable water entering the factory.

In practice, where recycling systems are applied, an increase of compounds is not uncommon. Zhang et al. [144] for example describe the accumulation of dissolved and colloidal substances in recycled water in the paper industry, caused by the release of these compounds during production. Water recycling in a milk bottle washer also results in an increase in chloride and total dissolved solids concentrations [134].

4. Conclusions

As demonstrated in Figures 4 and 5, an overall process evaluation is a useful tool to obtain quantitative insight into the process and to determine critical points in the process. This case study showed that the modelling approach described by Zwietering and Hasting [148] is not only applicable for micro-organisms but also for other compounds affecting food quality. Since these kind of models contain several simplifying assumptions of reality, they can only be applied to obtain orders of magnitude and can not easily give accurate predictions of reality.

It was found that for the potatoes the most important step is the first step where the potatoes are washed. The most critical step in the recycling process is the addition of salt to the system. Addition of compounds will always lead to accumulation of those compounds in a recycling system; hence this will lead to accumulation of compounds in the product. The amount of accumulation can be controlled by the percentage of water that is recycled or by reducing the addition of salts.

The addition of $FeCl_3$ to the membrane system, however, has to remain at the original level in order to achieve flocculation. Therefore, only the addition of salts prior to the wastewater treatment can be adjusted to make water system closure possible without affecting the product quality.

Thus, it is demonstrated that the developed model can be used to adapt the total process system to assure constant product quality. Instead of chloride ions it is also possible to use the model for other compounds affecting the product quality.

Acknowledgements

The work for this paper was supported by NOVEM. The authors would like to thank the employees of Triqua BV and in particular Lex van Dijk for the co-operation in this work. Dick Goudriaan and Guido Kieven from Smiths Food Group are kindly thanked for their assistance in obtaining the necessary data for the model.

Nomenclature

A_p: area of potatoes (m^2)
C_p: chloride concentration in potatoes (kg m^{-3})
$C_p(0)$: ingoing concentration of chloride in potatoes (kg m^{-3})
C_w: chloride concentration in water (kg m^{-3})
$C_w(0)$: ingoing chloride concentration in potable water (kg m^{-3})
D: diffusion coefficient (m^2 s^{-1})
d_p: thickness of potato slice (m)
J: flux of chloride ions between water and potatoes (kg $m^{-2}s^{-1}$)
V_p: volume of a potato slice (m^3)
V_{pl}: volume of one layer of a potato slice (m^3)
V_w: water volume (m^3)
t: time (s)
x: depth in the potato slice (m)

Greek symbols

Δx: layer thickness (m)
ϕ_p: flow rate of the potato slices (m^3 s^{-1})
ϕ_{pl}: flow rate of one layer of a potato slice (m^3 s^{-1})
ϕ_w: water flow rate (m^3 s^{-1})
τ_p: residence time of the potato slices (s)
τ_{pl}: residence time of one layer of a potato slice (s)
τ_w: residence time of the water (s)

6

Discussion: application of recontamination models

1. Introduction

Over the years, many mathematical models have been developed to describe microbiological processes. One advantage of these predictive models is that they allow a more efficient design of experiments to check safety or shelf life of products. Furthermore, they help to identify knowledge gaps that need further research.

Various models have been developed that describe the effect of temperature, *pH* and water activity on the growth and survival of micro-organisms [131]. These models can be combined with process engineering models to evaluate the effect of food processing steps on microbial spoilage and food safety of the product [148].

The same approach can be used to evaluate processes for other factors than microbiological hazards. An example is given in chapter 5 in which mathematical models are applied in the evaluation of food processing on the final quality of potato products. The application of this type of models allowed an easy detection of the most important steps in the process. Furthermore, the effect of closing the water recycling system could be investigated. This shows the advantage of using predictive models: even potential production processes that are not operational yet can be evaluated for implications on the properties of the final product.

Recently, predictive models have been applied in microbial risk assessment (MRA) to assess the probability of becoming ill after consuming food products. Once a microbial hazard is identified, an exposure assessment is performed to determine the level of the pathogen in the product at the moment of consumption. It is recommended to use a farm-to-fork approach to include all factors influencing the level of pathogens [70]. Apart from growth and inactivation in the production chain, also possibilities for recontamination should be considered, since 25% of all foodborne illnesses were found to be related to recontamination [140]. However, as was described in chapter 2, there are not many recontamination models available to perform this task quantitatively. This thesis, therefore, is aimed to contribute to the quantification of recontamination by the development of models for two recontamination routes. One route is via biofilm formation in food processing equipment (chapter 3) and another route is via the air (chapter 4).

The following sections will give two examples in which the biofilm model and air recontamination model are applied in a process evaluation to assess the importance of recontamination during food production. Since biofilm formation is more important in closed processing systems, section 2 describes the effect of biofilm formation in the production of an acid-based spread. The developed biofilm model yields point estimates (constant single values) for the level of pathogens at the moment of consumption.

Air recontamination can be important in ‘open’ systems in which the product comes into direct contact with the air. Section 3, therefore, describes the effect of aerial recontamination in the production of smoked salmon. The aerial recontamination model was based on stochastic distributions, which will give a distribution of the level of pathogens at the moment of consumption. Stochastic distributions are more realistic than point estimates, since both

variability and uncertainties can be incorporated in the distributions [70]. In section 3 both point estimates and stochastic distributions were used to estimate the level of bacteria at the point of consumption. The outcome of this exposure assessment is combined with dose-response models in section 4 to estimate the probability of becoming ill after consumption of contaminated salmon.
Finally, section 5 focuses on implementation of recontamination models and possibilities for future research to enlarge knowledge about recontamination and improve food safety.

2. Example 1: biofilm formation in acid based spread production

Van Gerwen [129] used acid based spread as an example to demonstrate the usefulness of a stepwise approach determining the most important process steps. According to her hazard identification procedure, *Staphylococcus aureus* was the most important pathogen determining the safety of the product. Since the parameters of our biofilm model are available for *S. aureus* (see chapter 3), this product was chosen to assess the importance of biofilm formation in production equipment. In order to evaluate the overall production process, all process steps were incorporated to assess the possibilities for growth and inactivation. A schematic picture of the production process of acid based spread is given in figure 1.

It is assumed that the different production steps (in figure 1) are batch processes, in which microbial growth can be described by:

$$\frac{dN_P}{dt} = vN_P \qquad (1)$$

with N_P: concentration of bacteria in the product stream (cfu m^{-3})
v: μ_p for $T < T_{max}$ and $-k_p$ for $T > T_{max}$
μ_P: specific growth rate in product stream (s^{-1})
k_P: inactivation parameter in product stream (s^{-1})

Equation 1 can be solved as:

$$N_{Pi} = N_{P(i-1)} \exp(v\tau) \qquad (2)$$

with N_{Pi}: concentration of bacteria at the end of the process step (cfu g^{-1})
$N_{P(i-1)}$: concentration of bacteria at the end of the previous process step (cfu g^{-1})
τ: residence time (s)

The current production process of acid based spread was evaluated using the so-called step characteristic (*SC*), which gives the logarithmic change in bacteria during a process step. *SC* is defined as: log ($N_{Pi}/N_{P(i-1)}$). A large *SC* value for a process step indicates an important step regarding food safety [130].

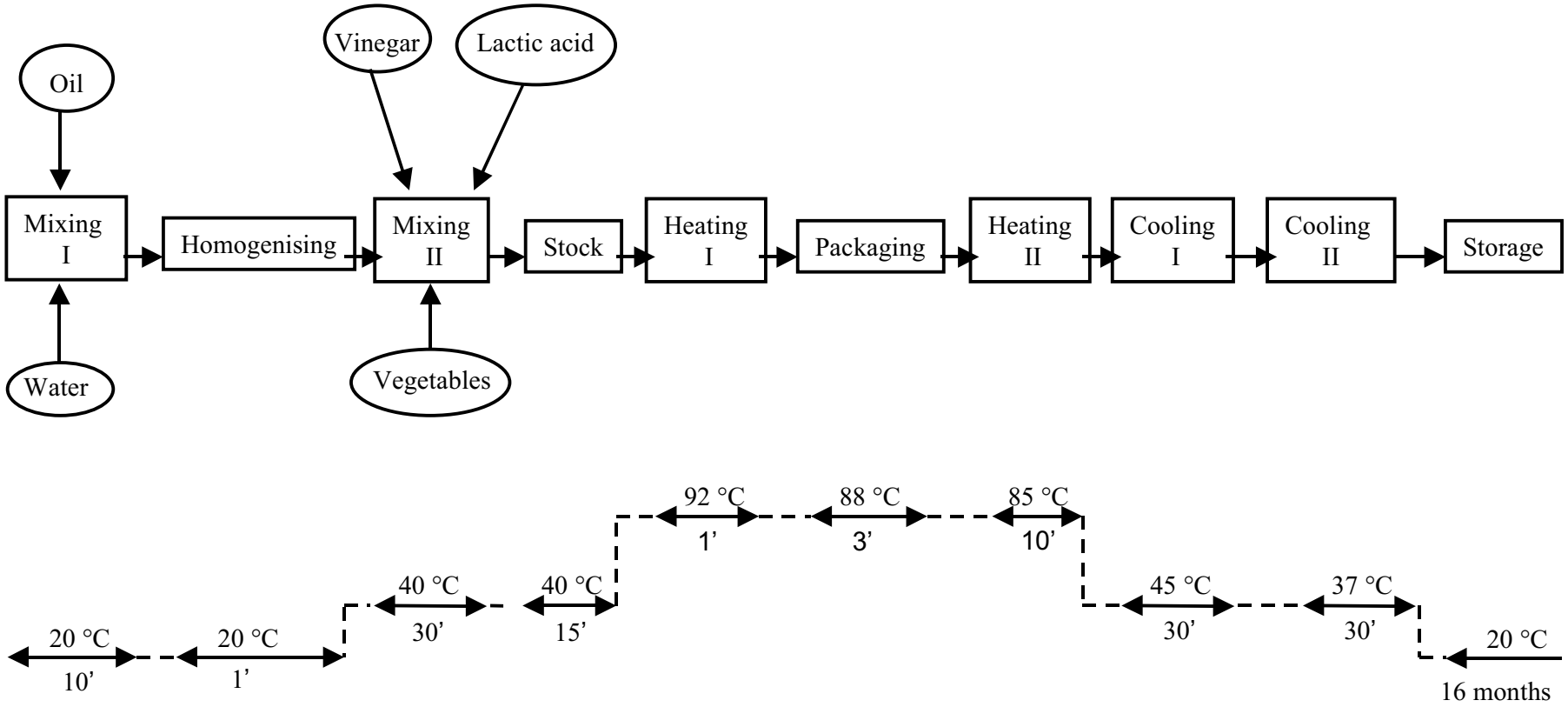

Figure 1. Production process of acid based spread together with residence times (in minutes) and temperatures per process step.

The specific growth rate in each process step (μ_P) is calculated using the cardinal temperature and *pH* model of Rosso et al. [116] with the cardinal factor for temperature (*t(T)*) and *pH* (*p(pH)*). This was combined with the gamma concept of Zwietering et al. [147] to include the effect of water activity on the growth rate ($\gamma(a_w)$):

$$\mu_P = \mu_{opt} t(T) p(pH) \gamma(a_w) \quad (3)$$

The cardinal and gamma factors depend on the product characteristics and the growth characteristics of *S. aureus*. The growth characteristics of *S. aureus* used were: T_{min} = 7 °C, T_{opt} = 37 °C, T_{max} = 48 °C, pH_{min} = 4, pH_{opt} = 6.5, pH_{max} = 10, $a_{w,min}$ = 0.83 and μ_{opt} = 2.3 h^{-1} [58]. For inactivation, an Arrhenius equation was used. The inactivation parameters k_{inf} (inactivation rate at infinite temperature) and *Ea* (activation energy) were estimated using linear regression on *D* values for *S. aureus* in milk [58] and yielded k_{inf} = 3.27E34 s^{-1} and *Ea* = 228.6 kJ mol^{-1}. Since milk has a different *pH*, a_w and fat content than acid based spread, the *D* values might be different for this product. However, *D* values for milk were only used to obtain orders of magnitude for inactivation of *S. aureus*.

The *pH* of the product was 7 before the second mixing step (worst-case estimation). At the second mixing step, vinegar and lactic acid were added resulting in a *pH* of 4.25 (worst-case estimation: rejection value of the product). The water activity of the product was 0.95 in all process steps [129]. The product temperatures and *pH*, together with the residence times in each process step are given in table 1. The obtained *SC* values for the different process steps are also given in table 1.

Table 1. Production process of acid based spread [129] together with step characteristics (*SC*) for the different production steps. An initial concentration of 1 cfu g^{-1} is assumed in the raw product. Bold values indicate important process steps.

	Process step	τ_p	*T* (°C)	*pH*	*v* (h^{-1})	*SC*
1	Mixing 1	10 min	20	7	0.536	0.04
2	Homogenising	1 min	20	7	0.536	0.00
3	Mixing 2	30 min	40	4.25	0.341	0.07
4	Stock/magnet/deaerating	15 min	40	4.25	0.341	0.04
5	Heating 1	1 min	92	4.25	-2.32E5	**<<-20** (-1680)
6	Packaging	3 min	88	4.25	-1.01E5	**<<-20** (-2188)
7	Heating 2	10 min	85	4.25	-5.32E4	**<< -20** (-3855)
8	Cooling 1	30 min	45	4.25	0.195	0.04
9	Cooling 2	30 min	37	4.25	0.359	0.08
10	Storage	16 mnth	20	4.25	0.122	**>>10** (609)

τ_p: residence time of the process step

v: μ_p for $T < T_{max}$ and $-k_p$ for $T > T_{max}$

μ_P: specific growth rate in product stream

k_P: inactivation parameter in product stream

When the current production process without biofilm formation is evaluated, it can be seen that the most important step is the heating step, causing a reduction of much more than 20 log units of *S. aureus*, which is a more than sufficient inactivation of this pathogen. Although the inactivation parameters from another product were used, the predicted order of inactivation is such that it can be assumed that the inactivation is total for acid-based spread.
Another important step is storage, resulting in an increase of 10 log units. This can only occur when the product is recontaminated after the heating step. Since the product is then already packed, such recontamination can only occur at consumer level. Therefore, once the product is opened it should be stored at low temperatures to prevent outgrowth of pathogens that may have re-entered the product.
The *SC* values as calculated in this study were slightly different from the ones obtained by van Gerwen [129]. This is caused by a different choice of the growth model and the parameters of *S. aureus*. For example for the second mixing step van Gerwen [129] found a *SC* value of 0.10 and in this study a value of 0.07 was found. These differences are, however, small and do not influence the conclusion regarding the most important steps in the process.
In order to evaluate the effect of biofilm formation in the production line, it was assumed that there is a stagnant area, where biofilms can be formed, in a pipeline connecting two process steps. A schematic picture is given in figure 2. Bacteria can only be exchanged with the main stream at the point where the stagnant area is connected to the pipeline, which is shown by the dotted lines.

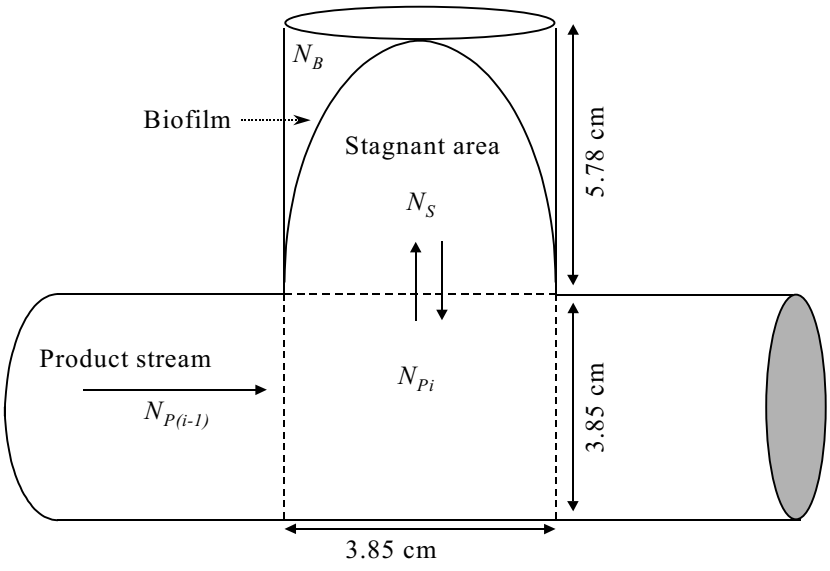

Figure 2. Biofilm formation in a stagnant area and exchange with the product stream (depicted with dotted lines). $N_{P(i-1)}$ is the ingoing concentration of bacteria, N_{Pi} the concentration of bacteria in the product stream, N_s is the concentration of bacteria in the stagnant area and N_B the concentration of bacteria in the biofilm.

The number of *S. aureus* in the product stream can be described using 3 mass balances:

Product phase:

$$\frac{dN_{Pi}}{dt} = \frac{1}{\tau_p}\left(N_{P(i-1)} - N_{Pi}\right) + \frac{\phi_S}{V_P}\left(N_S - N_{Pi}\right) + \mu_p N_{Pi} \quad (4)$$

accumulation in out exchange growth

Stagnant area:

$$\frac{dN_S}{dt} = \frac{1}{\tau_S}\left(N_{Pi} - N_S\right) + a_S k_D N_B^n - a_S k_A N_S + \mu_p N_S \quad (5)$$

accumulation in out desorption adsorption growth

Biofilm phase:

$$\frac{dN_B}{dt} = k_A N_S - k_D N_B^n + \mu_B N_B \quad (6)$$

accumulation adsorption desorption growth

with a_S: specific surface area (surface area divided by the volume of the stagnant area; m^{-1})
k_A: adsorption coefficient ($m\ s^{-1}$)
k_D: desorption coefficient ($m^{2n-2}\ cfu^{1-n} s^{-1}$)
n: power factor for non-linearity of desorption (-)
N_B: concentration of bacteria attached to the wall ($cfu\ m^{-2}$)
N_p: concentration of bacteria in the product stream ($cfu\ m^{-3}$)
$N_{P(i-1)}$: ingoing concentration of bacteria ($cfu\ m^{-3}$)
N_S: concentration of bacteria in the stagnant area ($cfu\ m^{-3}$)
V_P: volume product stream (m^3)
ϕ_S: flow rate into the stagnant area ($m^3\ s^{-1}$)
τ_P: residence time in product stream (s)
τ_S: residence time in stagnant area (s)
μ_P: specific growth rate in product (s^{-1})
μ_B: specific growth rate in biofilm (s^{-1})

Equations 5 and 6 are equal to equations 2 and 4 in chapter 3. In the present case, the biofilm is formed in a stagnant area instead of the inner side of a pipeline introducing an additional mass balance. The product phase (equation 4) was only described for the piece of pipeline in contact with the stagnant area (dotted lines in figure 2). The residence time of this part of the pipeline (τ_P) was incorporated in the model.

Biofilm experiments showed that the growth rate in the biofilm (μ_B) and the desorption coefficient (k_D) increased with the Reynolds number (chapter 3). Therefore, in order to describe biofilm formation in this system, the Reynolds number (Re) in the stagnant area needs to be estimated, which depends on the velocity, density and viscosity of the system.
The diameter of the pipelines transporting the product was 3.85 cm. It was assumed that the stagnant area had the same diameter with a length that is 1.5 times the diameter (5.78 cm). According to Grasshoff [42], the flow rate in the stagnant area is then approximately 10% of the flow rate in the main stream. In this production system, the flow rate in the main stream was 0.72 m s^{-1}, resulting in a flow rate in the stagnant area of 0.072 m s^{-1}.
Assuming a density of 1070 kg m^{-3} and a viscosity of 10.6 Pa.s near the wall (value for mayonnaise), the Reynolds number in the main stream is 3 and in the stagnant area 0.3. It was therefore decided to use the biofilm model parameters as determined for the lowest Re number in chapter 3 (Re = 3). All model parameters are given in table 2.
For this Re number, μ_B was 0.16 h^{-1}, whereas the specific growth rate in the bulk liquid was 0.6 h^{-1} (chapter 3). The ratio between μ_B and μ_P was therefore 0.27. This ratio was used for this production system to calculate the growth rate in the biofilm (μ_B) when the product growth rate (μ_P) is known (as a function of T, pH en a_w, see table 1).

Table 2. Values for biofilm parameters and parameters of the stagnant area.

Parameter	Symbol	Value	Unity
Diameter of stagnant area	d_S	3.85E-2	m
Length of stagnant area	l_S	5.78E-2	m
Specific area of stagnant area	$a_S=A_S/V_S=2/r_S$	103.9	m^{-1}
Flow rate in product stream	ϕ_P	3	$m^3 h^{-1}$
Flow rate in stagnant area	ϕ_S	0.3	$m^3 h^{-1}$
Residence time in product stream	$\tau_P = V_P/\phi_P$	0.054	s
Residence time in stagnant area	$\tau_S = V_S/\phi_S$	0.81	s
Adsorption coefficient	k_A*	7.41E-5	mh^{-1}
Desorption coefficient	k_D*	0.0014	$m^{0.3}cfu^{-0.15} h^{-1}$
Power factor	n*	1.15	-
Ratio between specific growth rates	μ_P/μ_B*	0.27	-

*: parameters obtained from the biofilm model at Re = 3 (chapter 3)

Four different scenarios were calculated assuming biofilm formation at different places in the production process. Simulink in Matlab (The MathWorks Inc, Natick, USA) was used to solve differential equation 1 to assess microbial growth and inactivation in each process step and equations 4 to 6 to evaluate biofilm formation (analogous to Zwietering and Hasting [148]).

It was assumed that no cleaning takes place and biofilms can grow to steady state conditions, which is a worst-case approach. Table 3 gives the results of the different scenarios. Scenario 1 is the current process where no biofilm formation has taken place (as in table 1). Scenario 2 assumes biofilm formation after the first mixing step and scenario 3 assumes biofilm formation prior to the first heating step. In scenario 4, it is assumed that the biofilm is formed inside the first mixing tank. In this case, only equations 5 and 6 were used to model biofilm formation on the wall of the mixing tank. For this scenario, the first mixing tank is modelled as a continuous system. The residence time in the tank (τ_S) is 10 minutes and a_S (the area divided by the volume of the tank) is 6 m^{-1}. All other parameters for equations 5 and 6 (k_A, k_D, n and μ_B/μ_P) are the same as in table 2.

Table 3. Step characteristics (*SC*) for *S. aureus* in the production of acid based spread for various scenarios. An initial concentration of 1 cfu g^{-1} is assumed in the raw product. Bold values indicate important process steps.

	Process step	Scenario1	Scenario 2	Scenario 3	Scenario 4
1	Mixing 1	0.04	0.04	0.04	**6.63**
	Biofilm after mixing 1	-	**3.92**	-	-
2	Homogenising	0.00	0.00	0.00	0.00
3	Mixing 2	0.07	0.07	0.07	0.07
4	Stock/magnet/deaerating	0.04	0.04	0.04	0.04
	Biofilm prior to heating	-	-	**2.30**	-
5	Heating1	<< **-20**[a]	<< **-20**[a]	<< **-20**[a]	<< **-20**[a]

[a]: complete inactivation

Scenario 1: no biofilm formation in the production process

Scenario 2: biofilm formation in a pipeline after the first mixing step

Scenario 3: biofilm formation in a pipeline prior to the heating step

Scenario 4: biofilm formation in the first mixing tank

Table 3 shows that biofilm formation between process step 1 and 2 causes an increase of 3.92 log units (scenario 2). Assuming an initial concentration of 1 cfu g^{-1}, the concentration of *S. aureus* increases to ca. 8 10^3 cfu g^{-1}. This level is inactivated at the heating step, suggesting that the product is still safe to eat. However, at a level of ca. 10^4 cfu g^{-1}, *S. aureus* starts to produce enterotoxins that are not inactivated by the heating step [62]. Furthermore, the concentration of *S. aureus* was much higher in the biofilm (10^9 cfu cm^{-2}), which might cause locally higher toxin levels that could be released to the product phase. This enterotoxin production was not studied further.

When scenarios 2 and 3 are compared, it can be seen that the place of biofilm formation influences the levels of *S. aureus* reached in the product phase. This is mainly caused by the different growth characteristics between the different process steps. In table 1, it can be seen that the specific growth rate in the product is higher in the first two steps compared to the

steps prior to heating. This causes a faster increase in biofilm formation and therefore a larger increase in the product phase. These growth characteristics were obtained in lab experiments using optimal growth media. The number of *S. aureus* in this production process might, therefore, be lower than presented in table 3. In the first mixing tank only water and oil are present, which may not contain enough nutrients to cause high growth of *S. aureus*. In the second mixing tank, acids are added causing a drop in *pH*. Although *S. aureus* can grow and produce toxins above *pH* 4, the type of acid used influences growth [62]. For mayonnaise and salad dressing products that contain acetic acid, such low *pH* values have been reported to inhibit growth of *S. aureus* due to the presence of organic acids [122]. The obtained values in table 3 can therefore be seen as worst-case values.

Scenario 4 shows that a longer residence time causes more biofilm formation and thus a much higher increase in the product stream. An increase of 6.63 log units suggests that enterotoxins can be formed in the mixing tank, which can cause food poisoning. However, these values were calculated for steady state conditions assuming there was no cleaning in the system. Presumably, the tank is cleaned before steady state is reached. The most effective cleaning moment can be obtained by determining the increase in cells during time (figure 3). Assuming that the number of cells in the biofilm should not exceed 10^4 cfu cm^{-2}, figure 3 shows that the mixing tank should be cleaned within 90 hours. The number of *S. aureus* in the product will then be less than 1 log cfu g^{-1}. Regular cleaning can thus reduce the biofilm problem, but in order to prevent biofilm formation, a good hygienic design is more important than regular cleaning.

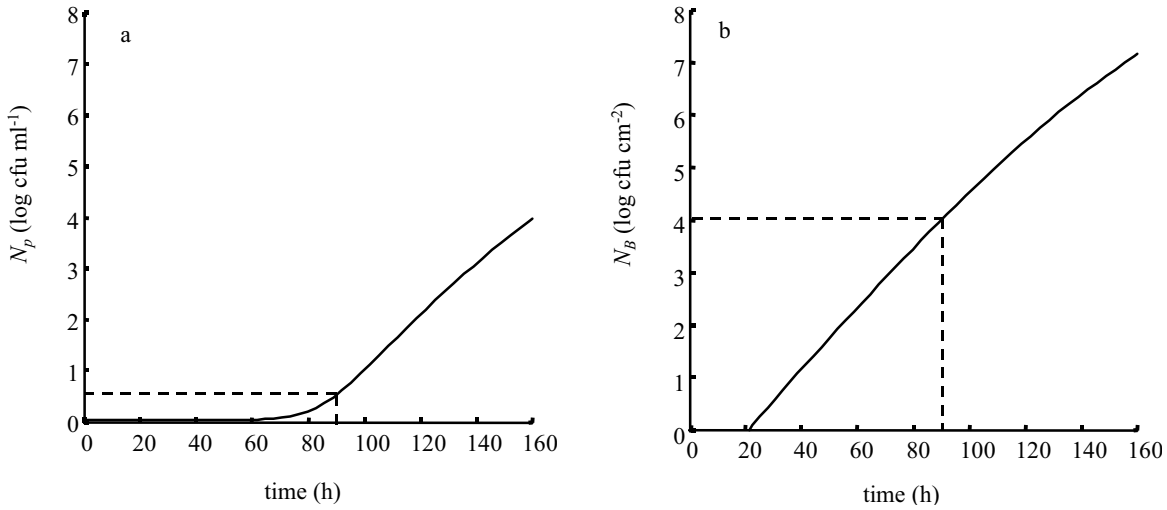

Figure 3. Concentration of *S. aureus* in product (a) and biofilm phase (b) for biofilm formation in the first mixing tank.

Since the different scenarios in table 3 were calculated for steady state conditions, the number of bacteria in the product streams can also be derived directly from the differential equations 4 to 6. For steady state conditions: $dN/dt = 0$, therefore equations 4 to 6 can be combined to obtain:

$$\underset{out}{\phi_P N_{Pi}} = \underset{in}{\phi_P N_{P(i-1)}} + \underset{growth\ product}{\mu_P V_P N_{Pi}} + \underset{growth\ dead\ end}{\mu_P V_S N_S} + \underset{growth\ biofilm}{\mu_B A_S N_B} \quad (7)$$

The number of bacteria in the stagnant area (N_s) can be obtained from equation 6:

$$N_S = \frac{k_D N_B^n - \mu_B N_B}{k_A} \quad (8)$$

For steady state conditions it can be assumed that the biofilm has reached its maximum concentration (N_B = 3 10^9 cfu cm^{-2} as found in chapter 3). Using this assumption, the number of bacteria in the stagnant area can be estimated using equation 8 and the data from tables 1 and 2 (N_S is 9.4 10^8 cfu ml^{-1}). For scenario 2 (following equation 7), the number of bacteria in the product stream results in N_{Pi} = 4.33 log cfu ml^{-1}, which is comparable to the value as obtained with a numerical solution of the differential equations in Matlab/Simulink (N_{Pi} = 3.96 log cfu ml^{-1}).

This shows that for worst-case assumptions, equation 7 and 8 can be used to evaluate the effect of biofilm formation on the product concentration. For the prediction of the right cleaning moment (figure 3), it is essential to use the dynamic equations 4 to 6 instead of equation 7, since steady state conditions have not been reached yet.

The different scenarios used in this example demonstrate that the biofilm model as developed in chapter 3 can be incorporated in a total exposure assessment to determine the level of pathogens at the moment of consumption and investigate whether biofilm formation is important or not. The use of *SC* values showed that this approach is useful to obtain the most important steps in a process line and gain insight in the process. It can, for example, be seen that biofilm formation in a stagnant area in a pipeline with a high flow rate and therefore a short residence time is less important than in a system with a high residence time like the mixing tank. This shows that the hygienic design for such tanks may be even more important than for pipelines. However, in order to determine whether biofilm formation is important or not, not only the product phase should be looked upon, but also the increase in the biofilm phase, since toxins can be formed in the biofilm causing a health problem in the product. This is only important for toxin producing pathogens; for other pathogens the approach of *SC* is sufficient to determine whether increases are acceptable or not.

In this example, the most important production steps were the heating step in which all *S. aureus* were inactivated and the storage step where pathogens that have re-entered the product can grow out to cause problems. However, it was also shown that when biofilms are formed prior to the heating steps high levels of *S. aureus* can be reached locally, which can cause production of enterotoxins. These are not inactivated in the heating step and can thus cause foodborne illness. Therefore, regular cleaning and a good hygienic design are a prerequisite to prevent foodborne diseases.

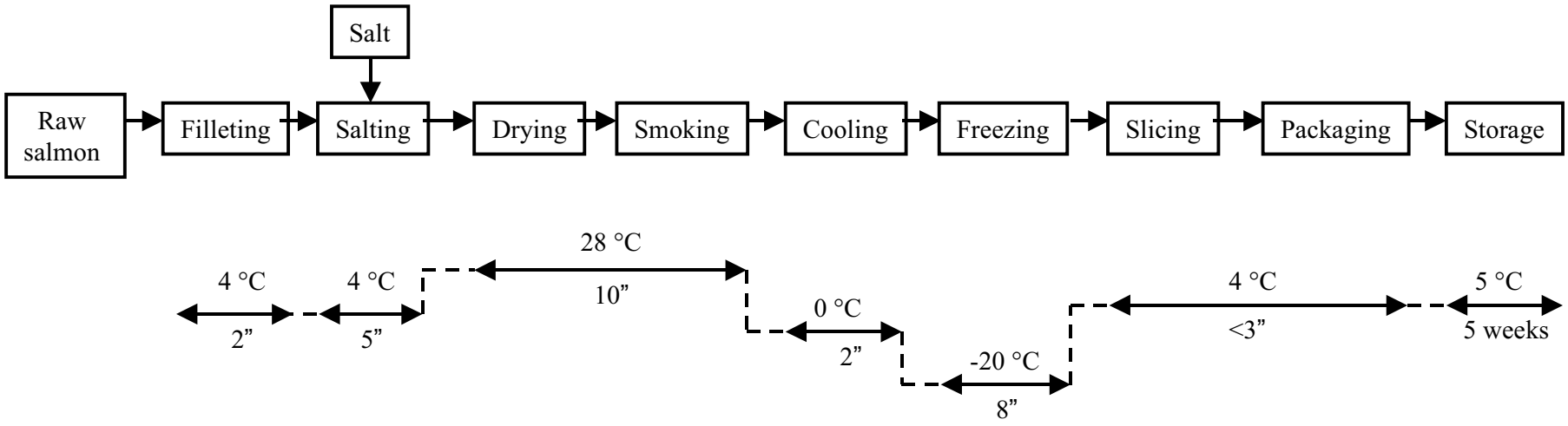

Figure 4. Production process of smoked salmon together with residence times (hours) and temperatures in each step.

3. Example 2: air recontamination and smoked salmon

Air recontamination is more important in open systems where the product comes into contact with the air. Therefore, in order to estimate the effect of recontamination via the air, smoked salmon is chosen as an example product. The most important microbiological hazards regarding the safety of smoked salmon are *Clostridium botulinum* and *Listeria monocytogenes* [41]. However, the combination of low temperatures and 3% NaCl in the water phase, prevents outgrowth of *C. botulinum*. *L. monocytogenes*, however, is capable of growing in the end product, regardless of the low storage temperatures. Indeed some cases of listeriosis have been reported related to the consumption of cold-smoked fish [41]. Therefore, in this study, only *L. monocytogenes* is regarded as a food safety hazard in cold-smoked salmon.

Contamination levels of *L. monocytogenes* in smoked salmon are between 0 and 75% with an overall prevalence of 10% [113]. In some factories, even 100% of the end product is contaminated with *L. monocytogenes* [29, 63]. The exact contamination route is unknown but many researchers state that the factory environment may be the source of contamination rather than the raw product [29, 4, 43].

In this case study, one possible contamination route, namely via the air, was investigated. For each process step a batch system was assumed as in the previous section. The production scheme is given in figure 4.

In order to evaluate the effect of airborne contamination, the airborne contamination model (chapter 4) was incorporated in equation 2 as [146]:

$$N_{Pi} = \left(N_{P(i-1)} + RC\right)\exp(v\tau) \tag{9}$$

with RC the level of recontamination (cfu g^{-1}), which can be calculated using the airborne contamination model (chapter 4):

$$RC = C_{air} v_s A \tau / W \tag{10}$$

with C_{air}: concentration of micro-organisms in the air (cfu m^{-3})
v_s: settling velocity (m s^{-1})
A: exposed product area projected on a horizontal plane (m^2)
W: weight of the product (g)

The weight of the product (W) was introduced in the air contamination model in order to transform the unity of contamination level in cfu g^{-1} instead of cfu per product.

The specific growth rate (μ_P) was calculated as mentioned in the previous section using the characteristics of *L. monocytogenes*: T_{min} = -0.4°C, T_{opt} = 37 °C, T_{max} = 45 °C, pH_{min} = 4.39, pH_{opt} = 7, pH_{max} = 9.4, $a_{w,min}$ = 0.92 and μ_{opt} = 1.01 h^{-1} [58]. The pH of the product was assumed to be 6.3 [115]. The temperature and water activity are given in table 4, for each process step together with the calculated specific growth rate.

Table 4. Production process of smoked salmon.

Process step	τ_P	T (°C)	a_w	μ_P (h^{-1})
Filleting	2 h	4	1	0.020
Salting	5 h	4	0.983[a]	0.016
Drying/Smoking	10 h	28	0.983	0.547
Cooling	2 h	0	0.983	1.3E-4
Freezing	8 h	-20	0.983	0.000
Slicing/Packaging	< 3 h	4	0.983	0.016
Storage	5 weeks	5	0.983	0.023

[a]: at the salting step ca. 3% salt is added (water-phase salt) resulting in a_w of 0.983

Chapter 4 describes the quantification of air contamination in which products were classified in low, medium and high counts categories regarding the concentration of airborne bacteria. Fish products belonged to the meat group, which was classified in the high counts category. The average air concentration for this category was 3.39 log cfu m^{-3} for total viable counts (TVC). Since there is scarce information about the number of pathogens and in particular the number of *L. monocytogenes* in the air, TVC was used to quantify airborne concentrations, which is a worst-case approach as was elucidated in chapter 4. The average log settling velocity was -2.59 log m s^{-1} (chapter 4).

The log values for airborne concentration and settling velocity need to be transformed to actual values in order to incorporate them in equation 10. The average and standard deviations of C_{air} and v_s can be calculated using:

$$mu_l = \exp\left(mu_n + \frac{1}{2}\sigma_n^2 \right) \quad (11)$$

$$\sigma_l^2 = mu_l^2 \left(\exp\left(\sigma_n^2\right) - 1 \right) \quad (12)$$

with mu_n = mu*ln(10) and σ_n = σ*ln(10). mu and σ are the average and standard deviations of the log values.

The normal distribution of the airborne concentration: normal (3.39, 0.73 log cfu m^{-3}) then results in a lognormal distribution with mu_l is 1.01E4 cfu m^{-3} and σ_l is 4.01E4 cfu m^{-3}. It can be seen that the median value of $10^{3.39}$ = 2.45E3 cfu m^{-3} is smaller than the average value of 1.01E4 cfu m^{-3} for the lognormal distribution. For the settling velocity, the normal distribution (-2.59, 0.45 log m s^{-1}) is transformed to a lognormal distribution (4.36E-3, 6.06E-3 m s^{-1}).

The effect of airborne concentration was calculated using as point estimates the average airborne concentration (C_{air} = 1.01E4 cfu m^{-3}) and settling velocity (v_s = 4.36E-3 m s^{-1}). The exposed area (A) is estimated to be 225 cm^2 (12.5 cm * 18 cm). The exposure time is assumed to be equal to the residence time of the process step. The weight (W) of the end product is estimated to be 100 g. RC can therefore be estimated as 9.91E-3 τ (cfu g^{-1}).

Several scenarios were calculated using the same approach with the step characteristics as in section 2. For the model calculations it is assumed that there is no effect of any competitive flora and that the fish has a shelf life of 5 weeks. In the first 2 scenarios, the current production process is calculated without air contamination. The salmon product can only come into contact with the air during the handling steps: filleting, salting or slicing and packaging. In scenarios 3 to 6 the effect of air contamination in either of these handling steps (scenario 3 to 5) or in all handling steps (scenario 6) is evaluated. The results of the model calculations is given in table 5.

Table 5. Step characteristics (*SC*) for *L. monocytogenes* in the production of smoked salmon for various scenarios. An initial concentration of 1 cfu per 10g is assumed on the raw fish. Bold values indicate important process steps.

	Process step	Scenario1	Scenario 2	Scenario 3	Scenario 4	Scenario 5	Scenario 6
1	Filleting	0.02	0.02	**2.87**	0.02	0.02	**2.87**
2	Salting	0.03	0.03	0.03	**3.27**	0.03	0.57
3	Drying/Smoking	**2.38**	0.00	0.00	0.00	0.00	0.00
4	Cooling	0.00	0.00	0.00	0.00	0.00	0.00
5	Freezing	0.00	0.00	0.00	0.00	0.00	0.00
6	Slicing/packaging	0.02	0.02	0.02	0.02	**3.00**	0.16
7	Storage	**6.55**[a]	**8.49**	**6.08**[a]	**5.70**[a]	**5.95**[a]	**5.40**[a]

[a]: These values represent the increase to the maximum concentration (assumed to be 10^8 cfu g^{-1})
Scenario 1: no air contamination in the production process
Scenario 2: no air contamination in the production process and assuming no growth during smoking
Scenario 3: scenario 2 with air contamination in the filleting step
Scenario 4: scenario 2 with air contamination in the salting step
Scenario 5: scenario 2 with air contamination in the slicing step
Scenario 6: scenario 2 with air contamination in the filleting, salting and slicing step

Table 5 shows that most increase takes place during storage, regardless whether or not air contamination takes place. Even when the raw fish is contaminated with only 0.1 cfu g^{-1} this already gives food safety problems after 5 weeks of storage. In the fist scenario, a large increase takes place in the smoking step due to the higher smoking temperature compared to the other steps (table 4). In reality, however, growth in the smoking step is usually not encountered [113, 115]. Smoke contains phenols, which inhibit the growth of *L. monocytogenes* [28]. Since this effect is not incorporated in the calculation of the growth rate (equation 2), it is assumed that the growth rate in the smoking step is zero in the other scenarios.

In scenario 2, even without growth in the smoking step, an initial level of 0.1 cfu g^{-1} in the raw fish causes a more than 8-log increase after 5 weeks of storage. These high levels are, however, never found in naturally contaminated fish [28, 63, 138]. It might be that *L.*

monocytogenes is injured due to the processing steps (like freezing) so that growth is reduced in naturally contaminated cold-smoked fish [28]. Another possibility is the so-called 'Jameson effect': the growth of all micro-organisms on the food is suppressed when the total microbial population achieves the maximum population density characteristic of the food [115]. In naturally contaminated cold-smoked salmon, TVC usually reach levels above 10^6-10^7 cfu g^{-1} within 1 to 2 weeks of storage at 5 °C. These high levels can suppress the growth of *Listeria* [28]. However, challenge tests, in which *L. monocytogenes* is inoculated to smoked fish, have shown that *L. monocytogenes* can indeed grow to high numbers. This demonstrates that when the salmon is infected with undamaged *L. monocytogenes* prior to packaging this may cause a food safety problem [112, 138].
Contamination at the filleting or salting step will therefore in practice probably not cause problems, since *L. monocytogenes* can hardly grow after smoking, cooling and freezing steps. Scenario 5 is then more realistic when undamaged *L. monocytogenes* enters the product after the freezing step, causing a 3-log increase in the fish. During storage this contamination level increases to 10^8 cfu g^{-1}.
Scenario 6 shows that the importance of contamination strongly depends on the level of pathogens already present in the product (equation 9). When the product is contaminated in the filleting step (*RC* is 71 cfu g^{-1}), this results in a level of 74 cfu g^{-1} in the product. Compared to the initial level of 0.1 cfu g^{-1}, this is an almost 1000 times increase. Further steps along the chain then contribute less to the final concentration of *L. monocytogenes* in the fish. Air contamination in the salting step (*RC* is 178 cfu g^{-1}) causes a 4 fold increase and in the slicing step (*RC* is 107 cfu g^{-1}) only 1.5 times increase.

Table 5 shows that air contamination can be an important source of recontamination (*SC* values between 2.9 and 3.3). However, Autio et al. [4] sampled the air in different sections of a salmon factory and could not detect any *Listeria* in the air. The concentration of *Listeria* in the air will, therefore, be much lower than the average airborne concentrations of total viable counts (3.39 log cfu m^{-3}) as assumed in this study. In order to apply the airborne contamination model (equation 9), it is therefore essential to first determine the concentration of *L. monocytogenes* in the air. This can be done using air samplers with a selective medium for *L. monocytogenes*. When counts are too low to detect in an air sampler, settling plates can be used, which give an estimate of the number of bacteria falling from the air in a certain time period. The sensitivity of settling plates can be increased using large plates and sampling times of several hours. A 14 cm settle plate exposed for four hours can detect airborne concentrations of around 1 cfu m^{-3} [142]. Using equation 10 without including the weight factor *W*, the minimum detection times and exposure areas can be determined (figure 5) considering that at least 5 cfu per plate (*RC* = 5 cfu) should be detected in order to obtain reliable results. For example, when the concentration of bacteria in the air is 10 cfu m^{-3} and the exposure time is 1 h the diameter of the settling plate should be at least 20 cm to obtain 5

cfu/plate. Or, when the diameter of the settling plates is 10 cm, the exposure time should be more than 4h to detect 5 cfu/plate.

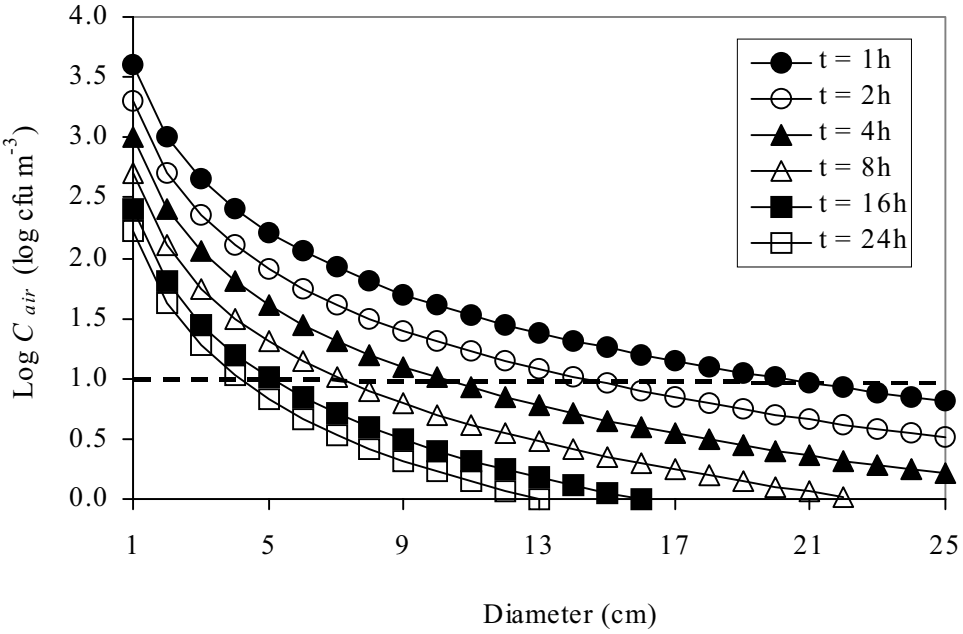

Figure 5. Combinations of exposure time and size of settling plates to obtain settling counts of 5 cfu/plate for different airborne concentrations.

Since no data are available at the moment, it is assumed that only 0.1% of the total concentration of bacteria in the air consists of *L. monocytogenes* (C_{air} is 10.1 cfu m^{-3}). In this case RC = 0.11 cfu g^{-1}, which is comparable to the initial concentration of 0.10 cfu g^{-1}. Therefore, the contamination levels are equilibrated (reducing the air contamination will not have a large impact). The concentration in the sliced fish will reduce around 3 log units to 0.23 cfu g^{-1} for scenario 5 (SC = 0.31). This concentration increases to 7.2 10^{7} cfu g^{-1} in smoked salmon after 5 weeks of storage.

The above described procedure shows that the use of quantitative numbers (as in table 5) compared with other information (e.g. from available literature) and qualitative reasoning helps to highlight the most important steps in the system. It showed that once salmon is contaminated with *L. monocytogenes*, this pathogen can grow out to high numbers in the product. Therefore, either the frequency of recontamination or possibilities for growth should be reduced to improve the safety of the product. The example given in this section shows that such an approach is transparent and makes it easy to challenge and improve the system. Once the most important steps are determined, these can be further quantified and characterised in probability density functions (PDFs) that can be used in an MRA.
The step characteristics as given in table 5 were calculated using average values for airborne concentration and settling velocity as point estimates. When PDFs have to be used, the level

of *L. monocytogenes* in smoked salmon at the point of consumption can be estimated using the lognormal distributions for C_{air} and v_s as defined earlier. Using Monte Carlo simulations for scenario 5 the average concentration of bacteria in the smoked fish prior to storage was found to be: 0.23 cfu g^{-1} with a 90% interval between 0.12 cfu g^{-1} and 0.52 cfu g^{-1}. The average level of *L. monocytogenes* at the moment of consumption is then 7.2 10^7 cfu g^{-1} with a theoretical 90% interval between 3.7 10^7 cfu g^{-1} and 1.6 10^8 cfu g^{-1}.
The advantage of using PDFs instead of point estimates is that they can give relevant information regarding the ranges of the obtained risk estimate, since especially the extreme values can cause illnesses. The assessment of the frequency of these high probability events determines the acceptance of a process rather than the mean or median probabilities [139].
In this case PDFs for concentration of bacteria in the air and settling velocity were obtained by analysing a large data set (chapter 4). However, usually not all PDFs are known to fulfil a complete MRA and several assumptions need to be made. It is then questionable whether a risk estimate based on PDFs yields more reliable results than using point estimates based on mean values or worst-case assumptions. Therefore, to reduce the uncertainty in the outcome of an MRA, it is essential to establish PDFs more accurately for the different steps of an MRA.

For this example product, the outcome of the exposure assessment is coupled to a dose-response relationship in order to estimate the probability of becoming ill after eating smoked salmon contaminated via the air. This is discussed in the following section.

4. Dose-response relationships

The most frequently used dose-response models are the exponential model and the beta-Poisson model [133], graphically presented in figure 6.
Exponential model:

$$P = 1 - \exp\left(-rD_p\right) \tag{13}$$

with D_p: level of micro-organisms at the moment of consumption (cfu/serving)
r: probability of one micro-organism causing infection.

beta-Poisson model:

$$P = 1 - \left(1 + D_P / \beta\right)^{-\alpha} \tag{14}$$

α and β are model parameters.

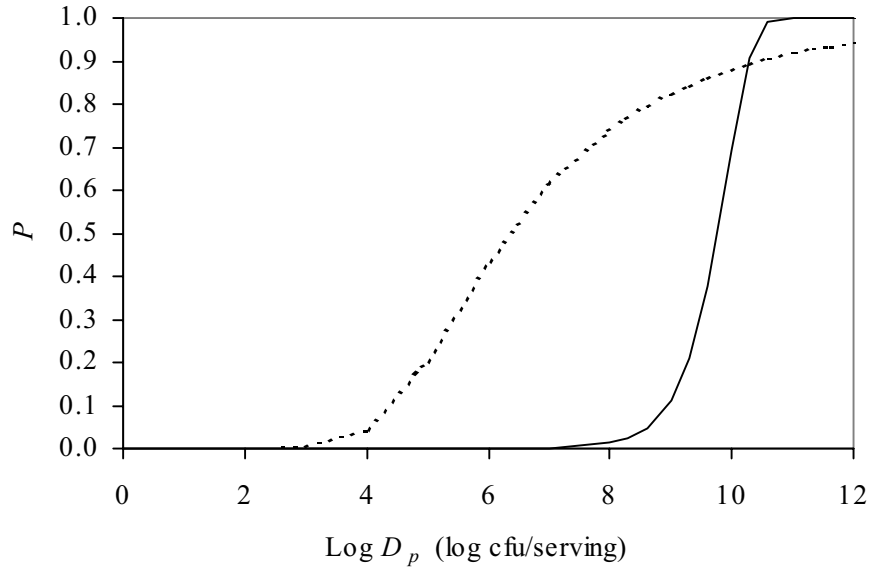

Figure 6. Dose-response curve for *L. monocytogenes* using r = 1.18E-10 [16] for the exponential model (solid line) and $\alpha = 0.17$ and $\beta = 3.62E4$ [44] for the beta-Poisson model (dotted line).

In practice, the aim is to keep the level of pathogens as low as possible and therefore only values of $P < 0.10$ are of interest [150]. For these low values there is a linear relationship between log N and log P with slope 1 as can be seen in figure 7 for both the exponential and beta-Poisson model.

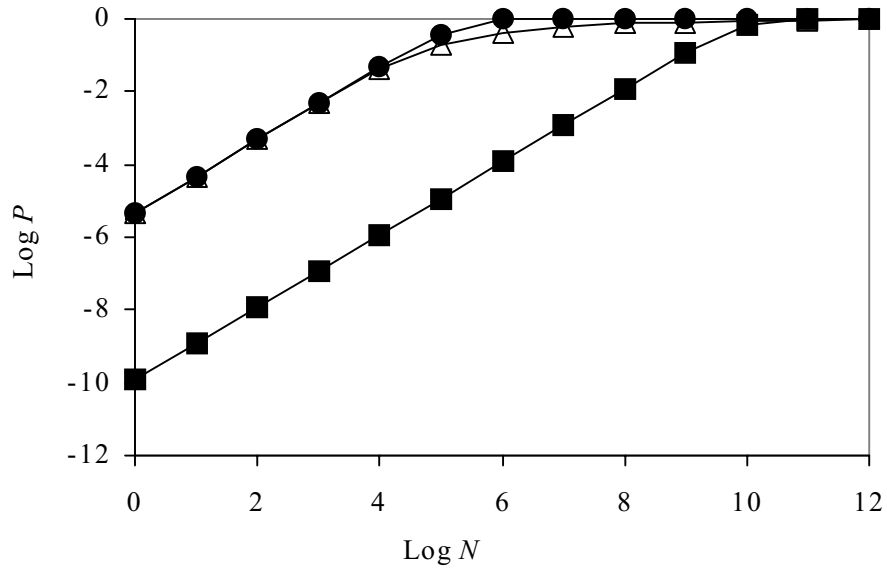

Figure 7. Dose-response curve for *L. monocytoge*nes on log-log scale for the beta-Poisson model (open triangles) using $\alpha = 0.17$ and $\beta = 3.62E4$ obtained from animal data [44] and for the exponential model (closed squares and circles) using r = 1.18E-10 obtained from epidemiological data (squares; [16]) and $r = \alpha/\beta$ (circles).

Figure 7 shows that both the exponential and beta-Poisson model show the same relationship with log P for low numbers of log N. Equations 12 and 13 can be simplified to:

$$P = rD_p \quad (15)$$

For the beta-Poisson model r is defined as: α/β.

In literature, apart from the exponential and beta-Poisson models, other dose-response relationships are used as well. Lindqvist and Westöö [76] for example used apart from the exponential model, the Weibull-Gamma model, which is an extension of the beta-Poisson model. According to their MRA, the exponential model described the number of outbreaks better than the conservative prediction of the Weibull-Gamma model. They concluded that the choice of dose-response model largely determines the outcome of an MRA. However, for low doses the beta-Poisson and exponential model are equal (equation 15 and figure 7). Therefore, it is rather the choice of parameter values (and thus dose-response data used and assumptions related to the parameters) that determines the outcome of the MRA, rather than the choice of the dose-response model.

In this case study, the probability of becoming ill after consumption of contaminated salmon is estimated based on scenario 5 from the previous section and assuming a serving size of 100 g (D_p = 100*N_p). The probability of illness is estimated by inserting the obtained lognormal distribution of the level of *L. monocytogenes* at the moment of consumption (section 3) into equation 15 using an r value of 1.18E-10 [16]. The results are given in table 6 for different storage times.

Table 6. Probability of illness after consumption of contaminated salmon after several weeks of storage including the 90% confidence interval.

Storage time (weeks)	average D_p (cfu/serving)	P	5th percentile	95th percentile
0	2.26E1	2.64E-9	1.40E-9	6.10E-9
1	1.13E3	1.33E-7	6.98E-8	3.25E-7
2	5.77E4	6.57E-6	3.49E-6	1.52E-5
3	2.86E6	3.39E-4	1.74E-4	8.03E-4
4	1.44E8	1.67E-2	8.71E-3	4.12E-2
5	7.18E9	8.69E-1	4.35E-1	1.93

This table shows that when equation 15 is used for high doses, as after 5 weeks of storage, unrealistic probabilities are obtained (the 95th percentile reaches a value above 1). In this case the original equation (equation 13) is better used rather than equation 15.
The maximum tolerable concentration of *L. monocytogenes* in ready-to-eat foods has been suggested as 100 cfu g^{-1} [57] or a concentration of 10^4 cfu per serving. When 0.1% of the

airborne concentration consists of *L. monocytogenes* and smoked salmon is contaminated via the air prior to storage, it can be concluded from table 6 that the product should be stored for less than 2 weeks to prevent foodborne illnesses. The probabilities obtained in this table are however based on a series of conservative assumptions. The *r*-value used in the exponential model is a conservative estimate of the probability of infection [16]. Furthermore, the exposure assessment determining the dose at the moment of consumption was based on the assumption that salmon has no competitive flora and is contaminated via the air with undamaged *L. monocytogenes*.

In order to perform a total MRA, apart from an exposure assessment and the establishment of dose-response relationships, the prevalence of contamination with *Listeria* should be included in the model as well as the number of exposures. According to the central limit theorem, the risk estimate approximates normality when the number of exposures is large enough [76]. This risk estimate can then be described by a normal distribution with the mean and standard deviation depending on the PDFs of the different steps of an MRA. For large number of exposures the standard deviation of this normal distribution approaches zero. The variability in the outcome of an MRA is thus reduced when the number of exposures increases. Generally, millions of products are produced, the outcome of an MRA can then be presented by the average risk estimate as a point estimate rather than a PDF describing the probability versus the probability of illness (as in Lindqvist and Westöö [76] or Cassin et al. [17]). The average risk from the final distribution can well be different from the deterministically determined risk based on the average value of the parameters.

5. Concluding remarks

The examples given in the previous sections were used to demonstrate how recontamination models can be used in an overall risk assessment. This showed that combining predictive microbiology with contamination models can help to identify the most important process steps and can be used to evaluate different scenarios to assess the influence on the level of pathogens at the moment of consumption.

Furthermore, a process evaluation can help to set performance criteria to meet food safety objectives (FSO). An FSO is defined as the maximum frequency and/or concentration of a microbial hazard in a food at the moment of consumption that provides the appropriate level of health protection. A performance criterion is the required outcome of one or more control measures to meet these FSOs [59].

The sum of the initial contamination, growth, inactivation and recontamination should be lower than the FSO:

$$H_0 - \sum R + \sum I_{G+RC} \leq FSO \qquad (16)$$

with FSO: food safety objective
H_0: initial level of the hazard
ΣR: total reduction of the hazard
ΣI_{G+RC}: total increase of the hazard due to growth (G) and/or recontamination (RC)
The values in equation 16 are given in log units [59].

For example, when the FSO is set at less than 1 cfu per 100 g, H_0 is 10^3 cfu g^{-1}, recontamination is negligible and growth causes a 1-log increase, the performance criterion for inactivation is:

$$3 - \sum R + (0+1) \leq -2 \Rightarrow \Sigma R \geq 6$$

The overall reduction should therefore be at least 6D reductions. When a reduction of only 5D is possible, then either the initial contamination or possibilities for growth should be reduced.

As explained in section 3, the importance of recontamination depends on the level of pathogens already present in the product. Therefore, process steps after an inactivation step are most sensitive to recontamination.

Graphically, a process evaluation including recontamination is presented in figure 8 for an imaginary production process.

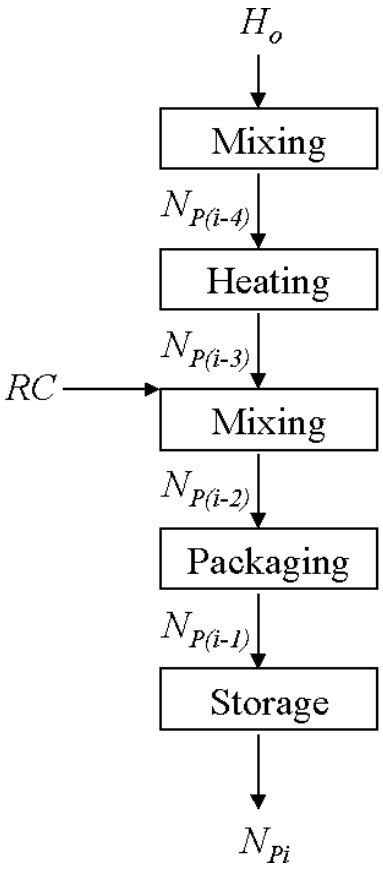

Figure 8. Imaginary production process with H_o the initial level of pathogens, $N_{P(i-n)}$ (n is 1 to 4) as the level of pathogens at the start of each production step and RC the recontamination factor.

When recontamination (*RC*) in figure 8 gives 10^{-1} cfu g^{-1} and the product itself ($N_{P(i-3)}$) contains 10^{-2} cfu g^{-1} after the heating step, the total concentration of bacteria in the product at the start of the second mixing step is $N_{P(i-3)} + RC = 0.11$ cfu g^{-1}. The increase or decrease during this mixing step can then be calculated using equation 9.
The recontamination factor can be quantified using the models as developed in this thesis.
For air contamination:

$$RC = C_{air} v_s A \tau / W \tag{10}$$

This equation can also be used to obtain clues for intervention in reducing airborne contamination by adjusting C_{air}, τ or A according to practical possibilities.

For recontamination via biofilms in steady state conditions (based on equation 7 and assuming that $\phi_P >> \mu_P V_P$):

$$RC = N_{Pi} - N_{P(i-1)} = \frac{\mu_P V_S N_S + \mu_B A_S N_B}{\phi_P} \tag{17}$$

The developed biofilm model is a mechanistic model based on mass balances that can be used to describe biofilm formation in time. This is useful to determine the appropriate cleaning moment so that recontamination through biofilms can be prevented (as can be seen in figure 3). When the model is applied in an MRA, initially steady state conditions can be assumed as a worst-case approach so that equation 17 can be used. An MRA is usually based on stochastic distributions that give a more realistic description of the actual situation than using point estimates. However, when the variability and uncertainty in the model parameters are unknown, or for the search of the most relevant factors, the use of point estimates can already indicate the most important factors influencing food safety.
For air contamination, *RC* should be added to the initial contamination and multiplied with growth or inactivation as given in equation 9. For the biofilm model (equation 17), the growth factor is already included in the equation; multiplication with a growth or inactivation factor is thus not necessary. Equations 10 and 17 can be used in a total process evaluation taken into account possibilities for recontamination, growth and inactivation in the different process steps. The outcome will then give an estimate of the level of pathogens at the moment of consumption, which should meet the predetermined FSO.

The philosophy of the developed recontamination models was not to obtain highly accurate models but to keep the models relatively simple and to minimise the number of parameters so that the models are suitable for MRA. The models should be validated further to determine whether these simplifications are justified. The biofilm model is for example only validated for laminar flow with *S. aureus* on silicon rubber surface. It is valuable to validate the model in other flow regimes and using other micro-organisms and surfaces. Furthermore, it would be useful to validate the model at higher temperatures. Then, it could also be applied for heat exchangers, which are known to be vulnerable to biofilm formation.

The air recontamination model should be further validated with industrial data on the number of contaminated products due to air contamination. The model can be extended with different types of airflows if necessary. Furthermore, section 3 showed that using TVC as a worst-case assumption resulted in unrealistically high levels of *Listeria* in the final product. Therefore, the concentration of specific pathogens in the air should be measured so that a more reliable estimation of air contamination can be made. TVC can, however, be used as a worst-case assumption resulting in a fail safe model for the potential magnitude of air contamination.

Overall, recontamination is an important potential source of foodborne illnesses and thus needs further attention. Quantification of recontamination can help to set performance criteria once FSOs are established. Furthermore, recontamination models can be incorporated in MRA to determine its importance and estimate the probability of becoming ill after consumption of the food item.
However, as described in chapter 2, there are not many recontamination models available at the moment that can be used for this purpose. Most predictive models so far have focussed on growth and inactivation rather than recontamination. For example recontamination via manual contact has not been modelled yet, but has been reported as a source of recontamination causing food illnesses [37, 47]. It is therefore relevant to quantify this type of recontamination. The work described in this thesis is an attempt to reduce the lack of recontamination models by proposing a model for biofilm formation and a model for air recontamination.
Further efforts should be made into quantifying and modelling recontamination routes. In addition, more data are necessary on the prevalence and impact of recontamination in production facilities. Such data are essential in the validation of recontamination models. Once reliable models are developed for all possible recontamination routes, this would be a step forward in applying a real farm-to-fork approach in MRA. When all relevant factors are included, a more accurate estimation of the exposure and thus the probability of illness after consuming a specific food product is possible.

References

1. **Al-Dagal, M. and Fung, D.Y.C.** (1990). Aeromicrobiology- a review. Food Science and Nutrition 29 (5), 333-340
2. **Allen, L., Polverari, M., Levesque, B. and Francis, W.** (1999). Effects of system closure on retention- and drainage-aid performance in TMP newsprint manufacture. TAPPI Journal 82 (4), 188-194
3. **Anonymous** (2001). ISO/DIS 4833. Microbiology of food and animal feeding stuffs-horizontal method for the enumeration of micro-organisms-Colony-count technique at 30 °C. International Organization for Standardization, Geneva, Switzerland
4. **Autio, T., Hielm, S., Miettinen, M., Sjöberg, A-M., Aarnisalo, K., Björkroth, J., Mattila-Sandholm, T. and Korkeala, H.** (1999). Sources of *Listeria monocytogenes* contamination in a cold-smoked rainbow trout processing plant detected by pulsed-field gel electrophoresis typing. Applied and Environmental Microbiology 65(1), 150-155
5. **Bakke, R., Trulear, M.G., Robinson, J.A. and Characklis, W.G.** (1984). Activity of *Pseudomonas aeruginosa* in biofilms: steady state. Biotechnology and Bioengineering 26, 1418-1424
6. **Barton, D.A., Stuart, P.R., Lagace, P. and Miner, R.** (1996). Experience with water system closure at recycled paperboard mills. TAPPI Journal 79 (3), 191-197
7. **Beer, T. and Ricci, P.F.** (1999). A quantitative risk assessment method based on population and exposure distributions using Australian air quality data. Environment International 25 (6/7), 887-898
8. **Belkhadir, R., Capdeville, B. and Roques, H.** (1988). Fundamental descriptive study and modelization of biological film growth-I. Fundamental descriptive study of biological film growth. Water Research 22 (1), 59-69
9. **Benefield, L. and Molz, F.** (1985). Mathematical simulation of a biofilm process. Biotechnology and Bioengineering 27, 921-931
10. **Benito, Y., Pin, C., Marin, M.L., Garcia, M.L., Selgas, M.D., and Casa, C.** (1997). Cell surface hydrophobicity and attachment of pathogenic and spoilage bacteria to meat surfaces. Meat Science 45 (4), 419-425
11. **Bemrah, N., Sanaa, M., Cassin, M.H., Griffiths, M.W. and Cerf, O.** (1998). Quantitative risk assessment of human listeriosis from consumption of soft cheese made from raw milk. Preventive Veterinary Medicine 37, 129-145
12. **Bloomfield, S.F. and Scott, E.** (1997). Cross-contamination and infection in the domestic environment and the role of chemical disinfectants. Journal of Applied Microbiology 83, 1-9
13. **Bonestroo, E.** (1996). Opsporing van nabesmettingsbronnen van verse, voorgebakken pommes frites. Report, Wageningen University, the Netherlands (Dutch publication)
14. **Bruhn, C.M. and Schutz, H.G.** (1999). Consumer food safety knowledge and practices. Journal of Food Safety 19, 73-87
15. **Bryers, J. and Characklis, W.** (1981). Early fouling biofilm formation in a turbulent flow system: overall kinetics. Water Research 15, 483-491
16. **Buchanan, R.L., Damert, W.G., Whiting, R.C. and van Schothorst, M.** (1997). Use of epidemiologic and food survey data to estimate a purposefully conservative dose-

response relationship for *Listeria monocytogenes* levels and incidence of listeriosis. Journal of Food Protection 60 (8), 918-922

17. **Cassin, M.H., Lammerding, A.M., Todd, E.C.D., Ross, W. and McColl, R. S.** (1998). Quantitative risk assessment for *Escherichia coli* O157:H7 in ground beef hamburgers. International Journal of Food Microbiology 41, 21-44
18. **Cassin, M.H., Paoli, G.M. and Lammerding, A.M.** (1998). Simulation modeling for microbial risk assessment. Journal of Food Protection 61 (11), 1560-1566
19. **Chang, H.T., Rittmann, B.E., Amar, D., Heim, R., Ehlinger, O. and Lesty, Y.** (1991). Biofilm detachment mechanisms in a liquid-fluidized bed. Biotechnology and Bioengineering 38, 499-506
20. **Characklis, W.G.** (1983). Process analysis in microbial systems: biofilm as a case study. In: Bazin, M. (Eds.), Mathematics in microbiology. Academic Press, London, 171-234
21. **Chen, Y., Jackson, K.M., Chea, F.B. and Schaffner, D.W.** (2001). Quantification and variability analysis of bacterial cross-contamination rates in common food service tasks. Journal of Food Protection 64 (1), 72-80
22. **Clement, T.P., Peyton, B.M., Skeen, R.S., Jennings, D.A. and Petersen, J.N.** (1997). Microbial growth and transport in porous media under denitrification conditions: experiments and simulations. Journal of Contaminant Hydrology 24, 269-285
23. **Cox, C.S.** (1987). The aerobiological pathway of microorganisms. John Wiley & Sons, Chichester, 293 p.
24. **Crank, J.** (1975). The Mathematics of Diffusion. Clarendon Press, London, 139-143
25. **Cunliffe, D., Smart, C.A., Alexander, C. and Vulfson, E.N.** (1999) Bacterial adhesion at synthetic surfaces. Applied and Environmental Microbiology 65 (11), 4995-5002
26. **Curiel, G.J., van Eijk, H.M.J. and Lelieveld, H.L.M.** (2000). Risk and control of airborne contamination. In: Robinson, R.K., Batt, C.A., Patel P.D. (Eds). Encyclopedia of Food Microbiology. Academic Press, San Diego, 1816-1822
27. **Dahi, E. and Thøgerson, J.** (1996). Bio-stabilization of drinking water in supply systems as observed in the tropics. World Journal of Microbiology & Biotechnology 12, 543-547
28. **Dalgaard, P. and Jørgensen, L.V.** (1998). Predicted and observed growth of *Listeria monocytogenes* in seafood challenge tests and in naturally contaminated cold-smoked salmon. International Journal of Food Microbiology 40, 105-115
29. **Dauphin, G., Ragimbeau, C. and Malle, P.** (2001). Use of PFGE typing for tracing contamination with *Listeria monocytogenes* in three cold-smoked salmon processing plants. International Journal of Food Microbiology 64, 51-61
30. **De Jong, P., Bouman, S., Langeveld, L.P.M. and Kiezebrink, E.H.** (1999). Predictive model for the adherence, growth and release of thermoresistant streptococci in production chains. In: Bird, M.R., Fryer, P.J., Grant, C.S., Graßhoff, A., Hasting, A.P.M., Spieß, W., Visser, H., Wilson, D.I. (Eds.), Fouling and cleaning in food processing '98, 118-124
31. **De Jong, P., te Giffel, M.C. and Kiezebrink, E.A.** (2002). Prediction of the adherence, growth and release of microorganisms in production chains. International Journal of Food Microbiology 74, 13-25
32. **Delignette-Muller, M.L. and Rosso, L.** (2000). Biological variability and exposure assessment. International Journal of Food Microbiology 58, 203-212
33. **Dickinson, R.B. and Cooper, S.L.** (1995). Analysis of shear-dependent bacterial adhesion kinetics to biomaterial surfaces. AIChE Journal 41 (9), 2160-2174

34. **Dickson, J.S. and Koohmaraie, M.** (1989). Cell surface charge characteristics and their relationship to bacterial attachment to meat surfaces. Applied and Environmental Microbiology 55 (4), 832-836
35. **Douben, P.E.T., Alcock, R.E. and Jones, K.C.** (1997). Congener specific transfer of PCDD/Fs from air to cows' milk: an evaluation of current modelling approaches. Environmental Pollution 95 (3), 333-344
36. **Duddridge, J.E., Kent, C.A. and Laws, J.F.** (1982). Effect of surface shear stress on the attachment of *Pseudomonas fluorescens* to stainless steel under defined flow conditions. Biotechnology and Bioengineering 24, 153-164
37. **Evans, M.R., Tromans, J.P., Dexter, E.L.S., Ribeiro, C.D. and Gardner, D.** (1996). Consecutive salmonella outbreaks traced to the same bakery. Epidemiology and Infection 116, 161-167
38. **Forster, H.W., Crook, B., Platts, B.W., Lacey, J. and Topping, M.D.** (1989). Investigation of organic aerosols generated during sugar beet slicing. American Industrial Hygiene Association Journal 50 (1), 44-50
39. **Gibson, H., Taylor, J.H., Hall, K.E. and Holah, J.T.** (1999). Effectiveness of cleaning techniques used in the food industry in terms of the removal of bacterial biofilms. Journal of Applied Microbiology 87, 41-48
40. **Gibson, L.L., Rose, J.B. and Haas, C.N.** (1999). Use of quantitative microbial risk assessment for evaluation of the benefits of laundry sanitation. American Journal of Infection Control 27 (6), S34-S39
41. **Gram, L. and Huss, H.H.** (2000). Fresh and processed fish and shellfish. In: Lund, B.M., Baird-Parker, T.C. and Gould, G.W. (Eds.), The microbiological safety and quality of food. Aspen Publishers, Gaithersburg
42. **Grasshoff, A.** (1983). Toträume in CIP-gereinigten Rohrleitungssystemen. Deutsche Milchwirtschaft 13, 407-414
43. **Guyer, S. and Jemmi, T.** (1990). Betriebsuntersuchungen zum Vorkommen von *Listeria monocytogenes* in geräucherten Lachs. Archiv für Lebensmittelhygiene 41(6), 144-146
44. **Haas, C.N., Thayyar-Madabusi, A., Rose, J.B. and Gerba, C.P.** (1999). Development and validation of dose-response relationship for *Listeria monocytogenes*. Quantitative Microbiology 1, 89-102
45. **Harrad, S.J. and Smith, D.J.T.** (1997). Evaluation of a terrestrial food chain model for estimating foodstuff concentrations of PCDD/Fs. Chemosphere 34 (8), 1723-1737
46. **Health Council of the Netherlands** (2000). Voedselinfecties. Publication no. 2000/09. Health Council of the Netherlands, The Hague (Dutch publication)
47. **Hedberg, C.W., Levine, W.C., White, K.E., Carlson, R.H., Winsor, D.K., Cameron, D.N., MacDonald, K.L. and Osterholm, M.T.** (1992). An international foodborne outbreak of shigellosis associated with a commercial airline. Journal of the American Medical Association 268 (22), 3208-3212
48. **Hedrick, T.I.** (1975). Engineering and science of aeromicrobiological contamination control in dairy plants. Chemistry and Industry October, 868-872
49. **Hedrick, T.I. and Heldman D.R.** (1969). Air quality in fluid and manufactured milk products plants. Journal of Milk and Food Technology 32 (7), 265-269
50. **Henriksson, E. and Haikara, A.** (1991). Airborne microorganisms in the brewery filling area and their effect on microbiological stability of beer. Monatsschrift für Brauwissenschaft 1, 4-8

51. **Hodgson, A.E., Nelson, S.M., Brown, M.R.W. and Gilbert, P.** (1995). A simple *in vitro* model for growth control of bacterial biofilms. Journal of Applied Bacteriology 79, 87-93
52. **Holah, J.T., Hall, K.E., Holder, J., Rogers, S.J., Taylor, J. and Brown, K.L.** (1995). Airborne microorganism levels in food processing environments. R&D-report no. 12, Campden & Chorleywood Food Research Association, United Kingdom, 22p.
53. **Holah, J.T. and Kearney, L.R.** (1992). Introduction to biofilms in the food industry. In: Melo, L.F, Bott, T.R., Fletcher, M. and Capdeville, B. (Eds.), Biofilms-Science and Technology. Kluwer Academic Publishers, Dordrecht, 35-41
54. **Hollander, A., Heederik, D., Denen, B. and Pothuis, J.** (1994). Onderzoek naar blootstelling aan bio-aerosolen in de aardappelverwerkende industrie. SDU uitgeverij, The Hague, 46 p. (Dutch publication)
55. **Holmberg, S.D. and Blake, P.A.** (1984). Staphylococcal food poisoning in the United States. Journal of the American Medical Association 251 (4), 487-489
56. **Hood, S.K. and Zottola, E.A.** (1995). Biofilms in food processing. Food Control 6 (1), 9-18
57. **ICMSF** (1994). Choice of sampling plan and criteria for *Listeria monocytogenes*. International Journal of Food Microbiology 22, 89-96
58. **ICMSF** (1996). Microorganisms in foods. Vol. 5. Microbiological specifications of food pathogens. Roberts, T.A., Baird-Parker, A.C. and Tompkin, R.B (Eds.). Blackie Academic & Professional, London
59. **ICMSF** (2002). Microbiological testing in food safety management. Wolters-Kluwers, USA (in press)
60. **ILSI** (1997). A simple guide to understanding and applying the hazard analysis critical control point concept. 2nd edition. Brussels: ILSI Europe Scientific Committee on Food Safety
61. **Jacobs, R.J., Grover, S.F., Meyerhoff, A.S. and Paivanas, T.A.** (2000). Cost effectiveness of vaccinating food service workers against hepatitis A infection. Journal of Food Protection 63 (6), 768-774
62. **Jay, J.M.** (1996). Modern food microbiology. Chapman & Hall, New York
63. **Jørgensen, L.V. and Huss, H.H.** (1998). Prevalence and growth of *Listeria monocytogenes* in naturally contaminated seafood. International Journal of Food Microbiology 42, 127-131
64. **Käferstein, F.K., Motarjemi, Y., Moy, G.G. and Quevado, F.** (1999). Food safety: a worldwide public issue. In: van der Heijden, K., Younes, M., Fishbein, L. and Miller, S. (Eds.), International food safety handbook. Marcel Dekker, New York
65. **Kang, Y-J. and Frank, J.F.** (1989). Biological aerosols: a review of airborne contamination and its measurement in dairy processing plants. Journal of Food Protection 52 (7), 512-524
66. **Kleiss, T.** (1992). Staphylococci in a whey powder plant environment. Thesis, University Zürich, Switzerland
67. **Kotula, A.W. and Emswiler-Rose, B.S.** (1988). Airborne microorganisms in a pork processing establishment. Journal of Food Protection 51 (12), 935-937
68. **Kumar, C.G. and Anand, S.K.** (1998). Significance of microbial biofilms in food industry: a review. International Journal of Food Microbiology 42, 9-27
69. **Kwok, W.K., Picioreanu, C., Ong, S.L., van Loosdrecht, M.C.M., Ng, W.J. and Heijnen, J.J.** (1998). Influence of biomass production and detachment forces on biofilm structures in a biofilm airlift suspension reactor. Biotechnology and Bioengineering 58 (4), 400-407

70. **Lammerding, A.M.** (1997). An overview of microbial food safety risk assessment. Journal of Food Protection 60 (11), 1420-1425
71. **Langeveld, L.P.M., van de Corput, P. and Faasen, M.J.M.G.** (1993). Kans op besmetting van gepasteuriseerde melkprodukten met *Listeria*. Voedingsmiddelentechnologie 7 (21), 13-16
72. **Larrauri, J.A., Borroto, B. and Crespo, A.R.** (1997). Water recycling in processing orange peel to a high dietary fibre powder. International Journal of Food Science and Technology 32, 73-76
73. **Lau, Y.L. and Liu, D.** (1993). Effect of flow rate on biofilm accumulation in open channels. Water Research 27 (3), 355-360
74. **Lindsay, D., Georgnaras, I. and von Holy, A.** (1996). Biofilms associated with poultry processing equipment. Microbios 86, 105-116
75. **Lindsay, D. and von Holy, A.** (1997). Evaluation of dislodging methods for laboratory-grown bacterial biofilms. Food Microbiology 14, 383-390
76. **Lindqvist, R. and Westöö, A.** (2000). Quantitative risk assessment for *Listeria monocytogenes* in smoked or gravad salmon and rainbow trout in Sweden. International Journal of Food Microbiology 58, 181-196
77. **Lorber, M., Cleverly, D., Schaum, J., Philips, L., Schweer, G. and Leighton, T.** (1994). Development and validation of an air-to-beef food chain model for dioxin-like compounds. The Science of the Total Environment 156, 39-65
78. **Lu, C., Biswas, P. and Clark, R.M.** (1995). Simultaneous transport of substrates, disinfectants and microorganisms in water pipes. Water Research 29 (3), 881-894
79. **Luppens, S.B.I., Reij, M.W., Rombouts, F.M. and Abee, T.** Development of a standard test to assess the resistance of *Staphylococcus aureus* biofilm cells to disinfectants (submitted)
80. **Lutgring, K.R., Linton, R.H., Zimmerman, N.J., Peugh M. and Heber A.J.** (1997). Distribution and quantification of bioaerosols in poultry-slaughtering plants. Journal of Food Protection 60 (7), 804-810
81. **Mackintosh, C.A. and Hoffman, P.N.** (1984). An extended model for transfer of micro-organisms via the hands: differences between organisms and the effect of alcohol disinfection. Journal of Hygiene 92, 345-355
82. **Malone, J.A. and Caldwell, D.E.** (1983). Evaluation of surface colonization kinetics in continuous culture. Microbial Ecology 9, 299-305
83. **Marks, H.M., Coleman, M.E., Jordan Lin, C.-T. and Roberts, T.** (1998). Topics in microbial risk assessment: dynamic flow tree process. Risk Analysis 18 (3), 309-328
84. **Maté, J.I. and Singh, R.P.** (1993). Simulation of the water management system of a peach canning plant. Computers and Electronics in Agriculture 9, 301-317
85. **McNab, W.B.** (1998). A general framework illustrating an approach to quantitative microbial food safety risk assessment. Journal of Food Protection 61 (9), 1216-1228
86. **Montville, R., Chen, Y. and Schaffner, D.W.** (2001). Glove barriers to bacterial cross-contamination between hands to food. Journal of Food Protection 64 (6), 845-849
87. **Morgenroth, E., van Loosdrecht, M.C.M. and Wanner, O.** (2000). Biofilm models for the practitioner. Water Science and Technology 41 (4-5), 509-512
88. **Mossel, D.A.A., Corry, J.E.L., Struijk, C.B. and Baird, R.M.** (1995). Essentials of the microbiology of foods- a textbook for advanced studies. John Wiley & Sons, Chichester, 250-257
89. **Mueller, R.F.** (1996). Bacterial transport and colonization in low nutrient environments. Water Research 30 (11), 2681-2690

90. **Mueller, R.F., Characklis, W.G., Jones, W.L. and Sears, J.T.** (1992). Characterization of initial events in bacterial surface colonization by two *Pseudomonas* species using image analysis. Biotechnology and Bioengineering 39, 1161-1170
91. **Nicolella, C., van Loosdrecht, M.C.M. and Heijnen, J.J.** (1999). Identification of mass transfer parameters in three-phase biofilm reactors. Chemical Engineering Science 54, 3143-3152
92. **Nielsen, L.A., Price, R.J. and Carroad, P.A.** (1983). Water re-use in processing of Pacific shrimp. Journal of Food Science, 48, 1056-1060
93. **Nieuwenhuijsen, M.J., Kruize, H. and Schenker, M.B.** (1998). Exposure to dust and its particle size distribution in California agriculture. American Industrial Hygiene Association Journal 58, 34-38
94. **Noguera, D.R., Pizarro, G., Stahl, D.A. and Rittmann, B.E.** (1999). Simulation of multispecies biofilm development in three dimensions. Water Science and Technology 39 (7), 123-130
95. **Notermans, S.** (1994). The significance of biofouling to the food industry. Food Technology 7, 13-14
96. **Notermans, S., Dormans, J.A.M.A. and Mead, G.C.** (1991). Contribution of surface attachment to the establishment of micro-organisms in food processing plants: a review. Biofouling 5, 21-36
97. **Notermans, S., Dufrenne, J., Teunis, P. and Chackraborty, T.** (1998). Studies on the risk assessment of *Listeria monocytogenes*. Journal of Food Protection 61(2), 244-248
98. **Notermans, S., Gallhoff, G., Zwietering, M.H. and Mead, G.C.** (1994). The HACCP concept: specification of criteria using quantitative risk assessment. Food Microbiology 11, 397-408
99. **Peyton, B.M. and Characklis, W.G.** (1993). A statistical analysis of the effect of substrate utilization and shear stress on the kinetics of biofilm detachment. Biotechnology and Bioengineering 41, 728-735
100. **Picioreanu, C., van Loosdrecht, M.C.M. and Heijnen, J.J.** (1998). A new combined differential-discrete cellular automaton approach for biofilm modeling: application for growth in gel beads. Biotechnology and Bioengineering 57 (6), 718-731
101. **Picioreanu, C., van Loosdrecht, M.C.M. and Heijnen, J.J.** (1999). Discrete-differential modelling of biofilm structure. Water Science and Technology 39 (7), 115-122
102. **Picioreanu, C., van Loosdrecht, M.C.M. and Heijnen, J.J.** (2000). Effect of diffusive and convective substrate transport on biofilm structure formation: a two-dimensional modeling study. Biotechnology and Bioengineering 69(5), 504-515
103. **Picioreanu, C., van Loosdrecht, M.C.M. and Heijnen, J.J.** (2001). Two-dimensional model of biofilm detachment caused by internal stress from liquid flow. Biotechnology and Bioengineering 72 (2), 205-218
104. **Pielaat, A. and van den Bosch, F.** (1998). A model for dispersal of plant pathogens by rainsplash. IMA Journal of Mathematics Applied in Medicine & Biology 15, 117-134
105. **Powell, M.S. and Slater, N.K.H.** (1982). Removal rates of bacterial cells from glass surfaces by fluid shear. Biotechnology and Bioengineering 24, 2527-2537
106. **Radmore, K., Holzapfel, W.H. and Lück, H.** (1988). Proposed guidelines for maximum acceptable air-borne microorganism levels in dairy processing and packaging plants. International Journal of Food Microbiology 6, 91-95
107. **Radmore, K. and Lück, H.** (1984). Microbial contamination of dairy factory air. South African Journal of Dairy Technology 16 (3), 119-123

108. **Rahkio, M.** (1999). Airborne bacteria related to carcass contamination in slaughterhouses. Proceedings: 30th R3-Nordic Contamination Control Symposium, VTT, Espoo, Finland, 129-137
109. **Reij, M.W. and van Schothorst, M.** (2000). Critical notes on microbiological risk assessment of food. Brazilian Journal of Microbiology 31, 1-8
110. **Ren, T-J. and Frank, J.F. (1992).** Sampling of microbial aerosols at various locations in fluid milk and ice cream plants. Journal of Food Protection 55 (4), 279-283
111. **Richter, A., Smiths, R. and Ries, R.** (1999). Growth and morphology of biological thin films. Applied Surface Science 144-145, 419-424
112. **Rørvik, L.M., Yndestad, M. and Skjerve, E.** (1991). Growth of *Listeria monocytogenes* in vacuum-packed, smoked salmon, during storage at 4 °C. International Journal of Food Microbiology 14, 111-118
113. **Rørvik, L.M.** (2000). *Listeria monocytogenes* in the smoked salmon industry. International Journal of Food Microbiology 62, 183-190
114. **Ross, T.** (1996). Indices for performance evaluation of predictive models in food microbiology. Journal of Applied Bacteriology 81, 501-508
115. **Ross, T., Dalgaard, P. and Tienungoon, S.** (2000). Predictive modelling of the growth and survival of *Listeria* in fishery products. International Journal of Food Microbiology 62, 231-245
116. **Rosso, L., Lobry, J.R., Bajard, S. and Flandrois, J.P.** (1995). Convenient model to describe the combined effects of temperature and pH on microbial growth. Applied and Environmental Microbiology 61 (2), 610-616
117. **Rowe, B., Hutchinson, D.N., Gilbert, R.J., Hales, B.H., Begg, N.T., Dawkins, H.C., Jacob, M., Rae, F.A. and Jepson, M.** (1987). *Salmonella ealing* infections associated with consumption of infant dried milk. The Lancet October 17, 900-903
118. **Rozzi, A., Malpei, F., Bonomo, L. and Bianchi, R.** (1999). Textile wastewater reuse in northern Italy (Como). Water Science and Technology 39 (5), 121-128
119. **Sayeed, S.A. and Sankaran, R.** (1990). A study on the behaviour of air microflora in food industries. Journal of Food Science and Technology 27 (5), 340-344
120. **Scholte, R.P.M.** (1996). Spoilage fungi in the industrial processing of food. In: Samson, R.A., Hoekstra, E.S. (Eds.). Introduction to food-borne fungi, 5th ed. Centraalbureau voor Schimmelcultures, Baarn, the Netherlands, 275-288
121. **Siebel, M.A. and Characklis, W.G.** (1991). Observations of binary population biofilms. Biotechnology and Bioengineering 37, 778-789
122. **Smittle, R.B.** (2000). Microbiological safety of mayonnaise, salad dressings and sauces produced in the United States: a review. Journal of Food Protection 63 (8), 1144-1153
123. **Stewart, P.S.** (1993). A model of biofilm detachment. Biotechnology and Bioengineering 41, 111-117
124. **Stoodley, P., Dodds, I., Boyle, J.D. and Lappin-Scott, H.M.** (1999). Influence of hydrodynamics and nutrients on biofilm structure. Journal of Applied Microbiology Symposium Supplement 85, 19S-28S
125. **Swartz, J.B. and Carroad, P.A.** (1979). Recycling of water in vegetable blanching. Food Technology 33 (6), 54-59
126. **Thompson, K.M., Burmaster, D.E. and Crouch, E.A.C.** (1992). Monte Carlo Techniques for quantitative uncertainty analysis in public health risk assessments. Risk Analysis 12 (1), 53-63.
127. **Trulear, M.G. and Characklis, W.G.** (1982). Dynamics of biofilm processes. Journal Water Pollution Control Federation 54 (9), 1288-1301

128. **Van Buren, J.P.** (1979). The chemistry of texture in fruits and vegetables. Journal of Texture Studies 10, 1-23
129. **Van Gerwen, S.J.C.** (2000). Microbiological risk assessment of food. Thesis, Wageningen University, the Netherlands.
130. **Van Gerwen, S.J.C., te Giffel, M.C., van 't Riet, K., Beumer, R.R. and Zwietering, M.H.** (2000). Stepwise quantitative risk assessment as a tool for characterization of microbiological food safety. Journal of Applied Microbiology 88, 938-951
131. **Van Gerwen, S.J.C. and Zwietering, M.H.** (1998). Growth and inactivation models to be used in quantitative risk assessments. Journal of Food Protection 61 (11), 1541-1549
132. **Vanne, L.** (1999). Significance of air in food and package manufacturing. In: Proceedings: 30th R3-Nordic Contamination Control Symposium, VTT, Espoo, Finland, 503 p.
133. **Vose, D.J.** (1998). The application of quantitative risk assessment to microbial food safety. Journal of Food Protection 61 (5), 640-648
134. **Wallis, A.P.L.** (1977). A water recovery system for bottle and bulk tanker washing systems. The Milk Industry 79 (4), 8,17-18
135. **Wang, W-C. and Sastry, S.K.** (1993). Salt diffusion into vegetable tissue as a pretreatment for ohmic heating: determination of parameters and mathematical model verification. Journal of Food Engineering 20, 311-323
136. **Wanner, O.** (1995). New experimental findings and biofilm modelling concepts. Water Science and Technology 32 (8), 133-140
137. **Wanner, O. and Gujer, W.** (1986). A multispecies biofilm model. Biotechnology and Bioengineering 28, 314-328
138. **Ward, D.R.** (2001). Description of the situation. Journal of Food Science 66 (7), 1067S-1071S
139. **Whiting, R.C. and Buchanan, R.L.** (1997). Development of a quantitative risk assessment model for *Salmonella enteritidis* in pasteurized liquid eggs. International Journal of Food Microbiology 36, 111-125
140. **WHO** (1995). Sixth report of the WHO surveillance programme for control of foodborne infections in Europe. FAO/WHO collaborating centre for research and training in food hygiene and zoonoses, Berlin.
141. **Whyte, W.** (1986). Sterility assurance and models for assessing airborne bacterial contamination. Journal of Parenteral Science & Technology 40 (5), 188-197
142. **Whyte, W.** (1996). In support of settle plates. PDA Journal of Pharmaceutical Science & Technology 50 (4), 201-204
143. **Whyte, W., Matheis, W., Dean-Netcher M. and Edwards, A.** (1998). Airborne contamination during blow-fill-seal pharmaceutical production. PDA Journal of Pharmeutical Science & Technology 52 (3), 89-99
144. **Zhang, X., Beatson, R.P., Cai, Y.J. and Saddler, J.N.** (1999). Accumulation of specific dissolved and colloidal substances during white water recycling affects paper properties. Journal of Pulp and Paper Science 25 (6), 206-210
145. **Zock, J-P.** (1998). Organic dust exposure and respiratory health in the potato processing industry. Thesis, Wageningen University, the Netherlands, 148p.
146. **Zwietering, M.H.** (2002). Quantification of microbial quality and safety in minimally processed foods. International Dairy Journal 12 (2-3), 263-271
147. **Zwietering, M.H., de Wit, J.C. and Notermans, S.** (1996). Application of predictive microbiology to estimate the number of *Bacillus cereus* in pasteurised milk at the point of consumption. International Journal of Food Microbiology 30, 55-70

148. **Zwietering, M.H. and Hasting, A.P.M.** (1997). Modelling the hygienic processing of foods-A global process overview. Foods and Bioproducts Processing 75 (C3), 159-167
149. **Zwietering, M.H., Rombouts, F.M. and van 't Riet, K.** (1993). Some aspects of modelling microbial quality of food. Food Control 4 (2), 89-96
150. **Zwietering, M.H. and van Gerwen, S.J.C.** (2000). Sensitivity analysis in quantitative microbial risk assessment. International Journal of Food Microbiology 58, 213-221

Summary

Every year at least 1.5 to 6% of the Dutch population suffers from foodborne illnesses. This may result in symptoms like vomiting or diarrhoea but can in some cases also lead to death. Processes like pasteurisation or sterilisation reduce the number of pathogenic bacteria in food products. Food safety is further controlled by implementing systems like Good Manufacturing Practices (GMP) and Hazard Analysis Critical Control Points (HACCP). Although these preventive measures do improve food safety, the presence of pathogenic bacteria can never be completely eliminated. Therefore, there is always a probability of becoming ill after consuming a food product. This probability can be estimated using Microbiological Risk Asessment (MRA).

For one element of MRA, the exposure assessment, the food chain is evaluated from the raw materials to the final product to estimate the level of pathogens in a food product at the moment of consumption. Predictive modelling techniques are combined with process engineering models to evaluate the effect of food processing steps on microbial survival and food safety. The same approach can be used to evaluate processes for other factors than microbiological hazards as was demonstrated in the evaluation of food processing on the accumulation of salts in a potato product. This approach proved to be useful to obtain quantitative information of the process and find critical points in the system.

In MRA, usually, only growth or inactivation in the different process steps is considered and re-introduction of bacteria during the production process is not taken into account. However, when pathogens re-enter the product after an inactivation step, this can cause foodborne illness. It is therefore relevant to quantify this recontamination so that it can be incorporated in MRA. A literature review, however, revealed that not many available recontamination models are directly applicable to the food industry.

The objective of this thesis was therefore to quantify recontamination using predictive modelling techniques so that it can be incorporated in MRA. Two possible recontamination routes were investigated: recontamination via formation of biofilms (layers of bacteria and their extracellular products attached to a surface) and recontamination via aerial transfer (e.g. through the existence of aerosols).

Recontamination via biofilms was modelled using mass balances and growth kinetics. Parameters for the biofilm model were obtained in biofilm experiments in which both biofilm formation and the release of cells into the flowing liquid were measured in time for up to 9 days. *Staphylococcus aureus* was chosen as a model pathogen and silicon tubing was used as testing material. The experiments were performed in duplicate for different flow conditions

(Reynolds = 3.2, 32 and 170). It was shown that at higher Reynolds numbers, the biofilm developed faster and the desorption rate increased accordingly.
As a case study, the developed biofilm model was applied in an example process system: the production of an acid-based spread. Different scenarios were evaluated, which demonstrated that the developed biofilm model indeed can be incorporated in an exposure assessment to determine the level of pathogens at the moment of consumption and to investigate whether biofilm formation is important or not. It was shown that when biofilms have been formed prior to a heating step, high levels of *S. aureus* can be reached locally, which can cause production of enterotoxins. These toxins are not inactivated in the heating step and can thus cause foodborne illness. Therefore, regular cleaning and a good hygienic design are a prerequisite to prevent foodborne diseases due to such biofilm formation.
The second route that was quantified was recontamination via the air. Data on the number of airborne micro-organisms were collected from literature and industries. The settling velocities of different micro-organisms were calculated for different products by combining the data on aerial concentrations with sedimentation counts. Statistical analyses were performed to clarify the effect of different products and seasons on the number of airborne micro-organisms and the settling velocity. For both bacteria and moulds three significantly different product categories with regard to the level of airborne organisms were identified. The statistical distribution in these categories was described by a lognormal distribution. The settling velocity did not depend on the product, the season of sampling, or the type of micro-organism and could be described by a lognormal distribution as well. The probability of recontamination via the air was estimated using the number of bacteria in the air, the settling velocity, and the exposed area and time of the product.
The effect of aerial recontamination was investigated in the production of smoked salmon as a case study. Using worst-case assumptions, it was shown that once salmon is contaminated with *Listeria monocytogenes* via the air, this pathogen can grow out to high numbers in the product. Therefore, either the frequency of recontamination or possibilities for growth should be reduced to improve safety of the product. Based on this exposure assessment, it was shown that smoked salmon should be stored for less than 2 weeks at 5 °C to control illnesses due to aerial recontamination of the food.

Overall, the work described in this thesis contributes to the reduction in the lack of recontamination models by quantifying biofilm formation and air recontamination. The application of the models in two example production processes showed that they can be incorporated in MRA to determine its importance and estimate the probability of becoming ill after consumption of the food item. However, other recontamination routes should be quantified as well and more data are necessary to validate and improve the models. Reliable recontamination models can be used together with growth and inactivation models to obtain a more reliable outcome of a MRA.

Samenvatting

Elk jaar lijdt zeker 1.5 tot 6% van de Nederlandse bevolking aan een voedselinfectie of voedselvergiftiging. Dit kan resulteren in symptomen als overgeven of diarree, maar kan in sommige gevallen ook de dood tot gevolg hebben. Processen als steriliseren of pasteuriseren verminderen het aantal ziekteverwekkende micro-organismen in levensmiddelen. Voedselveiligheid wordt verder beheerst door systemen als Good Manufacturing Practices (GMP) en Hazard Analysis Critical Control Points (HACCP). Alhoewel deze maatregelen de veiligheid van voedsel verbeteren, zullen ze niet leiden tot een complete eliminatie van pathogene micro-organismen. Er is daarom altijd een kans op ziekte na consumptie van een levensmiddel. Deze kans kan geschat worden met behulp van Microbiological Risk Assessment (MRA).

In één onderdeel van MRA, de exposure assessment, wordt de gehele voedselketen van grondstof tot aan eindproduct geëvalueerd om een schatting te kunnen maken van de hoeveelheid pathogenen in het product op moment van consumptie. Het effect van processtappen op de overleving van micro-organismen en dus de voedselveiligheid kan bepaald worden door wiskundige microbiologische modellen te combineren met proceskundige modellen. Dezelfde aanpak kan gebruikt worden om proceslijnen door te rekenen voor andere factoren dan voor micro-organismen zoals is toegepast voor de ophoping van zouten in een aardappelproduct. Met deze aanpak kon kwantitatieve informatie over het proces worden verkregen en konden kritieke punten worden opgespoord.

In een MRA wordt meestal alleen groei of inactivatie in de verschillende processtappen onderzocht en wordt herbesmetting vaak niet meegenomen. Als pathogene micro-organismen echter na een inactivatiestap in het product terechtkomen, kan dit leiden tot voedselinfecties. Het is daarom belangrijk om deze herbesmetting te kwantificeren en mee te nemen in een MRA. Een literatuuronderzoek wees echter uit dat er weinig herbesmettingsmodellen zijn die direct toegepast kunnen worden voor de levensmiddelenindustrie.

Het doel van dit proefschrift was dan ook om herbesmetting te kwantificeren met behulp van wiskundige modellen zodat ze kunnen worden toegepast in MRA. Twee mogelijke herbesmettingsroutes werden bestudeerd: via biofilmvorming (lagen van bacteriën en hun extracellulaire producten die gehecht zitten aan een oppervlak) en via de lucht (bijvoorbeeld door de aanwezigheid van aerosolen).

Herbesmetting via biofilms werd gemodelleerd op basis van massabalansen en groeikinetiek. Parameters voor het biofilmmodel werden verkregen in experimenten, waarin zowel de biofilmvorming als het loslaten van de cellen naar de vloeistof in de tijd werden gemeten. *Staphylococcus aureus* werd gebruikt als modelpathogeen en siliconenrubber werd gebruikt

als testmateriaal. De experimenten werden in duplo uitgevoerd bij drie verschillende stroomsnelheden (Reynolds = 3.2, 32, 170). Hieruit bleek dat bij toenemende Reynolds, de biofilmvorming sneller verliep en de desorptiesnelheid ook toenam.
In een case-studie werd het ontwikkelde biofilmmodel toegepast in de productie van acid-based spread. De evaluatie van verschillende scenario's toonde aan dat het biofilmmodel toegepast kan worden in een exposure assessment om zo de hoeveelheid pathogenen op moment van consumptie te bepalen en tevens te onderzoeken wanneer biofilmvorming van belang is. Hieruit bleek dat biofilmvorming voor de verhittingsstap lokaal hoge concentraties *S. aureus* kan veroorzaken, wat kan leiden tot enterotoxineproductie. Deze enterotoxines worden niet geïnactiveerd tijdens verhitting en kunnen dus voedselinfecties veroorzaken. Daarom is een goed hygiënisch ontwerp en regelmatig schoonmaken noodzakelijk om voedselinfecties door biofilmvorming te voorkomen.
De tweede herbesmettingsroute die gekwantificeerd werd, was besmetting via de lucht. Uit de literatuur en van bedrijven werden gegevens verzameld van concentraties micro-organismen in de lucht. Deze gegevens werden vervolgens gekoppeld aan sedimentatietellingen om zo de uitzaksnelheid van verschillende micro-organismen te schatten. Statistische analyses werden uitgevoerd om de invloed van verschillende producten en seizoenen te bepalen op het aantal micro-organismen in de lucht en op de uitzaksnelheid. Voor bacteriën en schimmels werden drie significant verschillende productgroepen gevonden, die beschreven werden met een lognormale verdeling. De uitzaksnelheid bleek niet afhankelijk te zijn van het product of het bemonsterde seizoen en werd ook beschreven met een lognormale verdeling. De kans op besmetting vanuit de lucht kon geschat worden met de concentratie micro-organismen in de lucht, de uitzaksnelheid en de blootgestelde tijd en oppervlak van het product.
Het effect van luchtbesmetting werd onderzocht in een case-studie naar de productie van gerookte zalm. Op basis van worst-case aannames bleek dat wanneer zalm besmet wordt met *Listeria monocytogenes* vanuit de lucht, deze pathogeen tot hoge aantallen kan uitgroeien in het product. De veiligheid van het product kan verbeterd worden door ofwel mogelijkheden voor groei of de kans op nabesmetting te verkleinen. Op basis van deze exposure assessment bleek dat een voedselinfectie door de consumptie van gerookte zalm grotendeels voorkomen kan worden door deze maximaal 2 weken bij 5 °C te bewaren.

Het werk in dit proefschrift draagt bij aan het modelleren van herbesmetting doordat zowel biofilmvorming als luchtbesmetting gekwantificeerd zijn. De toepassing van de modellen in twee voorbeeld productieprocessen liet zien dat ze geschikt zijn voor MRA om het belang van herbesmetting te bepalen en de kans op ziekte na consumptie te kunnen schatten. Het is echter noodzakelijk om ook andere herbesmettingsroutes te kwantificeren. Bovendien zijn er meer gegevens nodig om de verschillende modellen te kunnen valideren en aanpassen. Herbesmettingsmodellen kunnen gecombineerd worden met groei- en inactivatiemodellen om zo een betrouwbare risicoschatting te verkrijgen.

Dankwoord

De laatste bladzijden die nog geschreven moeten worden, maar zeker niet de onbelangrijkste. Een AIO-schap gaat niet over rozen, maar de klus is nu dan toch geklaard. Diverse mensen hebben hieraan bijgedragen en op deze bladzijden heb ik de gelegenheid ze daarvoor te bedanken.

Allereerst wil ik mijn promotoren en copromotor bedanken voor de goede begeleiding in de afgelopen vier jaar. Mick, ik heb veel van je praktijkervaring geleerd en ik zal de verhalen uit "de oude doos" gaan missen. Marcel, ook op afstand bleef je betrokken bij mijn onderzoek en ik heb je kritische kijk op mijn werk altijd bijzonder gewaardeerd. Email bleek een uitkomst voor vele, nuttige discussies. Remko, zonder jouw enthousiasme en motiverende woorden was dit proefschrift er nooit gekomen. Je was soms de snelheidsbepalende stap, maar belangrijker nog de katalysator in het proces. Bedankt voor al je tijd en inzet voor een AIO die officieel niet eens je AIO was.
Naast de (co)promotoren heeft mijn begeleidingscommissie constructief bijgedragen aan mijn onderzoek. Meike, Rijkelt, Martine, Taco, Huub en Frans bedankt voor de vele ideeën en praktische adviezen.
De afgelopen jaren heb ik met veel plezier gewerkt bij zowel levensmiddelenmicrobiologie als proceskunde. Ik "hing" tussen twee groepen in en heb daar ook schromelijk misbruik van gemaakt door diverse mensen van beide afdelingen lastig te vallen.
Van de proceskunde-afdeling bedank ik Albert voor de begeleiding in het aardappelproject. Jammer dat je wegging, waarna ik voor statistische adviezen bij Karin aanklopte. Ook Lex van Dijk en Sjoerd Boom van Triqua bedankt voor de plezierige samenwerking binnen dit project en de gezellige uurtjes in de auto (de snelste weg was toch niet door de polder).
Pieter en Ed, bedankt voor de hulp bij Matlab-probleempjes en Suzanne, bedankt voor je bijdrage aan hoofdstuk 4.
Zelf ben ik niet zo technisch, dus ik ben Jos erg dankbaar voor de adviezen over pompen, opstellingen en andere technische aangelegenheden. Gerrit, bedankt voor alle hulp op computergebied. Formeel hoorde ik weliswaar niet bij proceskunde, maar ik kon gelukkig toch altijd bij je terecht.
Van de microbiologen wil ik met name Rijkelt bedanken voor de praktische hulp bij allerhande problemen. Ik kon altijd bij je binnenlopen voor advies of een gezellig praatje. Suzanne, de gezamenlijke organisatie van onze workshop en de diverse biofilmuitstapjes waren erg gezellig. Ik zal de bizon niet snel vergeten….. (en de "autopech" evenmin).

Jasper en Boudewijn, bedankt voor de hulp bij het lay-outen van dit proefschrift. En Harsi, we hebben veel van elkaars kennis en ervaring geleerd.
In de loop van mijn AIO-schap begon ik het modelleer- en bureauwerk steeds meer te waarderen, dus was ik erg blij met de praktische hulp van verschillende studenten. Liesbeth, Annemieke, Margot, Evelyn en Wouter het viel niet altijd mee om de biofilms te laten groeien, maar ik hoop toch dat jullie het een leerzame ervaring vonden.
Verder wil ik ook graag alle ondersteunende "hand- en spandiensten" bedanken: Hedy, Joyce en Gerda voor het secretariële werk, de werkplaats, glasblazerij, bibliotheek, mediaservice en centraal magazijn (en wat verder helaas is wegbezuinigd).

Werkplezier wordt voor een groot gedeelte bepaald door de werksfeer en daar hebben meerdere mensen positief aan bijgedragen.
Allereerst alle kamergenoten die ik in de afgelopen jaren "versleten" heb: Frans en Marian, bedankt dat jullie mij van de eenzaamheid hebben gered. Vervolgens kreeg de European Chair een eigen kamer; Meike: het was kort maar krachtig. Van nog kortere duur, maar niet minder gezellig was het samenwonen met Anneke. Na 3 maanden nam de opvolger van Meike je plaats in. Martine, bedankt voor al je praktische oplossingen voor mijn biofilmonderzoek en de medebegeleiding van mijn studenten. Chantal, jij kwam vorig jaar ons team versterken. Het is maar goed dat mijn werk nu af is, het was af en toe iets te gezellig. Claudia, you were always working in the lab or in Zutphen, but the time you spent in our room was a very pleasant one.
Verder wil ik iedereen bedanken voor alle sociale activiteiten buiten het werk: de diverse borrels, filmavonden, labuitjes en BBQs bij Anja of Frans in de tuin.
Familie en vrienden, jullie zorgden voor de nodig afwisseling. De vraag: " Hoe staat het met je proefschrift?" is hierbij beantwoord. Floor, leuk dat je mijn paranimf wilt zijn. We kennen elkaar al sinds onze studententijd en ik heb het erg leuk gevonden om ook een tijdje samen AIO te zijn.
De laatste regels zijn voor Arjan. Je hebt me uit menig AIO dip(je) weten te halen en me behoed voor al te veel gestress. Het werk is nu gedaan, tijd om samen te genieten!

Curriculum Vitae

Esther Daniëlle den Aantrekker werd geboren op 4 oktober 1971 te Vlaardingen. In 1990 behaalde zij het VWO diploma aan de Rijksscholengemeenschap Graaf Engelbrecht te Breda. In datzelfde jaar begon ze aan de studie Levensmiddelentechnologie aan de Landbouwuniversiteit te Wageningen. Afstudeervakken werden afgelegd in de richtingen Levensmiddelenmicrobiologie en –chemie. Haar stage liep ze bij Wall's Ice Cream Factory, Unilever in Pakistan. In juni 1996 behaalde ze haar doctoraal diploma.
Na haar studie werkte ze tijdelijk als projectmedewerker bij de Grolsche Bierbrouwerij te Enschede. In oktober 1997 startte ze met een gecombineerd promotieonderzoek bij de leerstoelgroepen Levensmiddelenproceskunde en –microbiologie, waarvan de resultaten beschreven zijn in dit proefschrift.